NOTICE

The quality of this microform is heavily dependent upon the quality of the original thesis submitted for microfilming. Every effort has been made to ensure the highest quality of reproduction possible.

If pages are missing, contact the university which granted the degree.

Some pages may have indistinct print especially if the original pages were typed with a poor typewriter ribbon or if the university sent us an inferior photocopy.

Reproduction in full or in part of this microform is governed by the Canadian Copyright Act, R.S.C. 1970, c. C-30, and subsequent amendments.

AVIS

La qualité de cette microforme dépend grandement de la qualité de la thèse soumise au microfilmage. Nous avons tout fait pour assurer une qualité supérieure de reproduction.

S'il manque des pages, veuillez communiquer avec l'université qui a conféré le grade.

La qualité d'impression de certaines pages peut laisser à désirer, surtout si les pages originales ont été dactylographiées à l'aide d'un ruban usé ou si l'université nous a fait parvenir une photocopie de qualité inférieure.

La reproduction, même partielle, de cette microforme est soumise à la Loi canadienne sur le droit d'auteur, SRC 1970, c. C-30, et ses amendements subséquents.

Canada

TWO-PHASE CLOSED THERMOSYPHON WITH TWO-FLUID MIXTURES

BY

ROHJOON PARK

A thesis submitted in partial fulfilment of

the requirements for the degree of

MASTER of APPLIED SCIENCE

in the

DEPARTMENT OF MECHANICAL ENGINEERING

UNIVERSITY OF OTTAWA

Ottawa, Ontario, Canada

ISBN 0-612-00563-1

Canada

UNIVERSITÉ D'OTTAWA
UNIVERSITY OF OTTAWA

ACKNOWLEDGEMENT

First of all, the author is greatly indebted to Dr. Y. Lee. His advice, encouragement, and valuable suggestions during the program are particularly appreciated.

Many thanks to the technical staffs of the Mechanical Engineering and Physics workshops for their manufacture and repair.

The author wishes to express his appreciation to his colleagues, especially Dr. Pioro, for their help and discussion.

The author also wishes to acknowledge to his parents for their moral and material support. Also his wife, Youngha, shows patience and support throughout the course of this work.

ABSTRACT

An experimental study was conducted to investigate the performance of stationary two-phase closed thermosyphons with two-fluid mixtures. Three mixtures were used as the working fluids: water-ethanol, water-ethyleneglycol and water-glycerol.

The results are presented to show the effects of ratio of two fluid component, mean operating temperature, different fluid mixtures, heat flux and inclination of the thermosyphon with respect to the direction of the gravitational force. An analytical model is presented to predict the variation of the overall heat transfer coefficients with mole fraction for the thermosyphon with binary mixtures. A good agreement between the prediction by the model and the experimental results was obtained.

TABLE OF CONTENTS

LIST OF TABLES

LIST OF FIGURES

NOMENCLATURE

A	surface area
c_{pl}	specific heat of liquid at constant pressure
d	diameter
h	heat transfer coefficient
h_{fg}	latent heat of vaporization
g	gravity
L	length of thermosyphon
L^+	length ratio; L_e/L_c
P	pressure
Q	power (heat transfer rate)
q	heat flux
q´	heat generation per volume
R	thermal resistance
T	temperature
t	thickness of tube
U	overall heat transfer coefficient

V	volume
V^+	dimensionless volume of the working fluid, V_l/V_T
X^+	mole fraction of the second fluid, first fluid: water

Subscript

a	adiabatic section
ave	average
c	condenser section
cr	critical
e	evaporator section
fc	coolant fluid
i	inside
l	liquid
o	outside
s	saturation
sur	surrounding
T	total
TS	thermosyphon
w	wall

Greek Letter Symbols

λ	thermal conductivity (= k)

μ	dynamic viscosity
θ	angle of inclination, 90° = horizontal position
ρ	density
σ	surface tension
φ	angle from horizontal position, 90° = vertical position

Chapter 1

INTRODUCTION

1.1 Thermosyphon

It has been known for a long time that high rates of heat transfer can be obtained by means of the evaporation-condensation process. There are two closed systems that utilize this process, namely, **heat pipes** and **two-phase closed thermosyphon.** Both the heat pipe and thermosyphon are devices which transport and distribute large amount of heat by means of evaporation and condensation of a working fluid with a very small temperature difference along its working length. Although the heat pipes and two-phase closed thermosyphons are similar, there is an important difference in the mechanism of condensate return in these elements. The two-phase closed thermosyphon is a simple tube which contains a small amount of working fluid in it. When the heat is applied to the lower section of the tube, some of the liquid vaporizes, rises toward the upper end and then condenses. The condensed liquid goes down along the surface of the tube wall due to the gravitational forces. The heat pipe, on the other hand, has a wick structure along the inside tube wall. This wick provides a capillary force for the return of the condensed liquid toward the lower section. The two-phase closed thermosyphon is called the wickless heat pipe which relies on an external force

field (gravity or centrifugal force).

The most characteristic feature of both systems is that they derive the power necessary for the circulation of the working two-phase fluid solely from the heat transfer process. Therefore, no external power supply is needed.

The advantageous characteristics of a two-phase closed thermosyphon (and heat pipe) are:

1. It is light, flexible and controllable.
2. It can act as a thermal diode and a heat flux transformer.
3. It has a simple structure and isothermal surfaces.
4. It can transport a large amount of heat.
5. It reacts fast and has no moving part.
6. It can work even in space (heat pipes).
7. It can work as a separate unit (open two-phase thermosyphon).
8. It is almost noiseless in operation.

Due to its excellent characteristics, the thermosyphon is used in many fields: cooling of gas turbine blade [1,2], heat exchanger [3-5], nuclear reactor cooling [6,7], preservation of permafrost [8,9] etc. Other examples of applications in the industry are listed in Table 1.

1.2 Working Fluids

There are many parameters which affect the heat transfer characteristics of the two-phase closed thermosyphon. For the proper selection of a working fluid, the following must

be considered:

1. operating range of temperature and pressure
2. maximum heat flux in the evaporator
3. thermophysical properties (boiling and melting point, latent heat of vaporization, surface tension, thermal conductivity, viscosity, density, etc.)
4. toxicity
5. fire and explosion hazard
6. operating conditions which must include the conditions when it is not in use (possibility of freezing of the liquid when the device is stopped, start-up conditions, accidental situations)

Theoretically, all kinds of fluid can be used as a working fluid, but water is found to be the best choice by considering all of the above parameters. Water permits the transmitting of heat more than all the other used working fluids, except liquid metals. Also water is cheap, easily available, safe from fire, etc.. On the other hand, there are some disadvantages of water such as high melting (freezing) temperature, tendency to react with some substances (alkali metals, etc.) which are accompanied by the release of hydrogen where under certain conditions may cause an explosion.

Although ethanol, esters and freons can be used as a working fluid at low temperatures, because of their harmful effects of humans, a great care must be taken in using them. Therefore, the use of two- or multi-component mixtures were considered as working fluids. The two-component mixture heat transfer in a closed thermosyphon is little investigated. For certain applications, a thermosyphon with two-component mixture of two

fluids may show a superior engineering quality over that of single fluid. For example, closed thermosyphons with water and ethanol, or water and ethyleneglycol may be more suitable for cold region applications. Use in conjunction with a solar panel heater can be another example where such a thermosyphon with two-fluid mixtures suit better for practical reasons. The use of multi-component fluids makes it possible to broaden the range of operating temperatures. A water-glycol mixture is an actual example of a binary mixture working fluid. By adding glycol to water, the range of boiling temperatures and freezing temperatures becomes wider. Chechetkin [10] showed that pure ethyleneglycol boiling for prolonged time periods does not decompose up to 250 °C which corresponds to a pressure of 0.45 MPa. For this reason, ethyleneglycol and its mixture with water are recommended as boiling working fluids. To prevent freeze damaging of water-filled thermosyphon, it has been suggested to add 1-2 % volume of ethanol to the water [11]. Such a mixture protects the tube from any damage up to -40 °C without the decrease of heat transferring properties.

It should be noted that only certain binary mixtures have an azeotrope (i.e., a binary mixture in which the liquid and the vapour in equilibrium have the same composition). At azeotropic point, the two components boil at the same temperature in spite of the large difference in the pressures of each component. These solutions exist only at a certain ratio between the components of the binary mixture and they do not separate into two pure components by distillation, i.e., a working fluid behaves like a single component. (It will be discussed in Chapter 4.)

The boiling and condensation of a mixture of two different liquid can show very different characteristics from those of a single, pure liquid. It is well documented, for

example, that the pool-boiling heat transfer curves for a mixture and for a pure liquid with the same physical properties exhibits that [12]:

i. For a mixture, the onset of nucleate boiling occurs at a larger temperature difference than for the pure liquid.

ii. The pool-boiling heat transfer coefficient in a mixture is lower than for the pure liquid.

iii. The critical heat flux is affected by the mixing effects but may be increased or decreased.

All these differences are considered due to the phase equilibrium effects.

For condensation, there is hardly any experimental work published, although simplified analyses for binary and multi-component condensation are available in the open literature [13].

1.3 Objective

As mentioned earlier, there are few investigations about the characteristics of two-phase closed thermosyphons with two-component mixture.

The object of the present study is, therefore, to make an experimental investigation into the performance of stationary two-phase closed thermosyphons with three two-fluid mixtures: water-ethanol, water-ethyleneglycol and water-glycerol. These three fluid mixtures were chosen for the range of their saturation pressures.

Based on the experimental data, new correlations were developed as a simple model to predict the overall heat transfer coefficient of the thermosyphon with a two fluid mixture.

Chapter 2

LITERATURE SURVEY

The first classification of thermosyphons was made by Davies et al. [14] according to:

i. the nature of boundaries (open or closed)

ii. the regime of heat transfer (free or mixed convection)

iii. the type of the body force (gravitational or rotating)

According to the above categories, D. Japikse [2] reviewed extensively all types of thermosyphons.

Some basic studies have been carried out in an attempt to achieve more understanding of the operation of the two-phase closed thermosyphon as well as establishing its performance characteristics.

Cohen and Bayley [1] carried out experiments on both rotating and static two-phase closed thermosyphon tubes for use in gas turbine blades. They found that the heat transfer coefficient was independent of the quantity of fluid until the volume of working fluid was reduced to a certain level. However, it increased with the increase of tube diameter. Also, dryout was observed at the bottom of the tube with a small quantity of liquid.

Larkin [15] made two experimental devices, one transparent and one opaque, to study

their heat transfer characteristics. Various heat transfer mechanisms flow phenomena in steady state and three types of evaporator dry-out were observed with the transparent device. The opaque device was designed to examine the effect of parameters on the steady-state operation of the two-phase closed thermosyphon. He found that the heat transfer coefficient of the condenser is strongly dependent on the amount of liquid, but not very sensitive to depth of water and heat flux respectively.

Lee and Mital [16] investigated the effects of the several parameters (amount of working fluid, heated length-cooled length ratio (L^+), mean operating pressure, heat flux and the type of working fluid) on the performance of the thermosyphon using a copper tube 1.37 m in length and 25.4 mm in diameter. In this parametric study, they concluded that the heat transfer coefficient is independent of the quantity of the working fluid above a certain amount; however, it decreases with increasing L^+, but increases with increasing pressure and heat flux. Additional parametric work was done by Lee and Clements [17] and it was shown that heat transfer coefficient decreases with increasing diameter. Imura et al. [18] obtained similar results using water and ethanol as the working fluids and also developed correlation equations for both evaporating and condensing heat transfer coefficient.

A mathematical model was introduced by Shiraish et al. [19] to predict the heat transfer characteristics of the thermosyphon based on the experimental results. They found that the overall thermal resistance is very sensitive to the operating pressure, the heat flux and the quantity of the working fluid.

It is important to know the correct heat transfer limitations of a thermosyphon. Many correlations [20-22] were developed by investigators to find a critical heat flux. Two

different heat transfer limitations were observed by Nguyen-chi [23]: dryout and burnout. The critical heat flux due to the dryout increases with increasing filling ratio and operating temperature but decreases with increasing length ratio (L^+). The critical heat flux due to burnout increases with increasing operation temperature and tube diameter.

Many investigators agree that there exists a range of inclination angle at which the heat transfer coefficient of the thermosyphon has better performance than the vertical position. Because the thermosyphon works under the assistance of gravity, its transport capability is highly dependent on the direction of gravity. Several experiments have been reported in this subject [24-35]. Tu et al. [24] have reported the effect of inclination angle on the thermosyphon using a carbon steel tube with water as the working fluid. The working length is 10 m with 25 mm O.D. They suggested an operation angle between 35° and 40° from vertical position. Hahne and Gross [29] investigated a steel thermosyphon using Freon 115 as a working fluid. The tube was 2 m long with 40 mm diameter. The optimum value was placed between 40° and 45°. Negishi and Sawada [31] carried out an investigation with a copper thermosyphon of 330 mm in length and 13 mm in diameter. The high heat transfer coefficient was found between 50° and 70° for water and between 45° and 65° for ethanol. Shiraish et al. [28] obtained maximum performance between 40° and 50° for freon 113 in a glass tube. As shown above and in Table 2, no uniform conclusions can be made due to the differences among the operating conditions.

An experimental study was made to find an optimum filling ratio by Chen [27]. He found that the maximum heat transfer was obtained when the liquid fill was about 20 % of the thermosyphon volume. This result agrees well with those of other reports [33,36].

Andros [37] designed a stainless steel tube to investigate extended ranges of parameters. He noticed that the heat transfer coefficient for the condenser is not dependent on the liquid fill ratio except for the large fill ratio and the deleterious effect of non-condensible gases on the heat transfer coefficient in the thermosyphon. And with a visual device, he observed four basic flow regimes in the evaporator section of the thermosyphon during steady state operation: a smooth continuous evaporating film regime, the breakdown of the film into a series of rivulets, a wavy film with unstable rivulets and wavy film with bubble nucleation. Other investigations [38-41] were also carried out to obtain the flow patterns of the two-phase closed thermosyphon using glass tubes.

The phenomena observed in a glass tube , however, are not the same as those occurring in a metal tube. Pioro [40] compared the flow patterns between a glass tube and a special rectangular device. Two opposite walls of the device were stainless steel plate and the other two opposite walls were Plexiglas. He found a very different boiling pattern. The different phenomena are caused by the surface condition of wall. While the boiling occurs within the body of the superheated liquid (volume boiling) in the glass tube, the boiling takes place on the surface of the wall (nucleate surface boiling) in the metal tube. Ma et al. [41] observed the flow pattern using a glass tube with coated metal film. They found that four basic patterns are dependent on the filling ratio of the working fluid and the applied power, i.e., annular flow, slug flow, vapour 'projectile' flow and stagnant liquid column.

First physical explanation for the reduction in heat transfer coefficient in the binary mixtures was given by Van Wijk et al. [42]. They noted that at a certain concentration the dew point on the vapour bubbles may become equal to the temperature of the surrounding

superheated liquid and in that case the vapour bubbles grow only by diffusional mass transfer. Hence the heat transfer coefficient is lowered. Sterling and Tichacek [43] attributed the decrease in heat transfer to the additional resistance to mass diffusion, which exists in mixtures and slows down bubble growth. Stephan [44] developed a correlation which describe the influence of mass transport on heat transfer in multi-component system. To predict the effect of oil concentration on the heat transfer coefficient for refrigerant mixtures, a correlation was developed by Chongrungreong and Sauer [45]. Thome [46] developed a method for predicting the variation of nucleate pool boiling heat transfer coefficients with composition for binary liquid mixtures. He used six binary mixtures which showed degradation when they were mixed. Three mixing rules were compared to predict the heat transfer degradation for refrigerant mixtures by Kedzierski and Kim [47] recently. From their investigations, the minimum heat transfer coefficient was found at a certain mole fraction of the binary mixture.

However, there is little investigation about the effect of binary mixture working fluid on the performance of two-phase closed thermosyphon. Therefore, this experimental data can be a guide for choosing a proper working fluid at a given condition.

Chapter 3

EXPERIMENTAL APPARATUS AND PROCEDURES

3.1 Apparatus

The experimental apparatus is illustrated in Fig. (3.1) and Fig. (3.2) shows a schematic diagram. The main heat transfer system consists of the test thermosyphon, a power supply, a cooling jacket, a cooling system and related instrumentation.

The test thermosyphon used was made of 25.4 mm standard stainless steel S.S.304 tube. The tube was 1.4 mm long and 22.2 mm I.D. with a wall thickness of 1.6 mm. The closure of the top thermosyphon was made with a high performance vacuum valve (Nupro SS-4BG) through a stainless tubing of 6.4 mm O.D. together with a cold trap, welded on the upper cap which provided a link to the vacuum system, the charging line of the working fluid(s) and pressure measuring instrument. This arrangement made it easy to exchange working fluid-mixtures at different mixture ratios. At the bottom end, a 22.2 mm diameter and 1.6 mm thick stainless disc was welded to act as a wall. The overall working length of the thermosyphon was 1.4 m. Heat was applied in the lower 0.6 m long evaporator section

and heat was removed in the upper 0.6 m long condenser section. The middle section of 0.2 m in length was an adiabatic zone.

The evaporator section was heated by direct electrical resistance, using the evaporator section itself as the heater. Two electrode were clamped on the thermosyphon at the top and bottom of evaporator. Provision was made so as to vary the length of the heating section length, L_e, which was wrapped by insulation tape and then completely covered with thick (about 30 mm) insulation. The power to the evaporator section was provided with an electric power supply, rated up to 15KVA at 1500A A.C. The electric power input to the test heater was measured directly with two leads embedded in the test evaporator section, 400 mm apart in the central portion, by a digital voltmeter and an ammeter through measuring circuits. This eliminated the uncertainty in estimating the electrical lead losses and thus little error was introduced in calculating the heat flux. The probable maximum error in the wall heat flux is estimated to be about 5% [Appendix B].

The heat from the test section was removed at the upper part of the test thermosyphon by a coolant jacket. The cooling fluid at a given temperature was provided through a Colora coolant supply system and the flow rate of the coolant was measured through three rotameters which can be switched to a particular range of flow rate. The antifreezing mixture (50%water-50%ethyleneglycol) was used as a coolant.

A total of 11 AWG-36 chromel-alumel (K-type) thermocouples were welded (TIG welding) on the outside wall of the test tube; 6 for the measurement of the outer surface temperature of the evaporator section of the test thermosyphon, 3 for the condenser section, 1 for the adiabatic section and 1 for the outer surface of the insulation of the apparatus. The

circumferential wall temperature distribution at the centre of the evaporator section was measured at 90° intervals. All the thermocouples were calibrated *in situ.*

The voltage was measured by a Micron multimeter. An ammeter, Yokogawa M015L124, was used to measure the electric current of the evaporator in conjunction with a current transformer(GE JP-1) because of its high current flow. Because a high current is required, the power to the test tube was applied through two transformers, a powerstat (Super Electric Co. 13.4KVA), and a stepdown transformer (Marcus Co. Dry type 15KVA).

An additional important parameter in this experiment was the inclination of the test thermosyphon with respect to the gravitational force. The thermosyphon was placed between 2 supporting rods and a provision was made so that the thermosyphon could be easily rotated in 5° increments from 0° (vertical position) to 90° (horizontal position).

For a given series of experiments, the amount of the working fluid of a given mixture ratio charged at a vacuum of about 10^{-3} torr was about 20% of the total test tube by volume (i.e., $V^{+} = 0.20$) which was chosen from the preliminary test results of several thermosyphons with different amount of fill. This finding is consistent with that previously reported on the optimum amount of fill. Due to this value of working fluid ratio, the level of the pool was 20 mm lower than the 4 thermocouples which were placed in the centre of the evaporator section and was 0.18 m higher than the last one in the evaporator section. Such an distribution of thermocouples at the given volume of working fluid allowed us to measure wall temperatures under the different working conditions of the thermosyphon.

3.2 Procedure

All tests reported here are those obtained at the steady state. Prior to the actual experiments the thermosyphon was thoroughly cleaned with acetone followed by rinsing in ethanol and finally distilled water. After it was vacuum dried, it was tested for vacuum, leaks checked and connected to a Leybold model S1TEL 147283 mechanical vacuum pump to remove air and other non-condensible gases. The pump ran for 10 hours to reach the magnitude of $5*10^{-3}$ torr.

After the system was evacuated, a known amount of the mixture of a given mixture ratio was charged into the tube. Non-condensible gases in the test thermosyphon must be minimized. During steady-state operation non-condensible gases are pushed to go up to the upper end of the thermosyphon and make an insulating layer. Such a layer reduces the actual condensing area. Therefore it decreases the efficiency of the system. Non-condensible gases are introduced mainly by the air and those which may be generated within the thermosyphon when the working fluid contacted the inside wall. Air, on the other hand, can enter the thermosyphon through a leakage or it can come in to it while the working fluid is charged. Thus, great care is necessary when the system is being charged with a working fluid and one has to ensure that the thermosyphon is completely sealed.

The power to the evaporator heating section was increased in steps to the desired heat flux. When a steady state was reached (within 30-50 min), the voltage and the current to the evaporator, temperatures of evaporator and condenser were acquired and reduced through a Hewlett-Packard data acquisition system. The data acquisition system used in the study consists of: a Hewlett Packard system 9835A with hard disks; 3456A digital voltmeter; 3495A scanner and HP Thinkjet printer. For each experiment, measurements were made

at 1 minute interval for 30 to 40 minutes. The average temperatures from the thermocouples over a period of 10 minutes once steady state was reached were used as the data.

To study the effect of an inclination of the thermosyphon, the adiabatic temperature was adjusted to a predetermined value by varying the flow rate and/or the temperature of the coolant to the condenser.

After each series of the test for a given fluid mixture ratio, the thermosyphon was thoroughly cleaned by repeated washing and then vacuum dried, tested for vacuum, checked for leaks and any leaks found were corrected. After the system was evacuated, a known amount at another mixture ratio was charged into the test tube and the next series of tests were repeated.

3.3 Data Reduction

Since the thermocouples were welded onto the outside tube wall of the thermosyphon, the solution of the "inverse" heat transfer problem was required in order to obtain the inside surface temperature. By solving the two dimensional steady state heat conduction equation with heat generation, the inside temperatures were obtained [Appendix C]. The inside temperature, T_{wi}, can be related to the outside temperature, T_{wo}, as following:

$$T_{wi} = T_{wo} + T_{corr} \tag{3.1}$$

In the above equation, T_{corr} is the temperature difference due to conduction between a thermocouple location and the heat transfer surface. For the inside temperature of the condenser, T_{ci}, we have:

$$T_{ci} = T_{co} + \frac{qt}{k} \tag{3.2}$$

For the inside temperature of the evaporator:

$$T_{ei} = T_{eo} - \frac{q't^2}{2k} \tag{3.3}$$

And for the inside temperature of the adiabatic zone:

$$T_{ai} = T_{ao} + \frac{h_{sur}(T_{ao}-T_{\infty})}{k}t \tag{3.4}$$

where h_{sur} is heat transfer coefficient in free convection in our case.

The evaporator section was calibrated to determine the heat loss under the test conditions. The two temperatures (the temperature on the evaporator section of the thermosyphon and the temperature on the outside of insulation at the same position) were measured. The curve between the power and the difference in temperature was plotted. This plot was used to calculate the heat loss from the entire power supplied, thereby providing the rate of heat transfer into the working fluid in the thermosyphon. Under the steady state conditions of the test, this net heat transfer rate must be equal to that leaving the condenser section. Therefore, no attempts was made to measure the heat lost in the condenser section.

A conductance model (Fig. (3.3)) was used to estimate the heat transfer rate of the thermosyphon. For the thermosyphon the total thermal resistance between the temperature of the hot section and cold section can be written as:

$$R_T = R_1 + R_2 + R_3 + R_4 \tag{3.5}$$

where R_1: external resistance on hot side

R_2: resistance from evaporation

R_3: resistance from condensation

R_4: external resistance on cold side

Here , all wall conductive thermal resistances were neglected because of their small values. In our model, the overall thermal resistance of the thermosyphon is defined as:

$$R_{TS} = R_2 + R_3 = \frac{1}{U_{TS}} \tag{3.6}$$

The heat transfer coefficients in the thermosyphon are defined as:

(a) Thermosyphon heat transfer coefficient

$$U_{TS} = \frac{q}{T_{ei}-T_{ci}} \tag{3.7}$$

(b) Evaporation heat transfer coefficient

$$h_e = \frac{q}{T_{ei}-T_{ai}} \tag{3.8}$$

(c) Condensation heat transfer coefficient

$$h_c = \frac{q}{T_{ai}-T_{ci}} \tag{3.9}$$

Chapter 4

ANALYTICAL MODEL

The overall heat transfer coefficient of the thermosyphon with the mixture, $U_{TS,X}$, can be defined by the following equation:

$$\frac{1}{U_{TS,X}A_e} = \frac{1}{h_{e,X}A_e} + \frac{1}{h_{c,X}A_c} \tag{4.1}$$

where $U_{TS,X}$ is the overall heat transfer coefficient of the mixture at ratio X

A_e and A_c are the areas of the evaporator and the condenser, respectively

To obtain the overall heat transfer coefficient from Eq. (4.1), the heat transfer coefficients of evaporator and condenser must be known. The heat transfer coefficients are strongly dependent on the properties of fluid. For the binary mixture, two components could have a coupled effect on heat transfer coefficients. This effect may be deduced from the phase equilibrium diagram of mixtures. The phase diagram effects can be expressed on a temperature-composition diagram. There are two main phase diagrams for two fluid-mixtures (Fig. 4.1(a), 4.1(b)).

1. For the normal mixture the temperature-composition diagram is shown in Fig.(4.1(a)). The lower line, the bubble point line, represents the variation of the

liquid saturation temperature with the composition. The upper line, the dew point curve, illustrates the variation of the saturated vapour temperature with the composition. The area between the curves represents a two phase mixture with a liquid of composition $x_{l,A}$ and a vapour composition $x_{v,A}$ in coexistence. At T_a mole fraction of liquid A is $x_{l,A}$ and vapour mole fraction is $x_{v,A}$.

2. In the case of azeotrope, Fig (4.1(b)), the vapour will first form at temperature T_b; that vapour has the same composition as the liquid ($x_{v,A} = x_{l,A}$); consequently, the distillate obtained has exactly the same composition as the original liquid. Therefore, azeotropes are useful since they behave like pure fluids in many ways because there is no composition difference between the phases.

When a liquid A of composition $x_{l,A}$ boils, the vapour A in equilibrium with the liquid A has a composition $x_{v,A}$. On the other hand, the liquid B has composition $1-x_{l,A}$ and vapour B has $1-x_{v,A}$. While the evaporator contains the working fluid, the heat transfer coefficient could be affected by the liquid mole fractions of each component and the condensing heat transfer coefficient should be influenced by the vapour mole fractions of each component. Therefore, the heat transfer coefficients of a mixture may be deduced from the heat transfer coefficients of the pure component using the following simple hypothesis:

$$h_{e,X} = h_{e,A}x_{l,A} + h_{e,B}x_{l,B} \tag{4.2}$$

$$h_{c,X} = h_{c,A}x_{v,A} + h_{c,B}x_{v,B} \tag{4.3}$$

where $h_{e,A}$ is evaporating heat transfer coefficient of liquid A

$x_{l,A}$ is liquid mole fraction of liquid A

$h_{e,B}$ is evaporating heat transfer coefficient of liquid B

$x_{l,B}$ is liquid mole fraction of liquid B (= 1 - $x_{l,A}$)

$h_{c,A}$ is condensing heat transfer coefficient of liquid A

$x_{v,A}$ is vapour mole fraction of liquid A

$h_{c,B}$ is condensing heat transfer coefficient of liquid B

$x_{v,B}$ is vapour mole fraction of liquid B (= 1 - $x_{v,A}$)

Vapour-liquid equilibrium data are very difficult to obtain in the literature, but it appears from the available data [48] that the ratios of vapour to liquid phases of the two fluid components are not strongly dependent on the temperature and pressure for the range studied in the present experiment. For this reason, we have used the vapour-liquid equilibrium data of P=760 mm.Hg for ethanol and of P=228 mm.Hg for the case of ethyleneglycol.

For the values of h_e and h_c, one can use any number of the empirical correlations available in the literature. For example, for h_e, we can use that of Imura [18] given as:

$$h_e=0.32\frac{\rho_l^{0.65}\lambda_l^{0.3}c_{pl}^{0.7}g^{0.2}q_e^{0.4}}{\rho_v^{0.25}h_{hg}^{0.4}\mu_l^{0.1}}\left(\frac{P_i}{P_o}\right)^{0.3} \tag{4.4}$$

For h_c, we can use that of Nusselt [49] given as:

$$h_c=0.943\left[\frac{\rho_l^2 g h_{hg}\lambda_l^3}{L_h\mu_l(T_a-T_c)}\right]^{0.25} \tag{4.5}$$

In spite of non linearity of the mole fraction on heat transfer coefficient, the model works well as seen in Figs. ((5.25),(5.26)), indicating that although the mass transfer of the

volatile liquid into the less volatile fluid should have affect heat transfer coefficient, for the working fluid used in the present study, it can be concluded that the effect is negligible.

Before an analytical model can be used with any confidence, it must first endure the validation process. This process consists of comparing theoretical predictions with actual experimental results. Different sets of experimental results are required covering a wide range of conditions to give the theory a greater range of validity. If the theoretical predictions are within acceptable limits of the experiment, some confidence can be gained in using the theory for predictions in other situations of interest. However, care must be taken that the theory is not extended to phenomena far outside the range of validation.

In chapter 5.2, it will be seen that our own correlations for h_e and h_c from the present study give better results over the other correlations such as those given in equations ((4.4), (4.5)).

Chapter 5

RESULTS AND DISCUSSION

The results are presented to show the effects of ratio of two fluid components, mean operating temperature, different fluid mixtures, heat flux and inclination of the thermosyphon with respect to the direction of the gravitational field on the performance of the thermosyphon. A comparison of the prediction of the heat transfer characteristics of the thermosyphon based on a simple analytical model with the experimental results was also made.

Ethanol, ethyleneglycol and glycerol in water are not surface active such as a trace of mercury which in sodium can cause considerable increase in the heat transfer coefficient under nucleate pool boiling conditions compared with that measured for the pure mercury [50]. However, the presence of the second component(non-surface active) in a pure liquid is known to cause considerable reductions in the heat transfer rate under the nucleate pool boiling condition. The cause of reduction in heat transfer coefficients is illustrated by many investigators [12, 42-48, 51]. In Fig. (5.1) the shaded area represents a layer of liquid. When the liquid starts to boil, the low boiling component in this layer is depleted. This causes the increase of the saturation temperature in the layer of liquid. Therefore, the superheat (T_w -

T_{sat}) which is required for the activation of bubble nuclei decreases. The bubble growth rates are consequently reduced and so are the heat transfer coefficients. This was seen throughout the present experimental study and the details are presented in the following.

5.1 Experimental Results

Before we consider the heat transfer performance of thermosyphon with two-component mixtures, the characteristics of boiling in the pure water thermosyphon is briefly discussed.

In Fig. (5.2), the variation of typical wall temperature histories over the length of the evaporator, condenser and adiabatic sections under several values of heat flux during the stable cooling conditions are illustrated. From Fig. 5.2, the following conclusions were observed:

I. When the heat input is low as seen in Fig. (5.2), e.g., Q = 4.7 W, the heat transfer is by natural convection only from the surface of the working fluid. As the power is increased, the temperature of the upper evaporator part which is above the pool level rises up rapidly, i.e., this part is overheated. Therefore the wall temperature of the upper evaporator is higher than that of the lower evaporator part. But the wall temperature under the pool level rises slowly and just a small quantity of vapour evaporates from the pool surface. On the other hand, because the temperature of the coolant is higher than the adiabatic temperature, the condensation does not occur. This shows that this is unstable and therefore, the thermosyphon does not function

properly.

II. With some increase of heat input (Q = 15 W), the wall temperatures of all the evaporator section increase. Especially the temperature of the wall under the pool becomes higher than that of above the pool. Due to the partial coverage of the wall by the rivulet, there is a temperature deviation (range of 0.5°C) around the wall. In this regime, the heat transfer consists of : conductance from wall to the vapour through the film, evaporation of the rivulet (the highest value of the heat transfer coefficient) and the convective heat transfer between the bare wall and the vapour.

III. At Q = 245 W, more liquid vaporizes and consequently more condensation occurs. The temperature distributions over the wall above the pool becomes more uniform. It indicated that all surface of the wall is covered with a liquid film and therefore, convective heat transfer between the wall and the vapour disappears. Besides the two kinds of heat transfer, there is also an occurrence of heat transfer by small vapour bubbles. Because these vapour bubbles take some quantity of heat by vaporization and make the border layers of fluid turbulent, convection heat transfer coefficient increases considerably. In the condenser, the temperature distributions makes it possible to notice the presence of non-condensible gases which are from the wall and working fluid. Due to the non-condensible gases, condensation does not occur in all part of the condenser.

IV. At Q = 622 W, temperature under the pool has a higher value than the

temperature above the pool. Increased pressure forced the non-condensible gases to move up to the top of condenser and made a new surface for condensation. This is because the heat transfer coefficient of surface nucleate boiling in the pool is less than that of the liquid film boiling at constant a heat flux.

V. With very increased power input, Q = 959 W, due to the rise of the fluid level by many vapour bubbles, the heat transfer coefficient becomes the same all over the evaporator section and accordingly the temperature distributions become uniform.

The temperature distributions of the condenser and evaporator sections are illustrated in Fig. (5.3) as a function of heat flux and the mixture ratio for a constant adiabatic section temperature, T_a. From such information as seen in Fig. (5.3), it can be expected that the heat transfer coefficient of pure water is higher than that of mixtures and pure ethanol.

5.1.1 Effect of Mole Fraction of Second Fluid, X^+

The effects of the mole fraction of the second fluid, X^+ on the overall heat transfer coefficient of the test thermosyphon, U_{TS}, are shown in Figs. (5.4(a)-5.6(b)) for the conditions shown in the figures. As was observed in the nucleate pool boiling of two-fluid mixtures, all show a decrease in the value of U_{TS} in all cases except for the case of water-ethanol.

For water-ethanol, the value of U_{TS} at X^+ of about 0.2 is, in general, slightly less than

that at X^+ of about 0.4 for all cases for the water-ethanol mixtures. The mixtures of water-ethyleneglycol did not display such phenomena as are seen in Figs. (5.5(a), 5.5(b)). Instead, the heat transfer rate seemed to decrease steadily with increasing value of X^+. Similar trends were also obtained in the case of water-glycerol. However, the minimum heat transfer coefficient is always found at the pure second fluid (the first fluid is water) not at the certain mole fraction of the binary mixture.

Since the equilibrium states of two-fluid two-phase mixtures are so complexly interrelated to the mole fraction of the fluids with the system temperature and pressure, no easy plausible physical explanation can be made to the heat transfer characteristics seen in these figures. Among three two-fluid mixtures examined in the present study, only the mixture of water-ethanol has azeotrope for the range of the system pressure studied and this may somehow have affected the results. The reduction of U_{TS} at X^+ of about 0.2 for the case of water-ethanol could have been the result of an increase of ethanol in the vapour phase at that value of X^+. This is because the condensation rate of ethanol is relatively low compared to that of the water vapour of U_{TS}. This is strictly an hypothesis based on the meagre data on the equilibrium of two-fluid mixtures available in the literature [48]. For these reasons, no further physical explanation is attempted for the phenomena.

5.1.2. Effect of the Adiabatic Temperature

For the definition of the heat transfer coefficients, h_c and h_e, it is logically more meaningful to use T_s instead of T_a as used in Eqs. (3.8) and (3.9). However, two pressure gauges connected to the vacuum line during the experiment did not last. Since $L^+ = 1$ and

heat loss is negligible it is safe to assume $T_a \fallingdotseq T_s$ as indicated in Ref. [9].

Typical results of the effect of T_a on the thermosyphon heat flux for the different mixture ratio are illustrated in Figs. (5.7(a)-5.9(b)) It can be seen that the heat flux increases as the adiabatic temperature increases.

Similarly, Figs. (5.10(a)-5.12(b)) show that the overall heat transfer coefficient of the test thermosyphon, U_{TS}, increases considerably with an increase in the adiabatic temperature, T_a, for all values of X^+. This is because the boiling heat transfer coefficient (or overall heat transfer coefficient) always increases with increasing pressure (Fig. (5.13)). Here P_o, 1 atm, is an outside pressure and P_a (adiabatic pressure) is derived from the adiabatic temperature. With an increase of pressure, the vapour density increases within the tube. At the constant heat flux, the mass flow rate of the vapour is steady and this results in a low vapour velocity, which may reduce the interfacial shear stress. Also an increase in temperature which results from the increased pressure, diminishes the effect to surface tension. And the reture flow of condensation increases because of a decrease of liquid viscosity. Due to these factors, the condensed liquid moves fast from the condensing section, which in turn increases the heat transfer coefficient.

Fig. (5.14) illustrates the effect of T_{fc} on U_{TS} in conjunction with T_a. It was found that U_{TS} increases slightly with the increasing of T_{fc}. With the increase of coolant temperature, the condenser temperature increases and consequently the temperature difference between the condenser and the adiabatic zone decreases. This increases the heat transfer coefficient.

5.1.3 Effect of Thermosyphon Inclination

The thermosyphon can mainly operate under the assistance of the gravity. Therefore, the heat transport capability of the thermosyphon is highly affected by the direction of the gravity. This means the inclination angle has a large effect on the operating characteristics of a thermosyphon. For this reason, it is necessary to study the effect of the inclination angle in order to search for the new application field and the clarification of the phenomena of the thermosyphon.

The effect of the orientation of the test thermosyphon with respect to the gravitational field is shown in Figs. (5.15(a)-5.17). It can be observed that for all X^+ at a given condition, the thermosyphon exhibits the highest heat transfer performance at the angle of about 60° from the direction of the gravitational field. Hahne and Gross [29] explained the higher heat transfer coefficients as a result of coupled effect of gravitational force and frictional force. As the angle of inclination is increased from the vertical to horizontal, both forces decrease. However, heat transfer coefficient is propotional to the gravity force and reversely propotional to the frictional force. Optimal angle could be anywhere between 0° and 90°. In our experiment, 60° is the angle where the coupled effect of gravitational force and frictional force on heat transfer coefficient is at the maximum. And Negishi and Sawada [31] explained that the heat transfer mechanism is considered to be affected by the condensation of vapour and forced convection by the dashing working fluid in the thermosyphon. As the inclination angle increased to 60° from the vertical position, the dashing tip of the working fluid went up along the condenser and finally reached the end of condenser. Also newly condensed surface was exposed to the vapour

after the surface was wiped by the dashing liquid. Due to these factors, the heat transfer performance may have a highest value at this angle.

5.1.4 Comparison with CHF of Pioro

Fig. (5.18) shows a comparison of the present results with the empirical correlation of Pioro [22] on the critical heat fluxes of two-phase closed thermosyphons with two-fluid mixtures. Pioro's equation is:

$$q_{cr} = 0.16 h_{kg} \rho_v^{0.5} [\sigma g(\rho_l - \rho_v)]^{0.25} [1 - \exp(-(\frac{d_i}{L_e})(\frac{\rho_l}{\rho_v})^{0.13} \cos^{1.8}(\varphi - 55))]^{0.86} \qquad (5.1)$$

The prpperties of mixture were found by using linear mixing rule. There was no direct collaboration between the two studies but it can be seen from the figure that the trend of the heat transfer characteristics of two studies is very similar which is a very encouraging aspect of the present study.

5.2 Comparison with Analytical Model

The heat transfer coefficients from present experimental study were compared with the heat transfer coefficients from the empirical correlation of Imura given as Eq. (4.4) and Nusselt's analysis, Eq. (4.5), for the heated section and cooled section, respectively. The heat transfer coefficients of the evaporator and the condenser were obtained in the heat flux range 8000-25000 W/m^2 with water, ethanol and ethyleneglycol as the working fluids.

5.2.1 Evapolating Heat Transfer Coefficient

Figs. (5.19-5.21) show the comparison of the present experimental data with Imura's correlation. The solid line indicates the values calculated by Imura's equation and the dotted line represents our new correlation. To develop our equation, we considered the following expression for the heat transfer coefficient in the evaporating section:

$$h_e = C_e \chi_e^{m_e} \tag{5.2}$$

where

$$\chi_e = \frac{\rho_l^{0.65} \lambda_l^{0.3} c_{pl}^{0.7} g^{0.2} q^{0.4}}{\rho_v^{0.25} h_{lg}^{0.4} \mu_l^{0.1}} \left(\frac{P_i}{P_o}\right)^{0.3}$$

The parameter χ_e is the same parameter proposed by Imura.

The constant C_e and the exponent m_e were determined from the experimental data so as to correlate the data best. The values are:

working fluid	C_e	m_e
water	0.251	1
ethanol	24.3	0.493
ethyleneglycol	21.2	0.389

5.2.2 Condensing Heat Transfer Coefficient

Nusselt's correlation and our empirical data are compared in Figs. (5.22-5.24). The solid line is for the Nusselt's equation and the dotted line is from our new correlation. As was the case for the evaporation heat transfer coefficient, we assumed:

$$h_c = C_c \chi_c^{m_c} \tag{5.3}$$

where

$$\chi_c = \frac{\rho_l^2 g h_{lg} \lambda_l^3}{L_c \mu_l (T_a - T_c)}$$

C_c and m_c are also obtained from the experimental data. The parameter χ_c is the same as in the Nusselt's equation, Eq. (4.5). The values for C_c and m_c are:

working fluid	C_c	m_c
water	$3.7*10^{-8}$	0.697
ethanol	$4*10^{-4}$	0.503
ethyleneglycol	$3.3*10^{-3}$	0.422

5.2.3 Overall Heat Transfer Coefficient

Figs. (5.25,5.26) show the comparison of the predicted values of U_{TS} with the experimental results. While the overall heat transfer coefficient, U_{TS}, using our correlation agrees well with the experimental data, there is a large deviation between U_{TS} calculated with the correlation using Imura's and Nusselt's equation and the present experimental results.

The comparison of the experimental values of U_{TS} with those calculated by our correlation and as well with those corrected using Imura's and Nusselt's equation is summarized in Figs. (5.27,5.28). The open circles are those obtained using our correlations and the closed ones are those using Imura's and Nusselt's equations. The overall heat

transfer, U_{TS}, predicted using our correlation based on the single model, Eq. (4.1) falls within ± 10 % of the experimental results in the case of water-ethanol mixtures. But deviation is high in the case of water-ethyleneglycol mixtures. This may be because some physical properties of ethyleneglycol are calculated using the methods given in Ref. [52] and the value of heat transfer coefficient of pure ethyleneglycol was found by extrapolation.

Chapter 6

CONCLUSIONS

The present experimental study provides practical design information on heat transfer characteristics of a closed two-phase thermosyphon with two-fluids mixtures in certain ranges. From the present study, the following conclusions are made:

1. Effect of X^+ was identified for three mixtures; i.e., water-ethanol, water-ethyleneglycol and water-glycerol.

2. The variation of the effect of X^+ on heat transfer depends on the kind of fluid mixtures but in all mixtures, the overall heat transfer coefficients of the test thermosyphon with a mixture is always lower than that with the first liquid (water) but higher than that with the second liquid (ethanol, ethyleneglycol and glycerol). Therefore, no minimum value of heat transfer coefficient was found in the mixture.

3. The overall heat transfer coefficient of the thermosyphon was found to increase considerably with increasing adiabatic temperature.

4. In the present experiment, the thermosyphon exhibits the highest performance at the angle of about 60° from the direction of the gravitational force for all values of X^+.

5. A simple analytical model which requires the equilibrium data of the binary mixtures is proposed to predict the overall heat transfer coefficient of the mixtures. This new correlation agrees well with the experimental results for which they were established.

REFERENCES

1. H. Cohen and F.J. Baylay, Heat Transfer Problems of Liquid Cooled Gas Turbine Blades, Proc. Inst. Mech. Eng, **169**, 1063-1080 (1955).
2. D. Japiski, Advances in Thermosyphon Technology, Advances in Heat Transfer, Academic Press, New York, **3**, 2-111 (1973).
3. Y. Lee and A. Bedrossian, A Two-Phase Closed Thermosyphon, Int. J. Heat Mass Transfer, **21**, 221-229 (1978).
4. D. Fetcu, V.B. Ungureanu and G. Bacanu, Gravity-Assisted Wickless Heat Pipe Heat Exchanger, 8th International Heat Pipe Conference, Beijing, Preprints E-12 (1992).
5. T. Wadowaski, A. Akabarzadeh and P. Johnson, Characteristics of a Gravity Assisted Heat Pipe Based Heat Exchanger, 7th IHPC, Minsk (1990)
6. S.N. Belousov, L.N. Kutin, V.I. Merkulov, S.M. Smirnov, Experience of the Developments and Investigatious of Passive Heat Removal Systerms Based on Heat Pipes for Nuclear Technology, 8th IHPC, Preprint E-P16 (1992)
7. N. Tsuyuzaki, T. Saito, M. Hishida, K. Negish, Y. Okamoto, Heat Removal Heat Pipe System of Nuclear Irradiation Facilities, 6th IHPC, Grenoble, 752 (1987)
8. B.S. Larkin, Heat Transfer in a Two-Phase Thermosyphon Tube, N.R.C. Report NO

DME/NAE 45-54 (3), 196 (1967)

9. S.H. Zahir, A Two-Phase Closed Thermosyphon at Low Temperature, M.A.Sc. Thesis, University of Ottawa (1972)

10. A.V. Chechetkin, High Temperature Heat Carriers, Pergamon Press, 307 (1963)

11. U.S Patient No 4664181, IC F28D 15/00

12. P.B. Whalley, Condensation and Gas Liquid Flow, Oxford University Press, Oxford, 167 (1991)

13. J.G. Collier, Convective Boiling and Condensation, 2nd ed., McGraw-Hill, 420 (1981)

14. T.H. Davies, W.D. Morris and W.D. Morris, Thermosyphons, Engineer's digest, **26**, No 11, 87-91 (1965).

15. B.S. Larkin, An Experimental Study of the Two-Phase Thermosyphon Tube, Transactions of the Canadian Society for Mechanical Engineering, 14, No.B-6 (1971).

16. Y. Lee and U. Mital, A Two-Phase Closed Thermosyphon, Int. J. Heat Mass Transfer, **15**, 1695-1707 (1972).

17. B. Clements and Y. Lee, Additional Parameters in Two-Phase Closed Thermosyphon: Effects of Tube Diameter and Wall Thickness, Int. J. Heat Mass Transfer, **24**, No.9, 1554-1555 (1981).

18. H. Imura, H. Kusuda, J. Ogata, T. Miyazaki and N. Sakamoto, Heat Transfer in Two-Phase Closed-Type Thermosyphon, Heat Transfer Japanese Research, **8**, No.2, 41-53 (1979).

19. M. Shiraish, K. Kikuchi and T. Yamanichi, Investigation of Heat Transfer Characteristics of a Two-Phase Closed Thermosyphon, 4th IHPC, London, 95 (1981).

20. H. Imura, K. Sasaguchi and H. Kozai, Critical Heat Flux in a Closed Two-Phase Thermosyphon, Int. J. Heat Mass Transfer, **26**, No.8, 1181-1188, (1983).

21. T. Fukano, K. Kadokuchi and C.L. Tien, Expermental Study on the Critical Heat Flux at the Operating Limit of a Closed Two-Phase Thermosyphon, Heat Transfer Japanese Reserch **17**, No.5, 43-60 (1988).

22. I.L. Pioro and M.V. Vorontsova, Calculation of the Ultimate Heat Flux for Liquid Boiling in Two-Phase Thermosyphons, J. of Eng. Physics, **53**, No.3, 376-383 (1987)

23. H. Nguyen-chi, M. Groll and Th. Dang-van, Experimental Investigation of Closed Two-Phase Thermosyphons, AIAA 14th thermophisics conference, Orlando, 193-200 (1979)

24. C. Tu, G. Xie, C. Hu, Z. Gao and R. Hong, The Two Phase Closed Thermosyphon: an Experimental Study with Flow Pattern and Optimum Fill Charge, China-U.S. Seminar on Two-Flows and Heat Transfer, Sian, 395-405 (1984).

25. H. Nguyen-Chi and M. Groll, Entrainment or Flooding Limit in a Closed Two-Phase Thermosyphon, 4th IHPC, London, 147-162 (1981).

26. M. Groll and Th. Spendel, Thermel Behavior of High-Performance Closed Two-Phase Thermosyphon, 5th IHPC, Tsukuba, 1-6 (1984)

27. M.M. Chen, Heat Transfer Performance of Two-Phase Closed Thermosyphons with Different Lengths, 6th IHPC, Grenoble, 647-651 (1987).

28. P. Terdtoon, M. Shiraishi and M. Murakami, Investigation of Effect of Inclination Angle on Heat Trancefer Characteristics of Closed Two-Phase Thermosyphon, 7th IHPC, Minsk, B9P (1990)

29. E. Hahne and U. Gross, The Influence of the Inclination Angle on the Performance of a Closed Two-Phase Thermosyphon, 4th IHPC, London, 125-135 (1981)

30. M. Yiwei, J.C.Y. Wang, L. Jifu and F. Yi, Theoretical and Experimental Studies on Condensation Heat Transfer Inside Vertical and Inclined Thermosyphons, 1989 National Heat Transfer Conference HTD-vol. 108, 111-116 (1989).

31. K. Negishi and T. Sawada, Heat Transfer Performance of an Inclined Two-Phase Closed Thermosyphon, Int. J. Heat Mass Transfer, **26**, No.8, 1207-1213 (1983).

32. M. Yiwei, L. Jifu and F. Yi, The Characteristics of Condensation Heat Transfer in Thermosyphons, 6th IHPC, Grenoble, 597-602 (1987).

33. A. Bontemps, C. Goubier, C. Marquet, J.C. Solecki and C. Nardi, Performance Limits of a Toluene Loaded, Closed Two-Phase Thermosyphon, 6th IHPC, Grenoble, 634-644 (1987)

34. S. Maezawa, K. Gi and S. Matsumura, Laminar Film Condensation on Inclined Two-Phase Closed Thermosyphon, 8th IHPC, Beijing, Preprint B-11 (1992).

35. Y. Wen and S. Guo, Experimental Heat Transfer Performance of Two-Phase Thermosyphons, 5th IHPC, Tsukuba, 43-49 (1984).

36. K.T. Feldman, Jr. and R. Srinivasan, Investigation of Heat Transfer Limits in Two-Phase Closed Thermosyphon, 5th IHPC, Tsukuba, 30-35 (1984).

37. F. Andros, Heat Transfer Characteristics of the Two-Phase Closed Thermosyphon (Wickless Heat Pipe) Including Direct Flow Observation, Ph.D. Thesis, Arizona State University (1980).

38. M. Shiraishi, P. Terdtoon and M. Murakami, Effect of Inclination Angle on Flow

Patterns in a Two-Phase Closed Thermosyphon, 8th IHPC, Beijing, Preprint B-22 (1992).

39. S. Roesler and M. Groll, Flow Visualization and Analytical of Interaction Phenomena in Closed Two-Phase Flow Systems, 8th IHPC, Beijing, Preprint A-4 (1992).

40. I.L.Pioro, Correction of Experimental Data on the Maximum Heat and Mass Transfers in Two-Phase Thermosyphons, Heat transfer-Soviet Research, **17**, No.5, 75-83 (1985).

41. T. Ma, X. Liu, and J. Wu, Flow Patterns and Operating Limits in Two-Phase Closed Thermosyphon, 6th IHPC, Grenoble, 576-581 (1987)

42. W.R. Van Wijk, A.S. Vos and S.J.D. Van Stralen, Heat Transfer to Boiling Binary Liquid Mixtures, Chem. Engng Sci. **5**, 68-80 (1956)

43. C.O. Sternling and L.J. Tichacek, Heat Transfer Coefficients for Boiling Mixtures, Chem. Engng Sci. **16**, 297-337 (1961)

44. K. Stephan, Heat Transfer with Natural Convection Boiling in Multicomponent Mixture, Heat Exchangers, 315-336 (1981)

45. S. Chongrungreong and H.J. Sauer,Jr., Nucleate Boiling Performance of Refrigerents and Refrigerent-Oil Mixture, J, of Heat Transfer, **102**, 701-705 (1980).

46. J.R. Thome, Prediction of Binary Mixture Boiling Heat Transfer Coefficients Using Only Phase Equlibrium Data, Int. J. Heat Transfer, **26**, No.7, 965-974 (1983).

47. M.A. Kedizierski and J.H. Kim, Causes of the Apparent Heat Transfer Degradation for Refrigerant Mixtures, HTD-vol.197, Two-Phase Flow Heat Transfer, 149-158

(1992).

48. W. Nusselt, Die Oberflchenkondensation des Wasserdampfes, VDI Z., **60**, 541 (1916), quoted from "Heat Transfer", J.P. Holman, 7th ed. (1990)

49. J.C. Chu, Distillation Equilibrium Data, Reinhold Pub. Co., New York (1950)

50. Y. Lee, Pool Boiling Heat Transfer with Mercury and Mercury Containing Dissolved Sodium, Int. J. Heat Mass Transfer, 11, 1807-1821 (1968).

51. R.A.W. Shock, Nucleate Boiling in Binary Mixtures, Int. J. Heat Mass Transfer, **20**, 701-709 (1977).

52. R.C. Reid, J.N. Prausnitz and T.K. Sherwood, The Properties of Gases and Liquids, 3rd ed., McGraw-Hill (1977)

53. S.J. Kline and F.A. McClintock, Describing Uncertainties in Single-Sample Experiments, Mechanical Engineering, 3-8, January (1953)

APPENDIX A

HEAT LOSS

Before beginning a test, heat loss must be calculated to determine the net power supply. The temperature difference between the thermosyphon outside wall (T_6) in the evaporator section and the outside insulation (T_{11}) which was placed at the same position against the power was plotted in Fiq. (A.1). In this pre-test, as much as two hours were required to obtain a single point in the steady state condition. This test was done without working fluid and vacuum.

i. $Q = 47A * 0.115V * 0.6/0.4 = 8.11$ (W)

$\Delta T = 53$

ii. $Q = 63.8 * 0.162 * 0.6/0.4 = 15.5$ (W)

$\Delta T = 94.4$

iii. $Q = 72.6 * 0.192 * 0.6/0.4 = 20.9$ (W)

$\Delta T = 124$

$Q = a\ \Delta T$

$a = \Sigma Q_i/\Sigma \Delta T_i = 44.5/271 = 0.164$

Heat Loss = $0.164 * (T_6 - T_{11})$ (A.1)

Therefore, Eq. (A.1) was used to subtract the heat loss from the entire power supplied.

APPENDIX B

ERROR ANALYSIS

The experimental errors were calculated using the method recommended by Kline and McClintok [53]. The evaluated uncertainties in the variables are:

D_i (inside diameter), ± 0.07 %

L (length), ± 0.25 %

T (temperature), ± 0.2 °C

E (voltage), ± 1.88 %

I (ampere), ± 1 %

Using these variables, followings were calculated.

1. Power

$$Q = VI - 0.164(T_6 - T_{11}) = 960$$

$$\frac{\partial Q}{\partial V} = I = 505$$

$$\frac{\partial Q}{\partial I} = V = 1.92$$

$$\frac{\partial Q}{\partial \Delta T} = -0.164$$

$$\omega_Q = [(\frac{\partial Q}{\partial V}\omega_V)^2 + (\frac{\partial Q}{\partial I}\omega_I)^2 + (\frac{\partial Q}{\partial \Delta T}\omega_{\Delta T})^2]^{\frac{1}{2}}$$

$$= [505*0.024)^2+(1.92*5)^2+(-0.164*0.2)^2]^{\frac{1}{2}}$$

$$= 15.4$$

$$Q = 960 \pm 15.4(1.6\%)$$

2. Area

$$A = \pi D_i L_e = 0.0418$$

$$\frac{\partial A}{\partial D_i} = \pi L_e = 1.89$$

$$\frac{\partial A}{\partial L_e} = \pi D_i = 0.0697$$

$$\omega_A = [(\frac{\partial A}{\partial D_i}\omega_{D_i})^2 + (\frac{\partial A}{\partial L_e}\omega_{L_e})^2]^{\frac{1}{2}}$$

$$= [(1.89*0.0000155)^2+(0.0697*0.0015)^2]^{\frac{1}{2}}$$

$$= 0.00002936$$

$$A = 0.0418 \pm 0.0000293(0.07\%)$$

3. Heat Flux

$$q = \frac{Q}{A}$$

$$\frac{\partial q}{\partial Q} = -\frac{Q}{A^2} = -\frac{960}{0.00175} = -549000$$

$$\frac{\partial q}{\partial Q} = \frac{1}{A} = 23.9$$

$$\omega_q = [(\frac{\partial q}{\partial A}\omega_A)^2 + (\frac{\partial q}{\partial Q}\omega_Q)^2]^{\frac{1}{2}}$$

$$= [(-549000*0.0000293)^2+(23.9*15.4)^2]^{\frac{1}{2}}$$

$$= 368$$

$$q = 23000 \pm 368(1.6\%)$$

4. Heat Transfer Coefficient

$$U_{TS} = \frac{q}{\Delta T} = \frac{23000}{16} = 1440$$

$$\frac{\partial U_{TS}}{\partial(\Delta T)} = -\frac{q}{\Delta T^2} = -89.8$$

$$\frac{\partial U_{TS}}{\partial q} = \frac{1}{(\Delta T)^2} = 0.0625$$

$$\omega_h = \left[\left(\frac{\partial U_{TS}}{\partial \Delta T}\omega_{\Delta T}\right)^2 + \left(\frac{\partial U_{TS}}{\partial q}\omega_q\right)^2\right]^{\frac{1}{2}}$$

$$= \left[(-89.9*0.2)^2+(0.0625*368)^2\right]^{\frac{1}{2}}$$

$$= 29.2$$

$$U_{TS} = 1440 \pm 29.2(2.02\%)$$

In the case of minimum heat flux, above procedures yielded a ± 5.09 % uncertainty in the heat transfer coefficient.

APPENDIX C

SAMPLE CALCULATION

A sample calculation is given in Appendix B. The conditions used for the calculation are:

Temperatures of the Condenser: T_1 = 44.2, T_2 = 45.2, T_3 = 43.8

Temperature of the Adiabatic Zone: T_4 = 49.5

Temperatures of the Evaporator: T_5 = 56.7, T_6 = 53.2, T_7 = 53.5, T_8 = 53.7, T_9 = 53.9, T_{10} = 55.1

Temperature of the Outside Insulation: T_{11} = 23.5

Current = 228 A

Voltage = 0.556 V

1. Power (Q)

Q = applied power - heat loss to the surrounding

= current * voltage * L_e/L^* (L^* = 0.4 m which is the distance between the embedded leads) - heat loss

= 228 * 0.556 * 0.6/0.4 - 0.164 * (T_6 - T_{11})

= 185 (W)

2. Heat Flux (q)

$$q = Q / A$$

$$= 185 / (\pi * D_i * L_e)$$

$$= 4420 \ (W/m^2)$$

3. Heat Generation Per Unit Volume (q')

$$q' = Q / \text{Volume}$$

$$= 185 / (\pi * (r_o + r_i) * t * L_e)$$

$$= 185 / (7.18 * 10^{-5})$$

$$= 2580000 \ (W/m^3)$$

4. Temperatures (T)

i. Inside Wall Temperature of the Condenser (T_{ci})

$$T_{ci} = T_{co} + \frac{qt}{k}$$

$$= 44.2 + \frac{4420 * 0.0016}{16.3}$$

$$= 44.6$$

ii. Inside Wall Temperature of the Adiabatic Zone (T_{ai})

(assume $h_{sur} = 20 \ W/m^{2o}C$, $T_\infty = 20 \ °C$)

$$T_{ai} = T_{ao} + \frac{h_{sur}(T_{ao} - T_\infty)}{k} t$$

$$= 49.5 + \frac{20 * (49.5 - 20)}{16.3} * 0.0016$$

$$= 49.6$$

iii. Inside Wall Temperature of the Evaporator (T_{ei})

$$T_{ei} = T_{eo} - \frac{q't^2}{2k}$$
$$= 56.7 - \frac{258000 * 0.0016^2}{2 * 16.3}$$
$$= 56.5$$

5. Heat Transfer Coefficients

i. Heat Transfer Coefficient in the Condenser (h_c)

$$h_c = \frac{Q}{A_c * (T_{ai} - T_{ci,ave})}$$
$$= \frac{185}{0.0418 * (49.6 - 44.8)}$$
$$= 921 (W/m^{2o}C)$$

ii. Heat Transfer Coefficient in the Evaporator (h_e)

$$h_e = \frac{Q}{A_e * (T_{ei,ave} - T_{ai})}$$
$$= \frac{185}{0.0418 * (53.9 - 49.6)}$$
$$= 1028 (W/m^{2o}C)$$

iii. Overall Heat Transfer Coefficient (U_{TS})

$$U_{TS} = \frac{Q}{A_e * (T_{ei,ave} - T_{ci,ave})}$$
$$= \frac{185}{0.0418 * (53.9 - 44.8)}$$
$$= 486 (W/m^{2o}C)$$

Table 1.1 Applications

Battery temperature control	Biological
Brakes	Coal Gasification
Cooking pin	Cooling electronic equipment
Cryosurgery	Die casting/molds
Domestic uses	Drying
Electric motors	Energy storage and conversion
Fibre drying	Fluidized beds
Food industry	Fuel preparation
Geothermal	Glass industry
Lasers	Ovens
Plasma torches	Recuperation
Rocket engine cooling	Space
Stirling engine	Solar collectors
Thermal drills	Thermionic applications
Tropical application	Ventilation

Table 2.1 The range of optimum angle (from vertical position)

ref	0	10	20	30	40	50	60	70	80	90
24										
25										
26										
27										
28										
29										
30										
31										
32										
33										
34										
35										

Table 5.1 $X^+ = 0.0$(water), $L^+ = 1$, $V^+ = 0.2$, $\theta = 0°$, $T_{fc} = -10°C$

No	Q	q	$T_{c,ave}$	T_a	$T_{e,ave}$	h_c	h_e	U_{TS}
1	17.5	418	-3.44	11.1	24.9	28.7	30.5	14.8
2	66.0	1580	1.10	15.1	44.8	113	53.3	36.1
3	149	3550	10.1	23.4	39.5	282	434	138
4	247	5890	19.1	29.4	36.2	606	1110	355
5	372	8870	27.8	35.9	40.2	1100	2140	721
6	499	11900	34.9	43.6	48.0	1370	2710	907
7	624	14900	42.0	51.7	56.8	1540	2940	1010
8	808	19300	51.9	61.8	67.0	1960	3670	1280
9	886	21100	58.7	69.4	75.0	1980	3790	1300

Table 5.2 $X^+ = 0.0$(water), $L^+ = 1$, $V^+ = 0.2$, $\theta = 0°$, $T_{fc} = 15°C$

No	Q	q	$T_{c,ave}$	T_a	$T_{e,ave}$	h_c	h_e	U_{TS}
1	15.8	379	16.1	22.7	33.7	57.1	34.5	21.9
2	66.2	1580	20.8	26.7	39.5	275	128	86.2
3	148	3530	25.9	33.1	44.6	463	360	197
4	247	5890	31.7	37.6	42.6	1060	1270	546
5	369	8800	37.6	44.6	48.0	1260	2580	846
6	497	11900	43.5	51.6	55.5	1470	3000	986
7	624	14900	50.0	58.8	63.3	1720	3260	1120
8	808	19300	54.5	67.0	71.9	2020	4000	1340
9	961	22900	63.0	73.9	79.4	2100	4210	1400

Table 5.3 $X^+ = 0.0$(water), $L^+ = 1$, $V^+ = 0.2$, $\theta = 0°$, $T_{fc} = 25°C$

No	Q	q	$T_{c,ave}$	T_a	$T_{e,ave}$	h_c	h_e	U_{TS}
1	14.9	356	26.0	30.2	40.4	85.7	35.8	25.2
2	64.8	1550	30.0	34.3	46.7	382	136	96.5
3	146	3490	34.8	40.7	47.9	631	617	276
4	245	5840	39.8	45.4	48.6	1080	1860	668
5	367	8750	45.4	51.8	55.0	1370	2770	914
6	491	11700	51.0	58.4	62.1	1580	3140	1050
7	622	14800	56.3	64.2	68.3	1870	3620	1180
8	805	19200	63.1	71.9	76.5	2180	4240	1440
9	959	22900	68.3	78.6	83.7	2220	4540	1490

Table 5.4 $X^+ = 0.2$(ethanol), $L^+ = 1$, $V^+ = 0.2$, $\theta = 0°$, $T_{fc} = -10°C$

No	Q	q	$T_{c,ave}$	T_a	$T_{e,ave}$	h_c	h_e	U_{TS}
1	18.5	442	-3.06	6.62	21.3	30.2	36.3	18.2
2	66.5	1590	3.58	10.8	33.4	223	78.6	56.1
3	149	3550	10.8	18.4	36.9	488	213	140
4	248	5920	18.4	27.3	43.8	829	389	239
5	368	8780	28.1	38.1	47.0	884	1000	465
6	495	11800	37.4	48.4	54.9	1077	1810	675
7	626	14900	44.0	57.8	63.2	1090	2760	783
8	808	19000	55.0	68.8	75.1	1400	3080	960
9	956	22800	63.2	78.0	84.9	1540	3310	1050

Table 5.5 $X^+ = 0.2$(ethanol), $L^+ = 1$, $V^+ = 0.2$, $\theta = 0°$, $T_{fc} = 15°C$

No	Q	q	$T_{c,ave}$	T_a	$T_{e,ave}$	h_c	h_e	U_{TS}
1	16.2	388	16.6	19.4	28.3	151	47.2	33.6
2	66.5	1590	21.3	26.0	35.3	368	195	117
3	148	3520	27.3	33.8	40.5	554	529	267
4	244	5830	32.8	40.3	45.3	781	1170	465
5	367	8750	39.6	48.6	53.3	967	1880	638
6	491	11700	45.0	56.0	62.4	1070	1840	671
7	622	14800	52.3	65.9	70.9	1090	2990	798
8	803	19200	61.5	76.7	82.6	1260	3270	911
9	958	22900	68.3	84.5	91.2	1410	3410	999

Table 5.6 $X^+ = 0.4$(ethanol), $L^+ = 1$, $V^+ = 0.2$, $\theta = 0°$, $T_{fc} = -10°C$

No	Q	q	$T_{c,ave}$	T_a	$T_{e,ave}$	h_c	h_e	U_{TS}
1	18.3	437	-2.77	11.5	17.6	30.7	75.1	21.5
2	69.2	1650	4.77	16.5	23.8	141	227	868
3	150	3570	14.4	24.7	30.6	355	634	221
4	248	5930	21.5	32.4	36.5	553	1451	400
5	369	8800	30.0	42.2	46.3	725	2190	543
6	492	11700	39.0	51.0	55.4	982	2640	716
7	624	14900	45.9	58.9	63.7	1140	3090	835
8	806	19200	55.1	69.6	75.1	1330	3470	960

Table 5.7 $X^+ = 0.4$(ethanol), $L^+ = 1$, $V^+ = 0.2$, $\theta = 0°$, $T_{fc} = 15°C$

No	Q	q	$T_{c,ave}$	T_a	$T_{e,ave}$	h_c	h_e	U_{TS}
1	17.5	418	17.1	22.7	25.8	75.9	133	48.3
2	67.6	1610	21.3	27.5	33.3	262	279	135
3	148	3540	27.9	34.0	44.4	585	363	220
4	247	5890	33.3	41.1	47.1	756	981	427
5	367	8750	40.1	50.9	54.6	807	2380	602
6	491	11700	46.4	58.1	62.2	998	2850	739
7	622	14800	51.9	64.8	69.4	1150	3200	847
8	806	19200	57.9	72.6	78.1	1310	3520	954
9	959	22900	62.9	78.9	85.0	1430	3800	1040

Table 5.8 $X^+ = 0.6$(ethanol), $L^+ = 1$, $V^+ = 0.2$, $\theta = 0°$, $T_{fc} = -10°C$

No	Q	q	$T_{c,ave}$	T_a	$T_{e,ave}$	h_c	h_e	U_{TS}
1	18.5	443	-2.99	14.9	18.0	24.7	144	21.1
2	68.8	1640	5.48	19.8	25.6	115	286	81.7
3	150	3580	14.2	26.4	36.7	295	362	162
4	249	5940	23.1	33.2	44.5	595	586	287
5	369	8800	31.2	44.0	48.3	687	2040	513
6	495	11800	38.8	51.4	56.3	928	2490	676
7	625	14900	46.1	61.0	66.3	1000	2820	740
8	806	19200	54.8	70.8	76.8	1200	3240	878
9	959	22900	61.1	78.7	85.1	1300	3560	954

Table 5.9 $X^+ = 0.6$(ethancol), $L^+ = 1$, $V^+ = 0.2$, $\theta = 0°$, $T_{fc} = 15°C$

No	Q	q	$T_{c,ave}$	T_a	$T_{e,ave}$	h_c	h_e	U_{TS}
1	16.8	401	16.5	25.1	27.2	46.9	190	37.4
2	67.7	1620	21.1	28.4	33.8	222	302	128
3	148	3540	27.6	35.2	39.8	475	821	290
4	247	5890	33.0	41.4	46.2	706	1220	447
5	367	8750	39.1	49.9	53.9	813	2150	590
6	491	11700	45.1	56.8	61.4	1000	2550	719
7	622	14800	50.8	64.33	69.4	1100	2940	799
8	807	19200	57.7	73.4	79.2	1230	3310	894
9	956	22800	63.3	80.9	87.3	1300	3570	951

Table 5.10 $X^+ = 0.8$(ethanol), $L^+ = 1$, $V^+ = 0.2$, $\theta = 0°$, $T_{fc} = -10°C$

No	Q	q	$T_{c,ave}$	T_a	$T_{e,ave}$	h_c	h_e	U_{TS}
1	17.7	423	-3.22	20.3	22.2	18.0	237	16.7
2	68.1	1620	3.52	23.8	27.9	80.3	430	67
3	149	3560	12.1	29.9	33.4	200	1020	167
4	248	5920	18.9	33.7	38.2	400	1317	307
5	368	8770	27.8	43.2	48.3	571	1730	430
6	491	11700	36.7	53.5	59.9	697	1830	505
7	622	14800	44.3	60.7	67.5	907	2180	641
8	804	19200	54.7	73.5	81.0	1030	2550	732
9	959	22900	57.5	78.3	87.0	1100	2620	775

Table 5.11 $X^+ = 0.8$(ethanol), $L^+ = 1$, $V^+ = 0.2$, $\theta = 0°$, $T_{fc} = 15°C$

No	Q	q	$T_{c,ave}$	T_a	$T_{e,ave}$	h_c	h_e	U_{TS}
1	16.7	398	15.4	27.8	30.9	32.2	130	25.7
2	66.9	1600	21.3	32.8	41.1	138	193	80.6
3	148	3540	27.5	37.6	43.7	351	610	221
4	246	5880	33.9	44.4	48.7	562	1380	399
5	366	8750	39.1	52.0	56.7	679	1860	498
6	490	11700	46.2	59.7	64.9	871	2230	626
7	621	14800	52.2	67.4	73.8	975	2320	686
8	804	19200	58.8	76.9	84.3	1060	2600	752
9	958	22900	66.7	86.0	94.1	1190	2810	834

Table 5.12 $X^+ = 1.0$(ethanol), $L^+ = 1$, $V^+ = 0.2$, $\theta = 0°$, $T_{fc} = -10°C$

No	Q	q	$T_{c,ave}$	T_a	$T_{e,ave}$	h_c	h_e	U_{TS}
1	16.3	389	-3.73	25.2	31.4	13.4	62.9	11.1
2	65.9	1570	4.92	28.3	46.2	67.6	96.1	39.1
3	148	3540	13.4	33.9	38.2	173	816	142
4	247	5890	21.9	40.5	46.0	316	1090	245
5	367	8750	30.2	47.8	53.8	497	1470	372
6	490	11700	37.4	56.2	63.2	623	1670	454
7	622	14800	43.3	63.0	71.9	756	1670	521
8	804	19200	53.7	75.3	85.9	885	1810	594
9	958	22900	56.0	80.5	92.9	933	1940	630

Table 5.13 $X^+ = 1.0$(ethanol), $L^+ = 1$, $V^+ = 0.2$, $\theta = 0°$, $T_{fc} = 15°C$

No	Q	q	$T_{c,ave}$	T_a	$T_{e,ave}$	h_c	h_e	U_{TS}
1	15.5	371	15.6	31.2	35.7	23.7	82.3	18.4
2	64.9	1550	19.8	35.1	48.7	101	138	54.8
3	147	3510	26.9	41.3	44.1	243	1260	204
4	246	5870	34.0	48.4	53.6	408	1120	299
5	366	8730	40.3	55.1	60.9	591	1490	423
6	490	11700	45.0	61.8	68.5	695	1760	498
7	620	14800	49.2	67.9	76.0	793	1810	552
8	803	19200	58.9	80.32	89.9	896	2000	618
9	956	22800	64.8	88.9	99.1	944	2250	665

Table 5.14 $X^+ = 0.2$(ethyleneglycol), $L^+ = 1$, $V^+ = 0.2$, $\theta = 0°$, $T_{fc} = -10°C$

No	Q	q	$T_{c,ave}$	T_a	$T_{e,ave}$	h_c	h_e	U_{TS}
1	18.9	450	-2.60	12.4	18.6	30.0	72.4	21.1
2	68.3	1630	3.07	16.2	29.4	126	148	62.8
3	149	3550	12.3	22.5	38.7	354	231	137
4	248	5910	21.0	31.6	42.8	562	695	286
5	368	8780	29.9	40.8	46.6	831	1590	535
6	492	11700	36.7	46.7	52.1	1180	2200	764
7	623	14900	44.6	55.5	61.0	1370	2790	910
8	806	19200	51.1	63.6	69.8	1540	3090	1030
9	960	22900	60.0	73.1	79.5	1740	3550	1170

Table 5.15 $X^+=0.2$(ethyleneglycol), $L^+=1$, $V^+=0.2$, $\theta=0^o$, $T_{fc}=15°C$

No	Q	q	$T_{c,ave}$	T_a	$T_{e,ave}$	h_c	h_e	U_{TS}
1	17.1	408	16.2	22.9	26.0	61.3	138	41.9
2	66.8	1600	21.4	27.9	34.3	249	283	126
3	148	3530	27.6	34.3	43.1	536	447	237
4	247	5900	33.1	39.7	45.7	902	1070	474
5	367	8760	39.1	47.4	51.7	1070	2070	699
6	491	11700	45.2	54.4	58.8	1270	2680	861
7	623	14900	49.4	59.9	64.8	1420	3000	964
8	805	19200	57.1	68.4	74.0	1700	3420	1140
9	959	22900	61.6	75.0	81.0	1710	3770	1180

Table 5.16 $X^+=0.6$(ethyleneglycol), $L^+=1$, $V^+=0.6$, $\theta=0^o$, $T_{fc}=-10°C$

No	Q	q	$T_{c,ave}$	T_a	$T_{e,ave}$	h_c	h_e	U_{TS}
1	16.7	398	-2.91	11.23	32.3	28.2	18.9	11.3
2	66.3	1580	2.70	16.3	42.3	117	79.4	43.3
3	147	3520	9.98	23.9	49.1	256	153	93.4
4	247	5880	17.9	33.7	53.2	382	379	176
5	367	8770	26.4	40.7	51.0	619	864	356
6	491	11700	33.6	49.0	57.5	766	1380	492
7	622	14900	40.9	57.3	66.8	910	1550	573
8	805	19200	49.4	66.8	77.1	1110	1860	694
9	958	22900	58.1	77.5	88.8	1180	2020	744

Table 5.17 $X^+ = 0.6$(ethyleneglycol), $L^+ = 1$, $V^+ = 0.2$, $\theta = 0^o$, $T_{fc} = 15°C$

No	Q	q	$T_{c,ave}$	T_a	$T_{e,ave}$	h_c	h_e	U_{TS}
1	16.6	395	16.4	21.2	29.3	83.5	48.4	30.7
2	66.6	1590	21.2	29.4	37.2	201	222	101
3	147	3500	26.1	34.3	52.5	436	210	137
4	246	5870	31.8	43.8	55.5	509	522	249
5	367	8750	38.5	50.1	56.9	756	1280	475
6	490	11700	45.1	57.8	65.6	922	1510	572
7	621	14800	50.9	65.4	73.5	1030	1820	658
8	804	19200	56.8	73.8	83.5	1130	1970	717
9	958	22900	61.6	80.5	91.4	1210	2100	769

Table 5.18 $X^+ = 0.8$(ethyleneglycol), $L^+ = 1$, $V^+ = 0.2$, $\theta = 0^o$, $T_{fc} = -10°C$

No	Q	q	$T_{c,ave}$	T_a	$T_{e,ave}$	h_c	h_e	U_{TS}
1	17.3	412	-1.75	15.1	29.5	24.6	29.1	13.2
2	67.2	1610	4.30	20.0	35.9	102	102	50.9
3	148	3540	9.98	26.0	45.5	222	182	99.9
4	247	5890	18.3	35.6	54.2	344	341	167
5	367	8760	26.4	43.1	52.9	524	896	330
6	491	11700	33.9	52.3	62.8	637	1110	405
7	622	14800	41.9	60.9	72.3	783	1310	489
8	804	19200	52.4	73.1	86.1	923	1480	568
9	957	22900	57.5	80.7	95.3	988	1560	605

Table 5.19 $X^+ = 0.8$(ethyleneglycol), $L^+ = 1$, $V^+ = 0.2$, $\theta = 0^o$, $T_{fc} = 15°C$

No	Q	q	$T_{c,ave}$	T_a	$T_{e,ave}$	h_c	h_e	U_{TS}
1	15.6	372	16.9	22.5	29.5	26.4	32.2	16.1
2	65.1	1550	21.9	30.9	49.5	180	93.2	57.7
3	147	3500	27.3	38.9	56.2	308	213	123
4	246	5860	31.6	45.2	58.6	436	457	218
5	366	8730	38.5	52.3	61.1	634	1000	388
6	489	11700	44.9	62.3	70.9	675	1350	450
7	620	14800	50.5	70.4	80.6	751	1450	492
8	803	19100	56.9	78.1	90.5	906	1550	572
9	957	22800	61.5	84.3	98.1	1000	1670	625

Table 5.20 $X^+ = 0.9$(ethyleneglycol), $L^+ = 1$, $V^+ = 0.2$, $\theta = 0^o$, $T_{fc} = -10°C$

No	Q	q	$T_{c,ave}$	T_a	$T_{e,ave}$	h_c	h_e	U_{TS}
1	10.3	247	-3.28	10.9	68.1	17.4	4.30	3.50
2	61.1	1460	2.71	20.8	76.5	84.1	28.9	20.2
3	143	3420	10.8	33.1	78.9	156	77.6	50.7
4	243	5790	17.4	42.3	82.6	238	146	89.0
5	364	8710	25.8	50.4	68.9	355	470	202
6	488	11600	32.6	63.7	81.6	375	651	238
7	618	14800	39.3	71.6	94.0	456	661	270
8	800	19100	46.9	81.0	109	561	693	310
9	951	22800	56.3	90.0	120	674	746	354

Table 5.21 $X^+ = 0.9$(ethyleneglycol), $L^+ = 1$, $V^+ = 0.2$, $\theta = 0^o$, $T_{fc} = 15°C$

No	Q	q	$T_{c,ave}$	T_a	$T_{e,ave}$	h_c	h_e	U_{TS}
1	10.5	252	17.9	21.2	70.8	77.0	5.14	4.80
2	61.7	1470	21.3	31.9	75.9	146	34.2	27.2
3	143	3410	25.9	43.0	83.1	206	87.5	60.0
4	241	5770	31.0	50.2	86.1	309	161	105
5	364	8690	38.4	57.8	74.7	443	518	238
6	486	11600	44.0	73.5	89.7	394	717	254
7	617	14700	49.4	82.6	102	445	746	279
8	799	19100	56.2	89.7	115	574	754	326
9	953	22700	59.8	95.0	124	645	779	353

Table 5.22 $X^+ = 0.2$(glycerol), $L^+ = 1$, $V^+ = 0.2$, $\theta = 0^o$, $T_{fc} = -10°C$

No	Q	q	$T_{c,ave}$	T_a	$T_{e,ave}$	h_c	h_e	U_{TS}
1	15.2	362	-0.68	11.3	30.9	29.7	25.1	9.73
2	67.7	1620	4.14	14.6	28.3	156	124	68.3
3	150	3570	9.46	19.8	34.5	357	362	161
4	248	5930	19.1	29.5	39.9	626	811	310
5	368	8790	26.1	37.1	44.0	839	1400	511
6	492	11800	34.7	45.4	51.0	1100	2090	722
7	623	14900	42.3	53.8	60.1	1290	2380	837
8	806	19200	52.1	64.9	71.3	1510	3010	1000
9	960	22900	59.0	72.9	79.7	1650	3360	1110

Table 5.23 $X^+ = 0.2$(glycerol), $L^+ = 1$, $V^+ = 0.2$, $\theta = 0^o$, $T_{fc} = 15°C$

No	Q	q	$T_{c,ave}$	T_a	$T_{e,ave}$	h_c	h_e	U_{TS}
1	17.0	406	16.4	22.2	26.7	69.2	99.0	39.7
2	66.7	1590	20.8	26.4	35.8	298	221	111
3	149	3550	27.4	33.4	39.5	602	586	294
4	247	5900	33.8	41.3	46.9	818	1140	455
5	367	8760	39.4	48.3	52.7	985	2000	658
6	491	11700	45.3	55.0	15.3	1140	2350	768
7	622	14900	50.9	61.5	66.7	1400	2860	940
8	805	19200	57.1	69.7	75.7	1520	3200	1030
9	959	22900	62.5	76.1	82.6	1680	3500	1140

Table 5.24 $X^+ = 0.6$(glycerol), $L^+ = 1$, $V^+ = 0.2$, $\theta = 0^o$, $T_{fc} = 15°C$

No	Q	q	$T_{c,ave}$	T_a	$T_{e,ave}$	h_c	h_e	U_{TS}
1	16.8	402	17.3	19.3	27.4	201	49.5	39.7
2	66.2	1580	21.3	25.2	38.88	490	135	94
3	147	3510	27.2	33.6	49.6	594	271	169
4	246	5880	33.6	41.6	51.6	748	599	327
5	366	8730	39.1	50.1	61.1	792	817	398
6	490	11700	44.8	58.3	69.5	871	1070	475
7	621	14800	50.5	66.1	75.8	948	1520	584
8	803	19200	57.1	75.0	86.6	1070	1660	650

Table 5.25 $X^+ = 0.8$(glycerol), $L^+ = 1$, $V^+ = 0.2$, $\theta = 0°$, $T_{fc} = -10°C$

No	Q	q	$T_{c,ave}$	T_a	$T_{c,ave}$	h_c	h_e	U_{TS}
1	15.8	377	0.85	6.86	36.3	71.8	13.3	10.76
2	67.6	1620	6.11	18.1	49.9	140	51.3	37
3	146	3490	12.8	27.7	54.4	239	133	84.1
4	253	6040	23.7	41.2	56.7	346	391	183
5	371	8860	30.8	50.0	66.4	461	542	249
6	485	11600	33.0	54.4	74.6	541	572	278
7	602	14400	38.1	63.9	85.6	558	662	303
8	778	18600	44.7	75.2	98.3	610	806	347
9	937	22400	48.1	83.0	108	642	884	372

Table 5.26 $X^+ = 0.8$(glycerol), $L^+ = 1$, $V^+ = 0.2$, $\theta = 0°$, $T_{fc} = 15°C$

No	Q	q	$T_{c,ave}$	T_a	$T_{c,ave}$	h_c	h_e	U_{TS}
1	15.8	378	18.0	19.1	38.7	355	19.3	18.3
2	65.0	1550	21.9	26.5	48.9	410	70.1	57.5
3	140	3340	27.2	39.8	55.5	274	225	119
4	250	5970	33.3	51.1	63.8	337	470	196
5	363	8670	39.4	59.8	73.4	424	637	255
6	485	11600	44.4	65.9	82.5	537	699	304
7	614	14700	49.5	73.5	92.0	609	794	345
8	791	18900	55.3	83.5	104	615	907	386
9	936	22400	61.1	90.3	113	766	983	431

Table 5.27 $X^+ = 0.0$(water), $L^+ = 1$, $V^+ = 0.2$, $\theta = 0°$

No	Q	q	$T_{c,ave}$	T_a	$T_{c,ave}$	h_c	h_e	U_{TS}
1	367	8760	43.5	51.1	54.5	1150	2600	797
2	367	8750	50.0	56.2	59.3	1400	2790	933
3	367	8770	56.3	61.6	64.4	1670	3110	1090
4	367	8750	60.4	65.3	67.9	1790	3310	1160
5	619	14800	42.6	54.2	58.7	1280	3220	917
6	617	14700	48.1	58.5	62.8	1440	3410	1010
7	617	14700	53.5	62.9	66.7	1570	3690	1100
8	619	14800	58.2	66.6	70.6	1760	3760	1200
9	901	21500	39.3	55.8	60.6	1310	4430	1010
10	901	21500	46.5	60.3	65.6	1550	4110	1130
11	901	21500	52.1	65.3	70.3	1620	4310	1180
12	900	21500	60.4	72.4	76.7	1800	4910	1320

Table 5.28 $X^+ = 0.2$(ethanol), $L^+ = 1$, $V^+ = 0.2$, $\theta = 0°$, $Q = 758w$

No	T_{fc}	$T_{c,ave}$	T_a	$T_{c,ave}$	h_c	h_e	U_{TS}
1	-17.5	30.5	50.0	56.8	931	2650	689
2	-15	31.8	50.9	57.7	952	2650	700
3	-10	32.7	50.9	57.8	989	2600	716
4	-5	32.9	51.0	57.8	999	2600	724

Table 5.29 $X^+ = 0.0$(water), $L^+ = 1$, $V^+ = 0.2$, $T_a = 58.4°C$, $Q = 623W$

No	θ	$T_{c,ave}$	$T_{e,ave}$	h_c	h_e	U_{TS}
1	0	49.0	62.5	1580	3640	1100
2	15	49.9	61.8	1770	4280	1220
3	30	49.8	61.8	1710	4500	1270
4	45	50.1	61.4	1800	4920	1320
5	50	50.6	61.5	1900	4790	1360
6	55	50.8	61.6	1920	4890	1380
7	60	50.6	61.4	1890	5090	1390
8	65	50.3	61.4	1830	5130	1350
9	75	50.2	61.3	1800	5280	1330
10	85	49.3	61.1	1640	5580	1270

Table 5.30 $X^+ = 0.0$(water), $L^+ = 1$, $V^+ = 0.2$, $T_a = 53.3°C$, $Q = 492W$

No	θ	$T_{c,ave}$	$T_{e,ave}$	h_c	h_e	U_{TS}
1	0	44.7	57.1	1390	2950	947
2	15	45.6	56.2	1540	3850	1100
3	30	45.5	55.8	1570	4210	1140
4	45	46.1	55.5	1670	4920	1250
5	55	46.6	56.0	1700	4740	1250
6	60	45.5	55.2	1650	5160	1250
7	65	45.8	55.4	1610	5400	1240
8	75	45.1	55.1	1500	5710	1190
9	85	45.3	55.4	1470	5620	1170

Table 5.31 $X^+ = 1.0$(ethanol), $L^+ = 1$, $V^+ = 0.2$, $T_a = 58.4°C$, $Q = 622W$

No	θ	$T_{c,ave}$	$T_{e,ave}$	h_c	h_e	U_{TS}
1	0	33.6	67.6	600	1600	436
2	15	37.1	65.9	701	1940	515
3	30	38.1	65.8	742	1940	536
4	45	38.4	65.8	748	1950	541
5	50	39.2	66.1	777	1920	553
6	55	39.5	66.2	789	1890	556
7	60	39.7	66.3	798	1870	558
8	65	39.7	66.6	802	1790	553
9	75	39.8	66.9	799	1730	547
10	85	38.0	68.2	731	1490	490

Table 5.32 $X^+ = 1.0$(ethanol), $L^+ = 1$, $V^+ = 0.2$, $T_a = 53.3°C$, $Q = 491W$

No	θ	$T_{c,ave}$	$T_{e,ave}$	h_c	h_e	U_{TS}
1	0	31.9	60.6	547	1630	409
2	15	33.2	59.7	582	1830	441
3	30	33.3	59.7	588	1840	446
4	45	34.7	59.7	629	1840	469
5	50	34.8	59.7	635	1820	471
6	55	34.4	59.7	622	1810	463
7	60	34.7	60.0	631	1750	464
8	65	34.6	60.1	628	1710	460
9	75	34.9	60.5	637	1640	459
10	85	34.0	59.9	610	1740	452

Table 5.33 $X^+=0.2$(ethanol), $L^+=1$, $V^+=0.2$, $T_a=58.4°C$, $Q=623W$

No	θ	$T_{c,ave}$	$T_{e,ave}$	h_c	h_e	U_{TS}
1	0	44.8	63.9	1100	2690	782
2	15	46.2	64.5	1260	2320	813
3	22.5	44.3	62.6	1070	3400	813
4	30	42.3	62.2	929	3860	749
5	45	44.7	62.2	1080	4070	852
6	60	45.0	62.2	1100	4070	863
7	75	44.7	62.8	1080	3540	825
8	85	43.6	65.3	1010	2180	688

Table 5.34 $X^+=0.2$(ethanol), $L^+=1$, $V^+=0.2$, $T_a=53.3°C$, $Q=493W$

No	θ	$T_{c,ave}$	$T_{e,ave}$	h_c	h_e	U_{TS}
1	0	42.5	60.4	1150	1550	658
2	15	39.8	57.3	867	3000	672
3	30	39.8	57.6	871	2790	663
4	45	40.2	57.1	887	3290	699
5	60	40.1	56.6	881	3690	711
6	75	40.5	56.6	915	3690	733
7	85	40.1	58.8	876	2230	627

Table 5.35 $X^+ = 0.4$(ethanol), $L^+ = 1$, $V^+ = 0.2$, $T_a = 58.4°C$, $Q = 624W$

No	θ	$T_{c,ave}$	$T_{e,ave}$	h_c	h_e	U_{TS}
1	0	43.8	63.4	1020	3030	763
2	15	45.7	62.5	1160	3680	884
3	30	43.9	61.9	1030	4260	829
4	45	46.0	61.9	1190	4290	933
5	50	46.6	61.9	1260	4230	970
6	55	46.7	62.0	1270	4200	976
7	60	46.9	62.1	1280	4050	972
8	65	46.6	62.4	1260	3720	944
9	75	46.5	63.1	1260	3130	900
10	85	45.5	63.3	1170	2930	836

Table 5.36 $X^+ = 0.4$(ethanol), $L^+ = 1$, $V^+ = 0.2$, $T_a = 53.3°C$, $Q = 491W$

No	θ	$T_{c,ave}$	$T_{e,ave}$	h_c	h_e	U_{TS}
1	0	42.3	57.5	1070	2800	774
2	15	41.5	56.9	1000	3260	766
3	30	41.1	56.4	966	3760	768
4	45	42.1	56.6	1050	3600	813
5	50	42.2	56.6	1050	3590	813
6	55	42.7	56.7	1100	3540	837
7	60	42.6	56.7	1100	3470	833
8	65	42.9	57.1	1120	3120	822
9	75	42.6	57.4	1110	2880	794
10	85	42.1	57.6	1040	2750	755

Table 5.37 $X^+ = 0.6$(ethanol), $L^+ = 1$, $V^+ = 0.2$, $T_a = 58.4°C$, $Q = 623W$

No	θ	$T_{c,ave}$	$T_{e,ave}$	h_c	h_e	U_{TS}
1	0	43.5	64.0	1010	2560	727
2	15	43.4	63.1	967	3150	757
3	30	45.0	62.9	1110	3280	831
4	45	47.3	62.7	1340	3410	963
5	50	47.4	62.8	1356	3390	969
6	55	47.7	62.9	1390	3400	985
7	60	47.5	62.9	1360	3290	963
8	65	47.1	63.0	1330	3150	935
9	75	47.1	63.7	1320	2820	899
10	85	45.9	63.9	1180	2710	824

Table 5.38 $X^+ = 0.6$(ethanol), $L^+ = 1$, $V^+ = 0.2$, $T_a = 53.3°C$, $Q = 491W$

No	θ	$T_{c,ave}$	$T_{e,ave}$	h_c	h_e	U_{TS}
1	0	38.6	58.1	791	2530	603
2	15	41.1	57.5	953	2860	715
3	30	42.2	57.3	1040	3050	777
4	45	42.6	57.3	1080	3060	798
5	55	42.9	57.3	1110	3040	813
6	60	42.9	57.4	1110	2960	809
7	65	42.8	57.7	1100	2800	791
8	75	42.8	58.2	1090	2500	761
9	85	43.2	58.6	1150	2260	760

Table 5.39 $X^+ = 0.8$(ethanol), $L^+ = 1$, $V^+ = 0.2$, $T_a = 58.4°C$, $Q = 623W$

No	θ	$T_{c,ave}$	$T_{e,ave}$	h_c	h_e	U_{TS}
1	0	39.9	65.9	804	1980	571
2	15	41.1	64.2	868	2510	645
3	30	40.0	64.1	817	2606	620
4	45	43.6	64.2	1000	2540	720
5	50	44.5	64.4	1070	2490	750
6	55	45.3	64.4	1140	2460	778
7	60	45.3	64.5	1140	2410	774
8	65	45.5	64.8	1160	2320	771
9	75	45.4	65.2	1140	2190	751
10	85	42.4	64.7	923	2400	666

Table 5.40 $X^+ = 0.8$(ethanol), $L^+ = 1$, $V^+ = 0.2$, $T_a = 53.3°C$, $Q = 491W$

No	θ	$T_{c,ave}$	$T_{e,ave}$	h_c	h_e	U_{TS}
1	0	35.5	59.5	659	1890	488
2	15	37.4	58.4	738	2300	558
3	30	38.3	58.3	781	2350	586
4	45	39.5	58.3	852	2340	625
5	50	39.8	58.3	872	2310	633
6	55	40.0	58.4	871	2300	632
7	60	41.3	58.5	900	2250	643
8	65	40.5	58.7	915	2160	643
9	75	39.2	58.8	836	2100	598
10	85	38.7	58.9	799	2100	578

Table 5.41 $X^+ = 0.2$(ethyleneglycol), $L^+ = 1$, $V^+ = 0.2$, $T_a = 58.4°C$, $Q = 623W$

No	θ	$T_{c,ave}$	$T_{c,ave}$	h_c	h_e	U_{TS}
1	0	47.3	63.8	1340	2840	910
2	15	47.4	62.6	1360	3600	988
3	30	48.6	62.2	1530	3860	1090
4	45	49.3	62.1	1640	3970	1160
5	50	49.4	62.0	1670	4140	1190
6	55	49.5	61.9	1680	4170	1200
7	60	49.5	61.9	1680	4240	1200
8	65	49.4	61.9	1660	4190	1190
9	75	49.1	62.0	1590	4210	1150
10	85	48.6	63.1	1510	3200	1030

Table 5.42 $X^+ = 0.6$(ethyleneglycol), $L^+ = 1$, $V^+ = 0.2$, $T_a = 58.4°C$, $Q = 623W$

No	θ	$T_{c,ave}$	$T_{e,ave}$	h_c	h_e	U_{TS}
1	0	41.8	67.6	893	1620	575
2	15	42.3	65.4	923	2110	642
3	30	42.2	65.1	922	2180	648
4	45	43.5	65.0	988	2220	689
5	50	43.9	65.2	1020	2210	699
6	55	44.5	65.1	1070	2230	724
7	60	44.4	65.0	1070	2230	724
8	65	44.4	65.4	1050	2160	708
9	75	43.3	65.8	998	1990	665
10	85	42.3	67.9	925	1570	582

Table 5.43 $X^+ = 0.8$(ethyleneglycol), $L^+ = 1$, $V^+ = 0.2$, $T_a = 58.4°C$, $Q = 623W$

No	θ	$T_{c,ave}$	$T_{e,ave}$	h_c	h_e	U_{TS}
1	0	38.1	69.9	729	1300	466
2	15	35.9	66.9	662	1690	480
3	30	37.4	66.8	698	1830	505
4	45	38.1	66.7	729	1810	520
5	50	38.5	66.5	751	1800	530
6	55	38.3	67.1	733	1760	517
7	60	38.2	67.0	735	1750	517
8	75	38.2	67.9	732	1580	500
9	85	36.7	72.3	678	1080	416

Table 5.44 $X^+ = 0.2$(glycerol), $L^+ = 1$, $V^+ = 0.2$, $T_a = 58.4°C$, $Q = 623W$

No	θ	$T_{c,ave}$	$T_{e,ave}$	h_c	h_e	U_{TS}
1	0	46.8	64.3	1290	2500	848
2	15	47.5	62.8	1360	3390	969
3	30	48.2	62.7	1440	3590	1030
4	45	48.7	62.4	1540	3740	1090
5	50	49.0	62.3	1580	3880	1120
6	55	49.1	62.4	1580	3880	1120
7	60	48.9	62.2	1570	3950	1130
8	65	49.1	62.2	1610	3950	1140
9	70	48.7	62.1	1540	4010	1110
10	85	48.3	62.1	1480	3960	1080

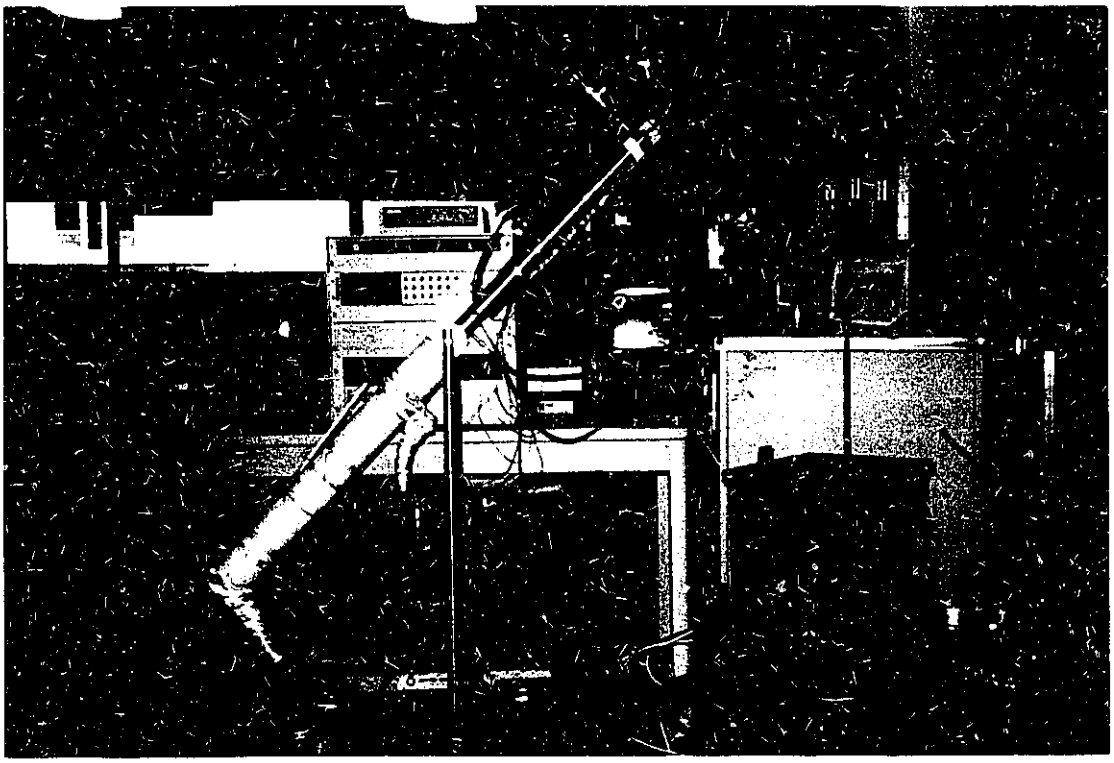

Figure 3.1 Experimental Set-up

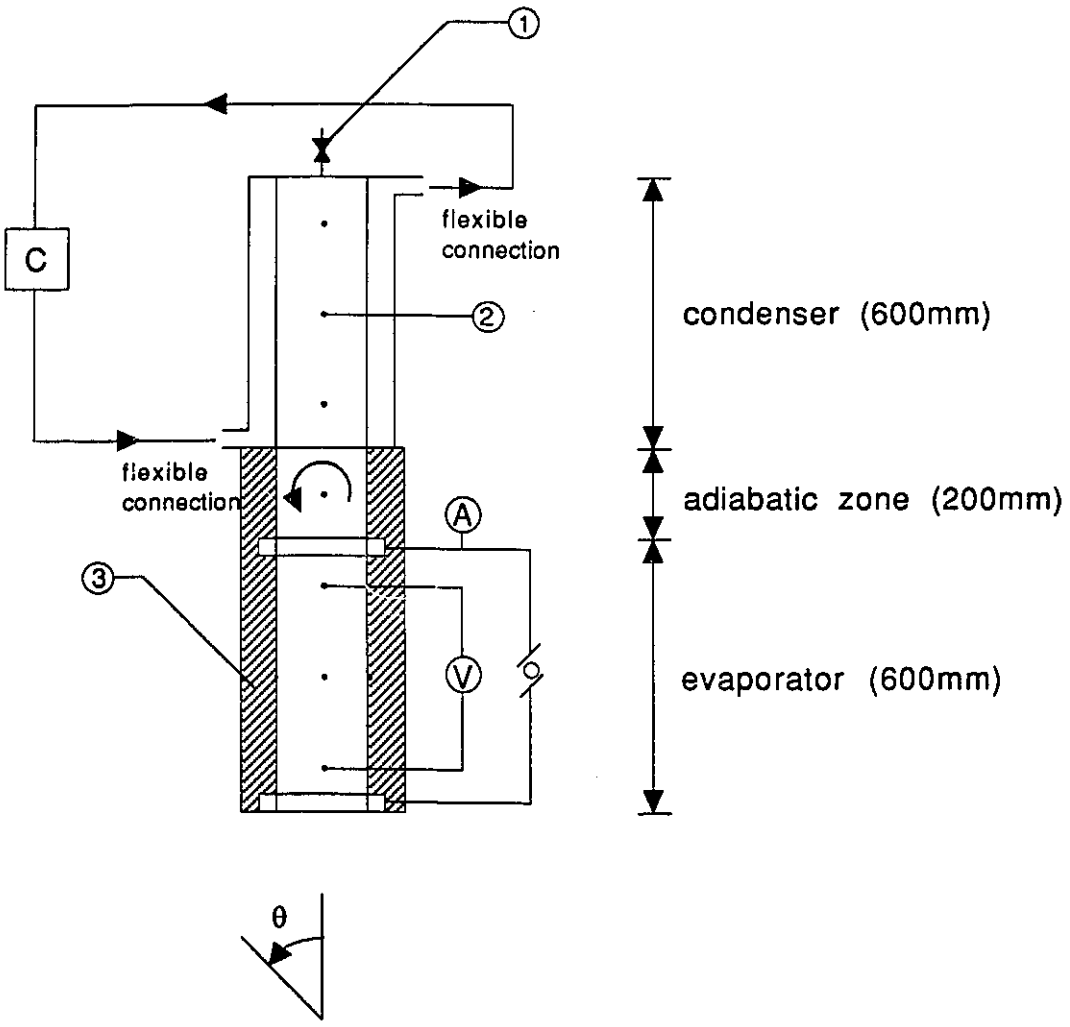

1. vacuum valve 2. thermocouples 3. insulation
Ⓥ voltmeter Ⓐ amperemeter [C] cooling system

Figure 3.2 Schematic Diagram of Experimental Apparatus

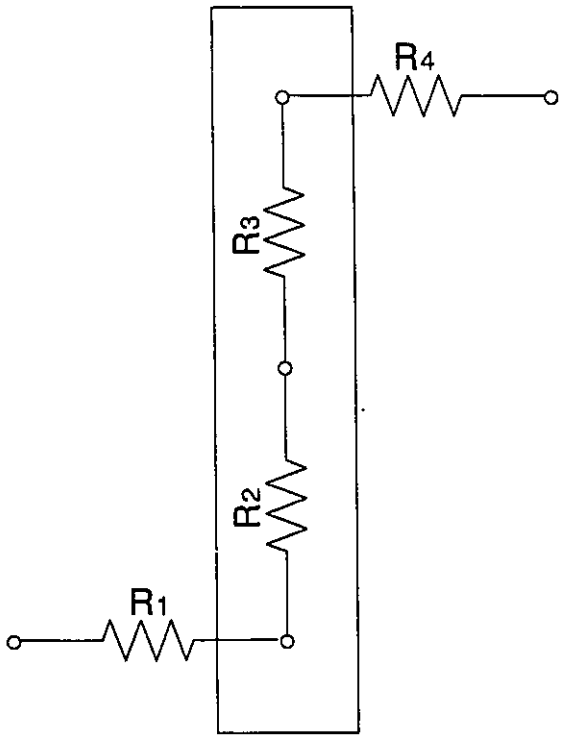

$$R_1 = 1/h_1A_1$$

$$R_2 = 1/h_eA_e$$

$$R_3 = 1/h_cA_c$$

$$R_4 = 1/h_4A_4$$

$$R_{TS} = R_2 + R_3$$

$$= 1/U_{TS}$$

Figure 3.3 Conductance Model

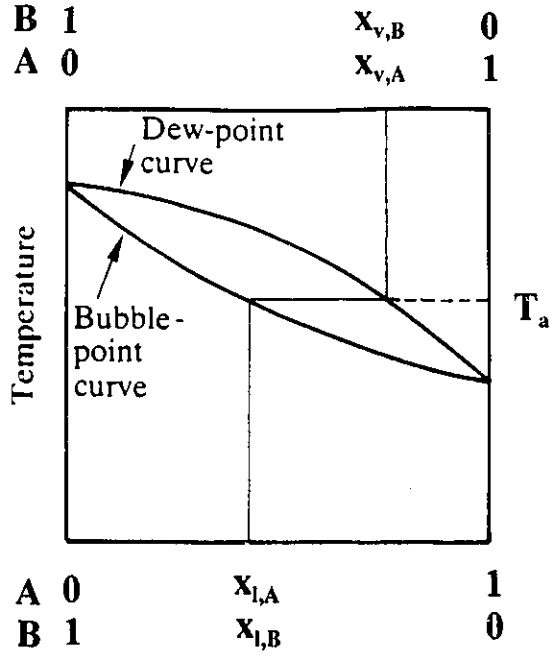

Figure 4.1(a) Phase Diagram for a Normal Mixture

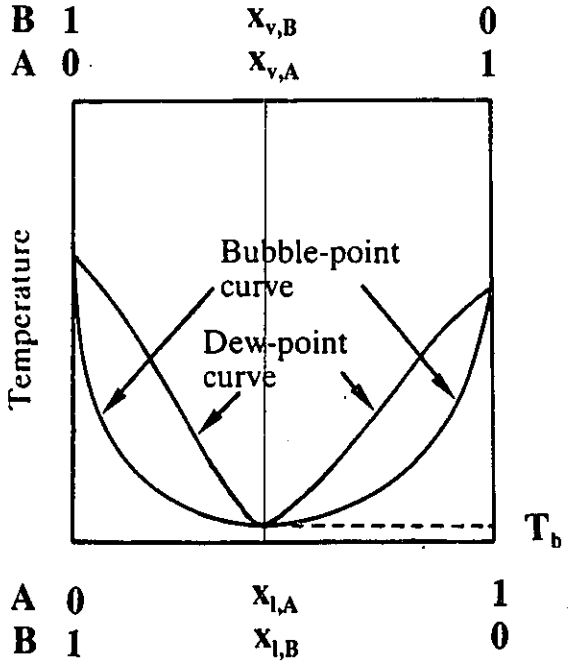

Figure 4.1(b) Phase Diagram for a Azeotrope

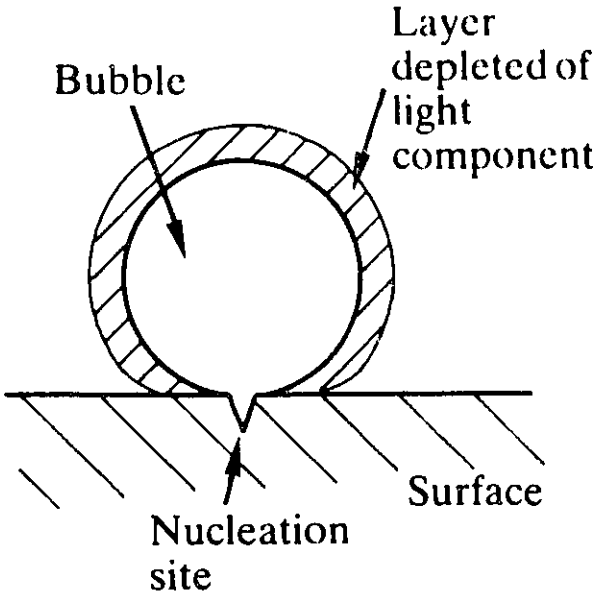

Figure 5.1 Model of the Reduction in Heat Transfer to a Bubble in a Mixture

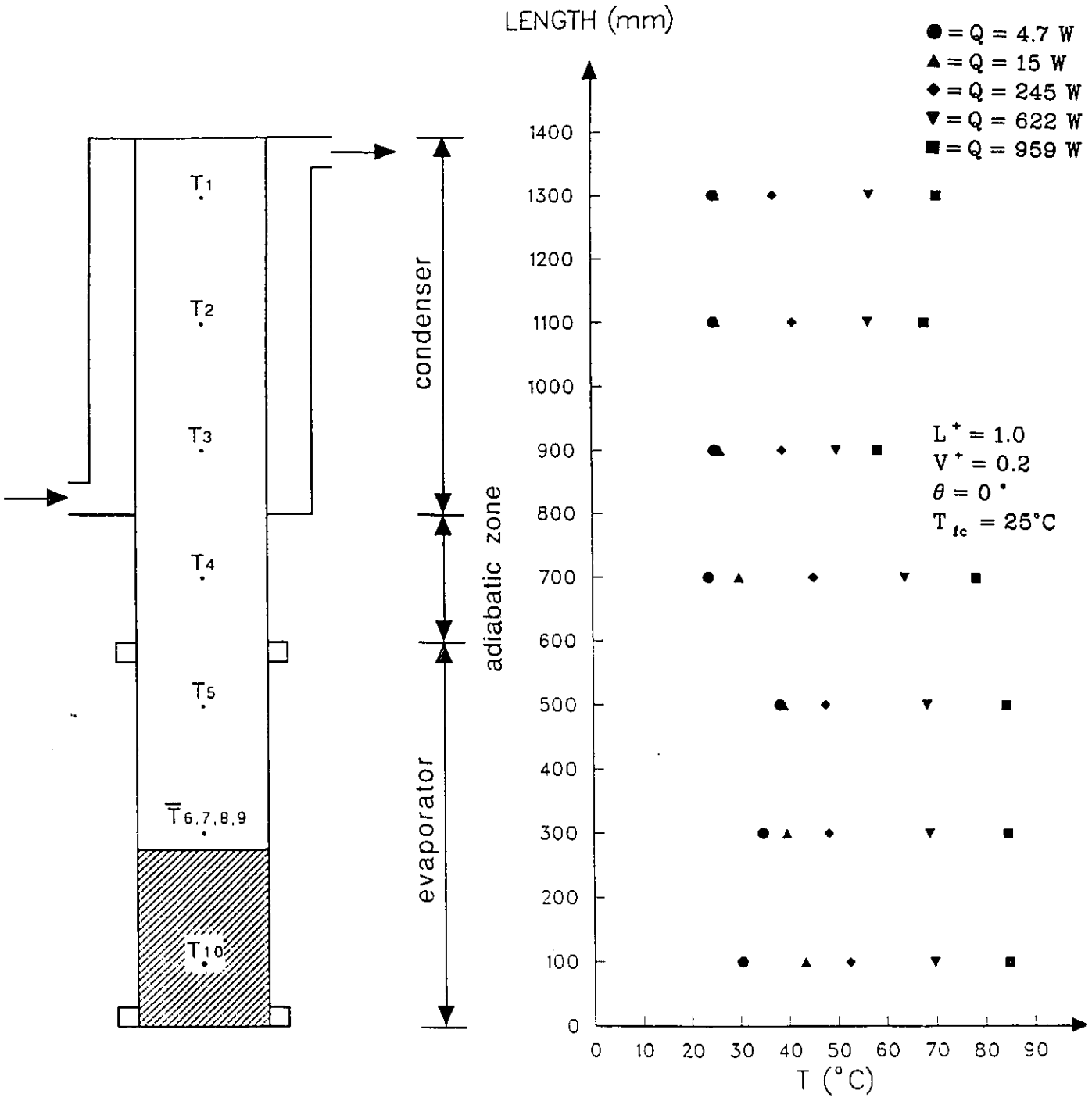

Figure 5.2 Temperature Distributions along the Length of Thermosyphon

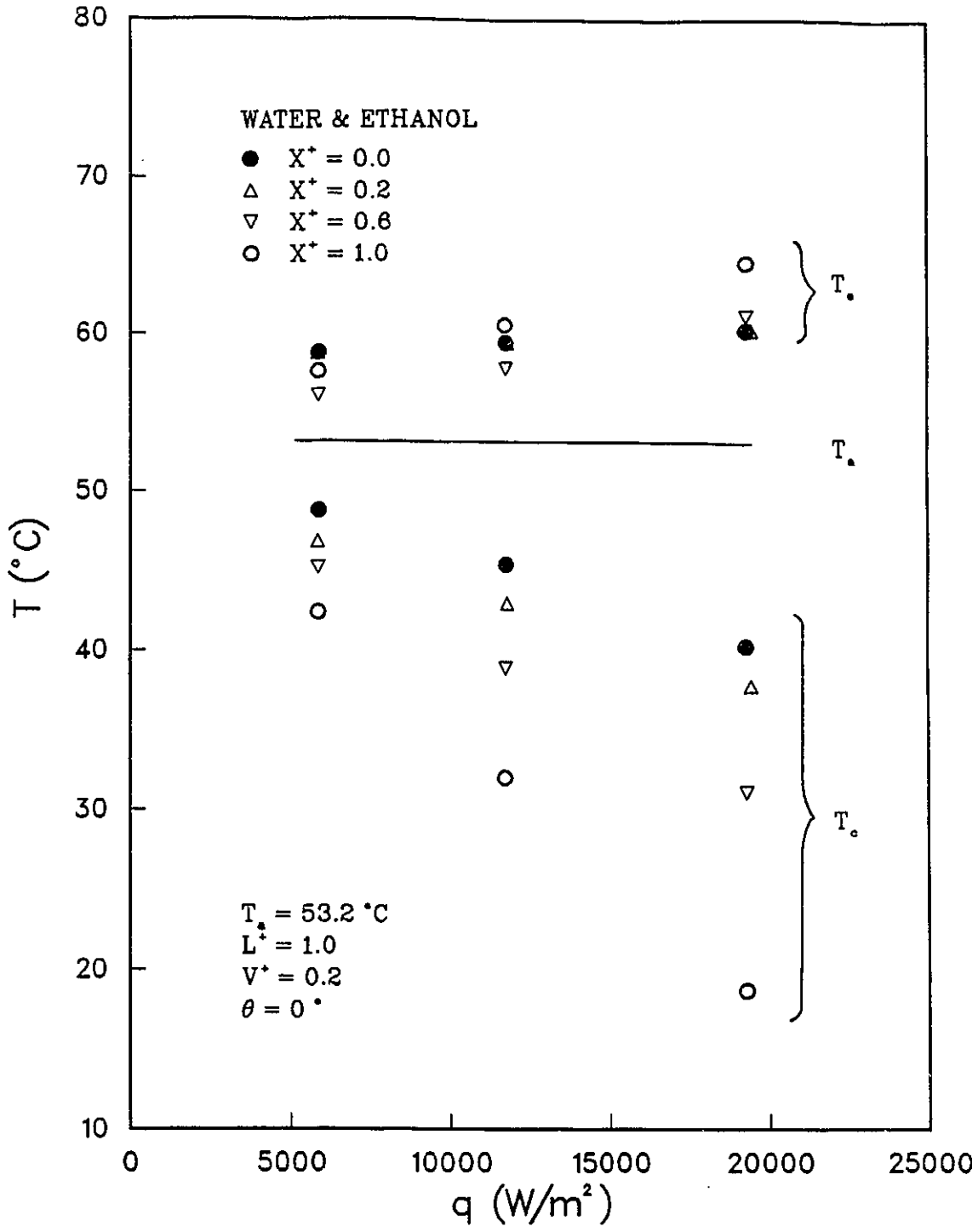

Figure 5.3 Temperature Distributions of Mixture at Constant Heat Flux

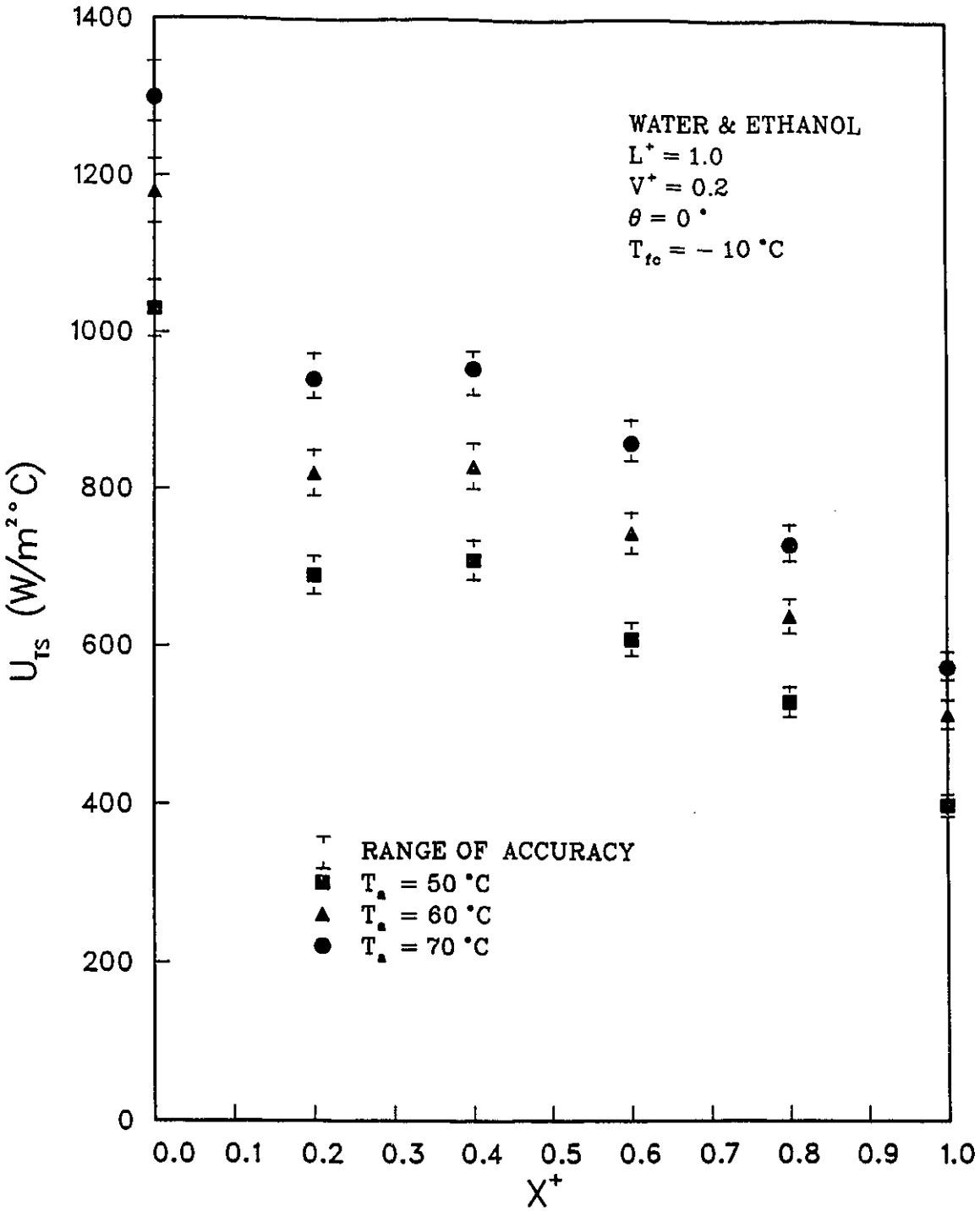

Figure 5.4(a) Effect of X^+ on U_{TS} (water-ethanol; T_{fc} = -10 °C)

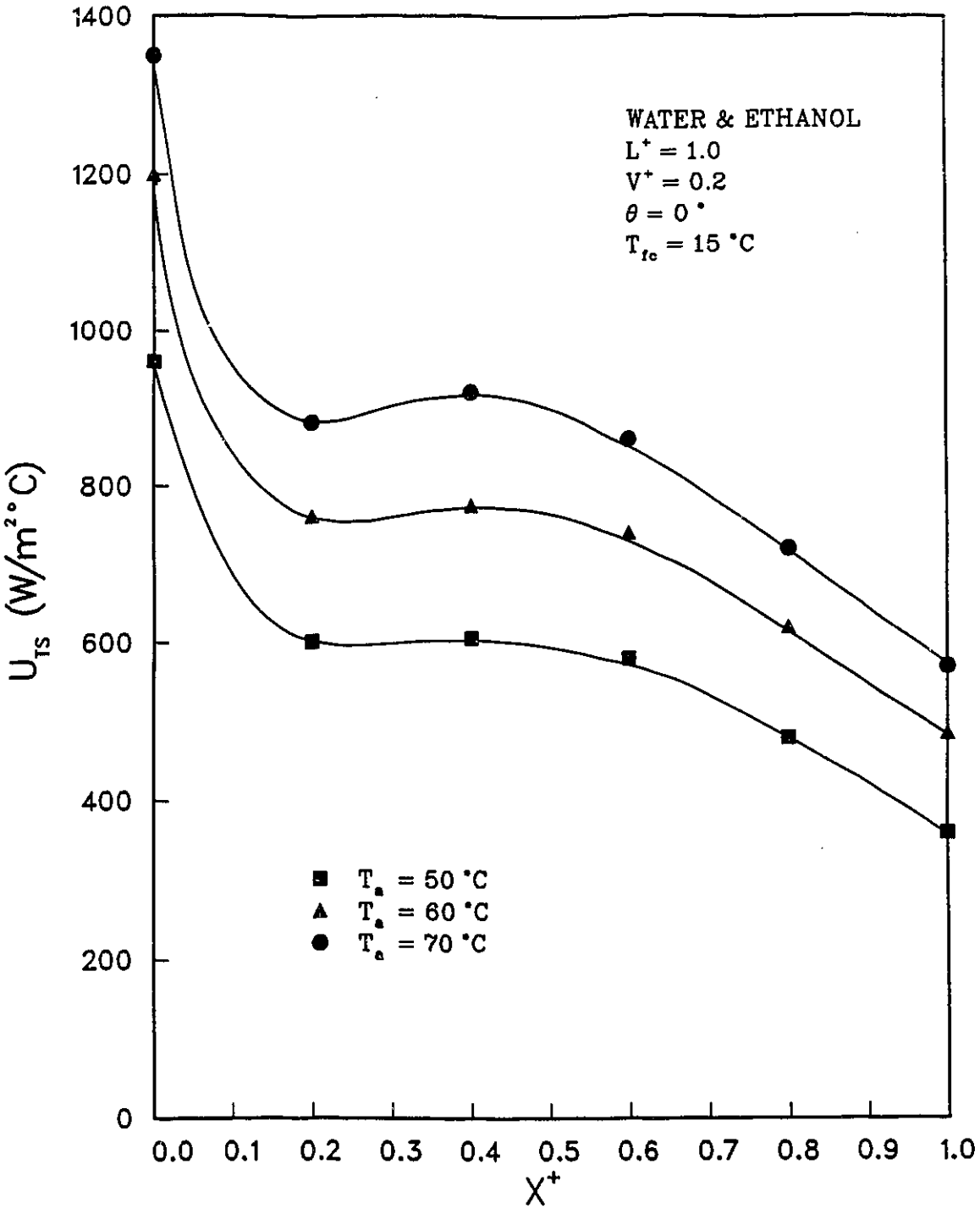

Figure 5.4(b) Effect of X^+ on U_{TS} (water-ethanol; T_{fc} = 15 °C)

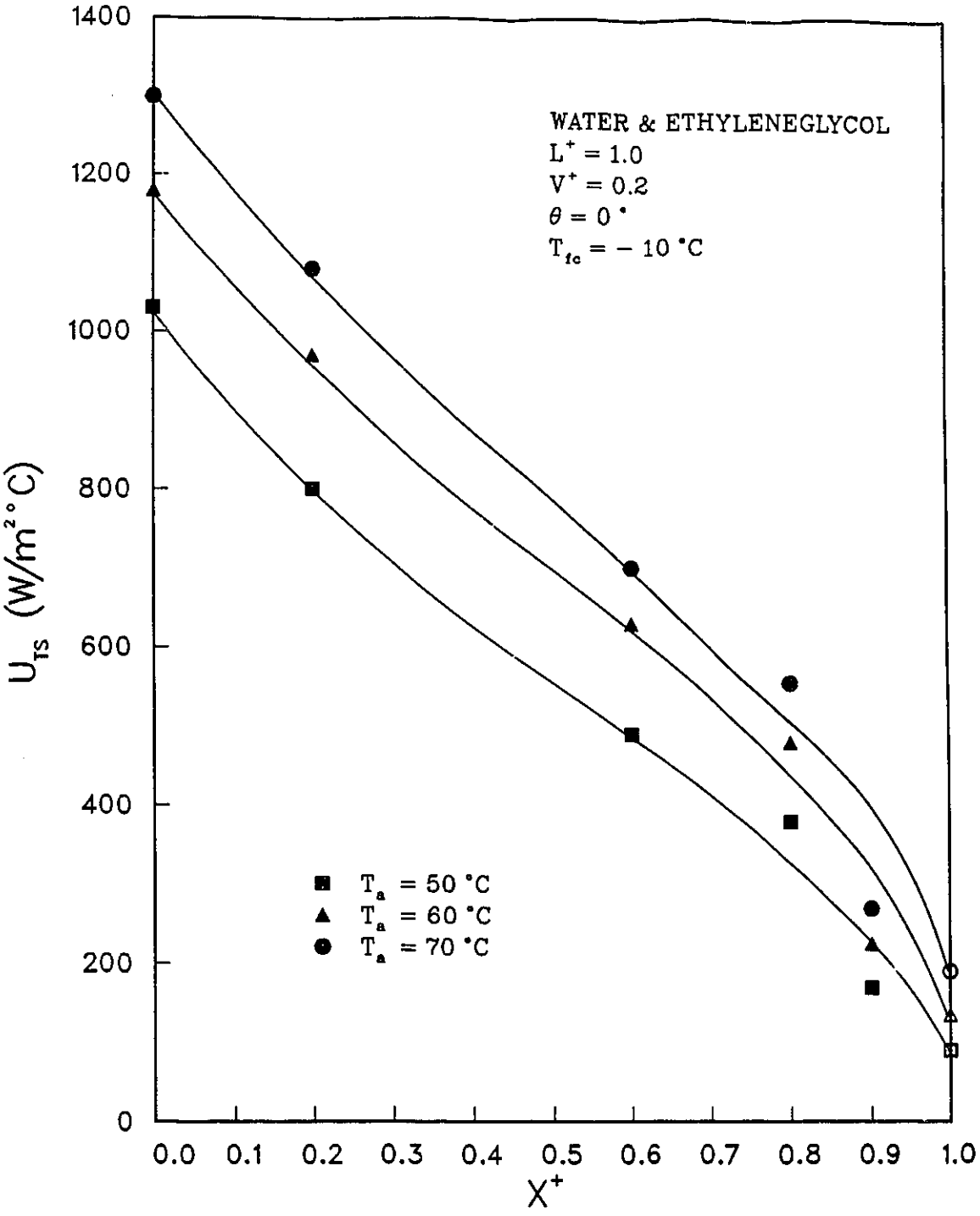

Figure 5.5(a) Effect of X^+ on U_{TS} (water-ethyleneglycol; T_{fc} = -10 °C)

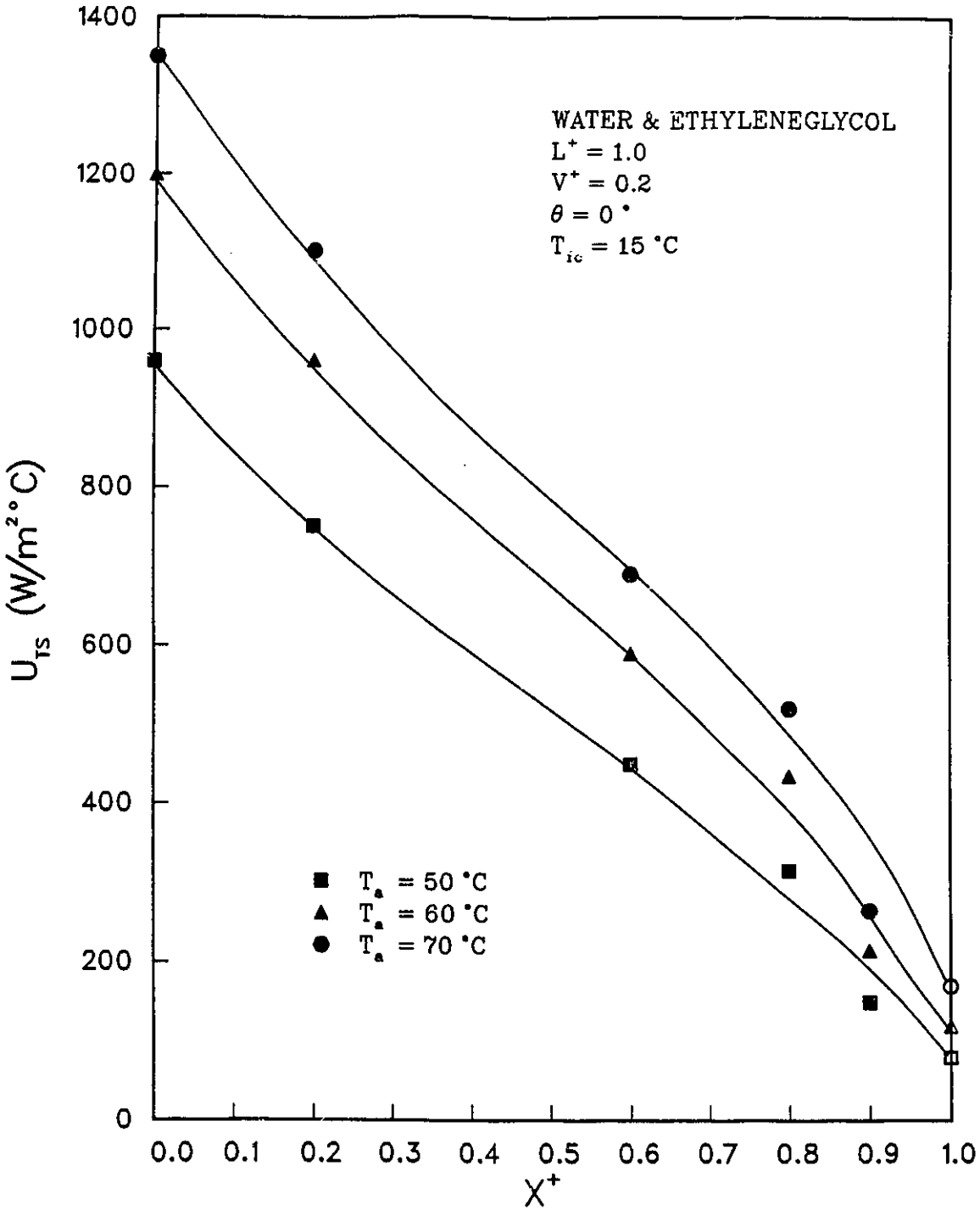

Figure 5.5(b) Effect of X^+ on U_{TS} (water-ethyleneglycol; T_{fc} = 15 °C)

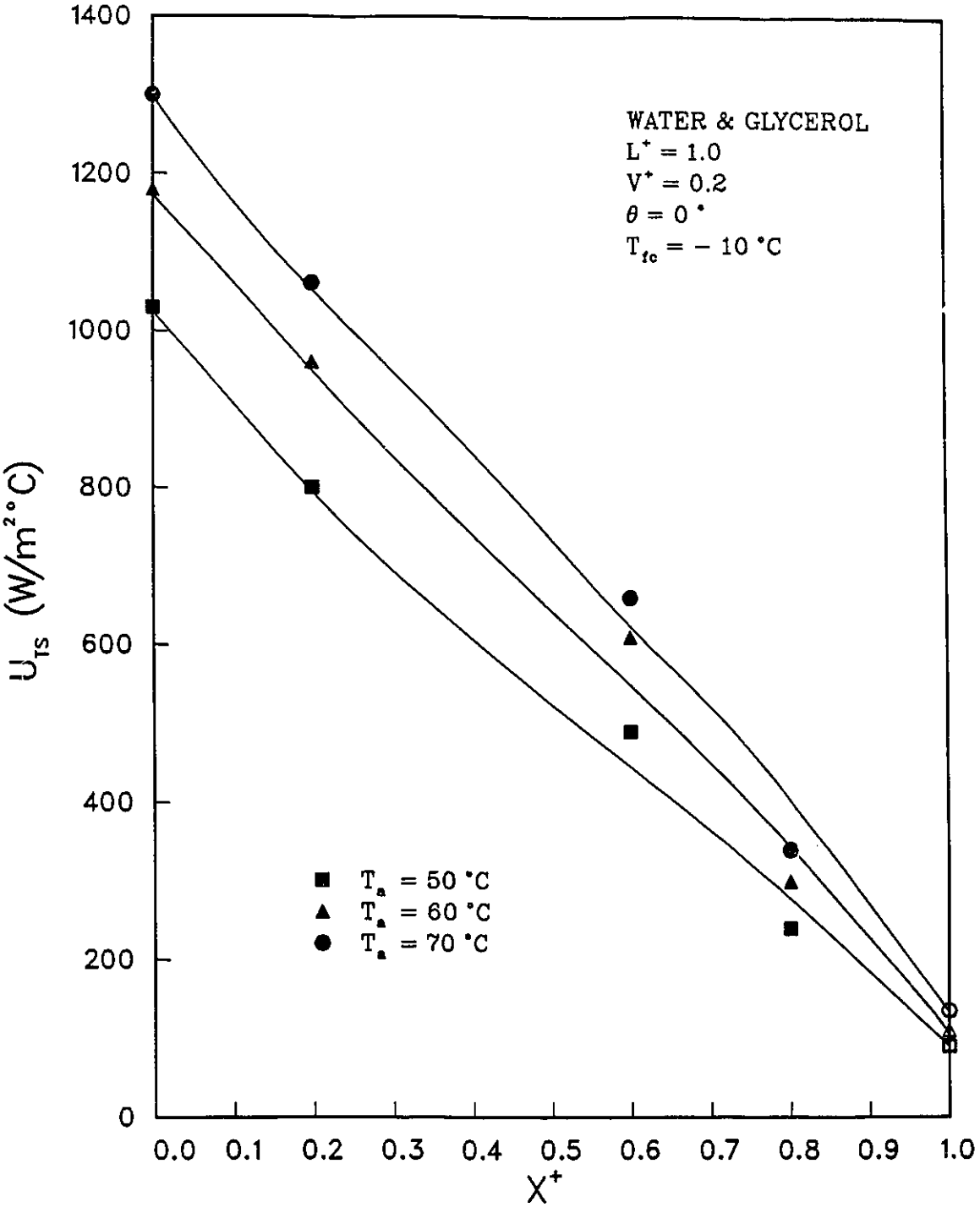

Figure 5.6(a) Effect of X^+ on U_{TS} (water-glycerol; T_{fc} = -10 °C)

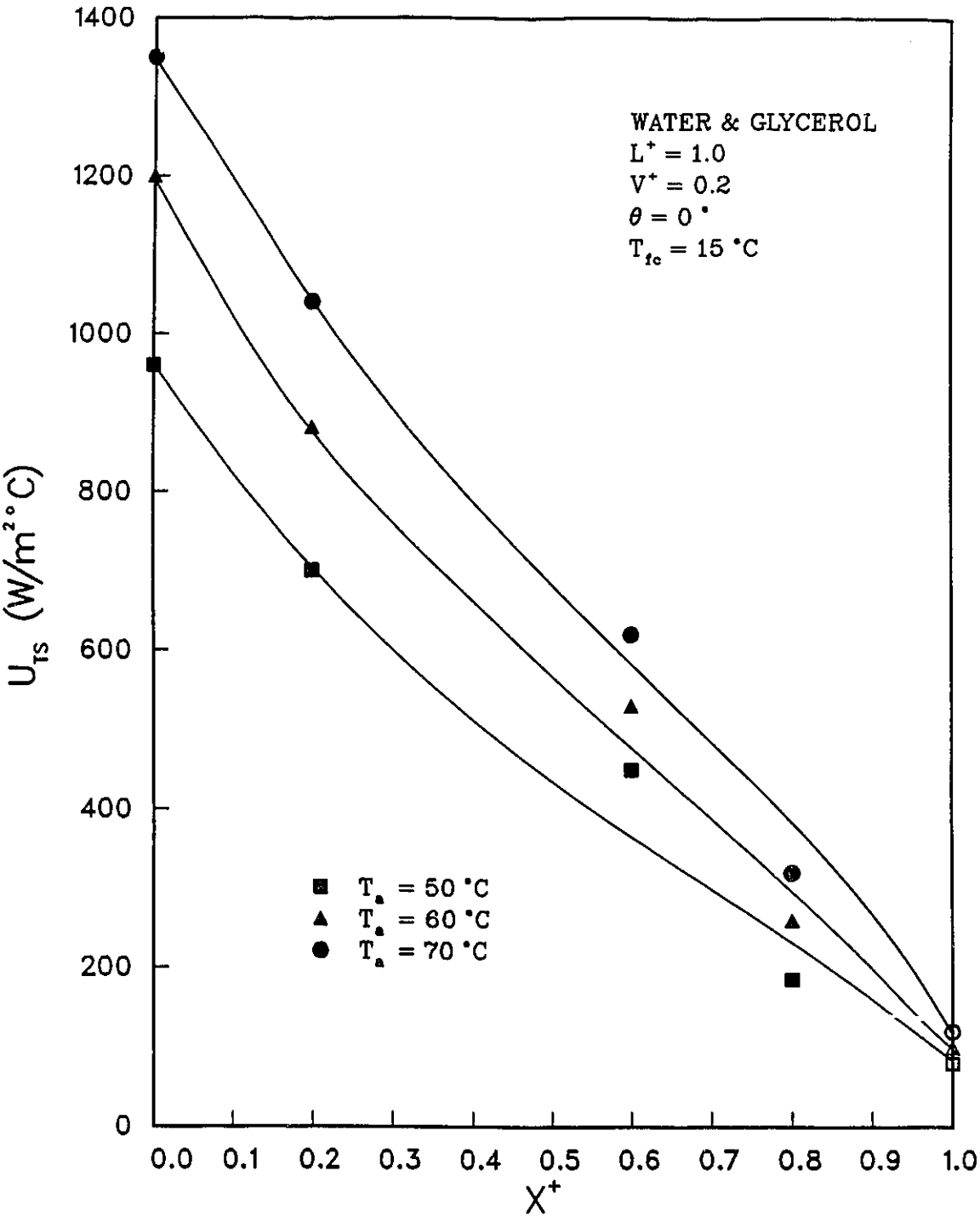

Figure 5.6(b) Effect of X^+ on U_{TS} (water-glycerol; T_{fc} = 15 °C)

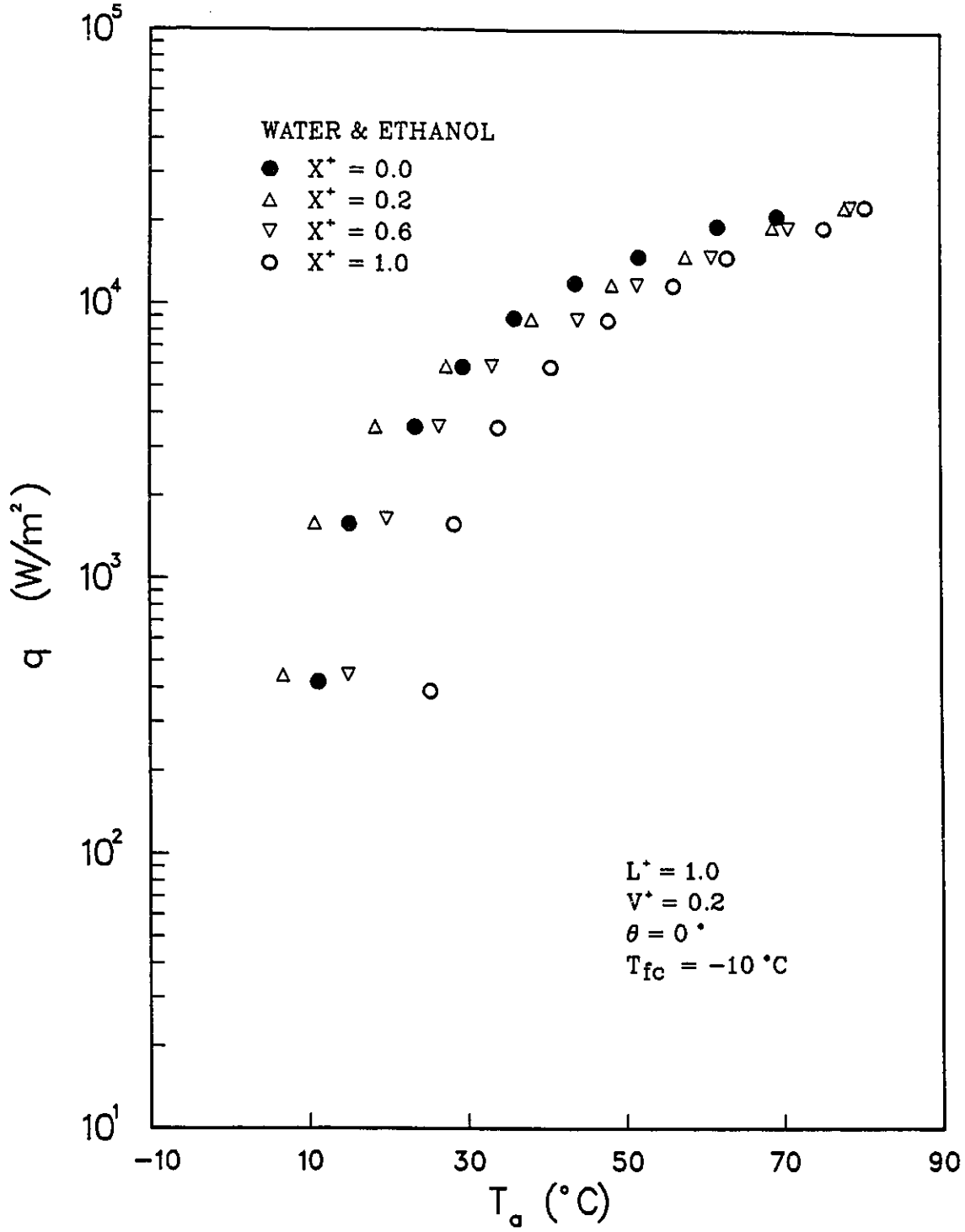

Figure 5.7(a) Effect of T_a on q (water-ethanol; T_{fc} = -10 °C)

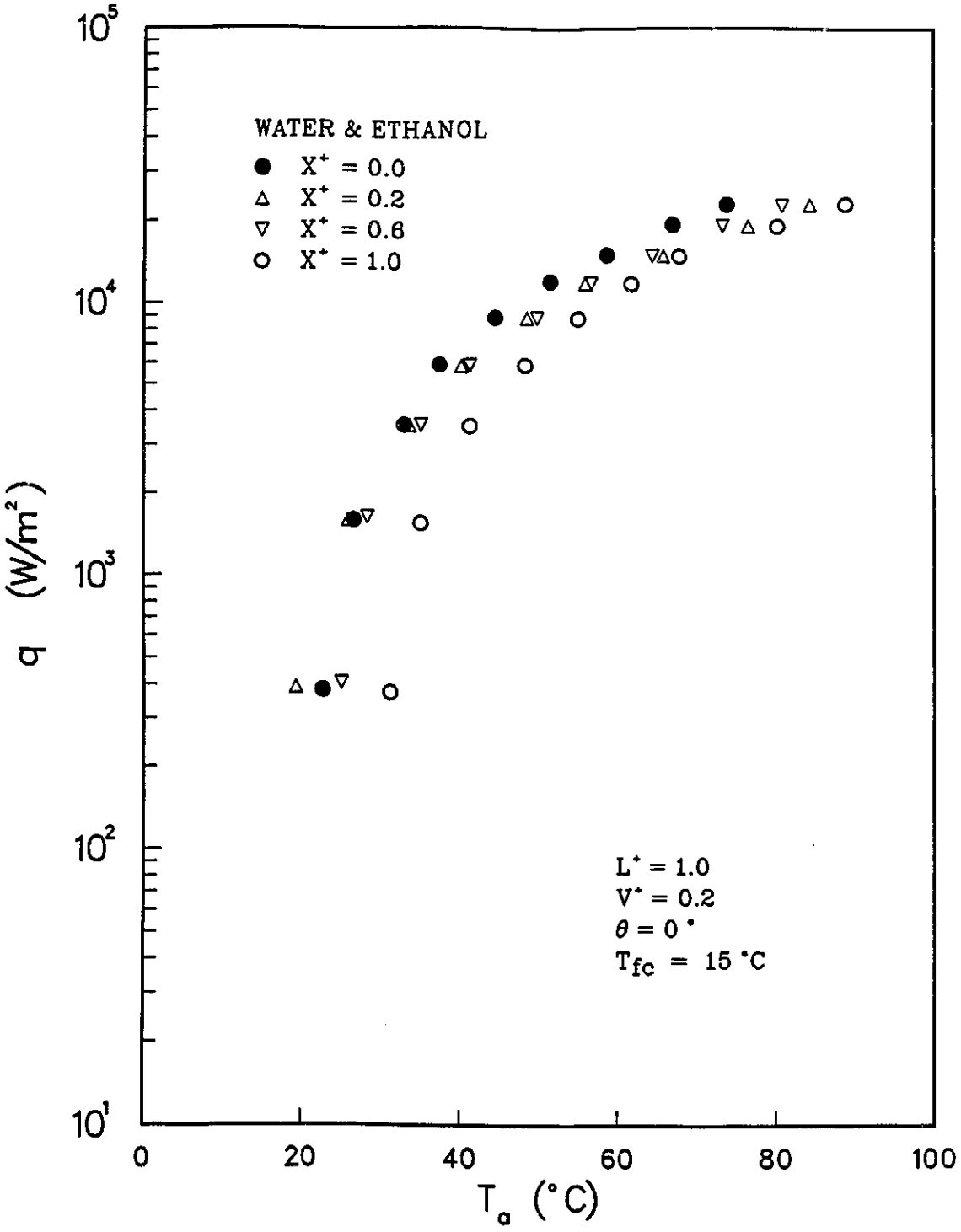

Figure 5.7(b) Effect of T_a on q (water-ethanol; T_{fc} = 15 °C)

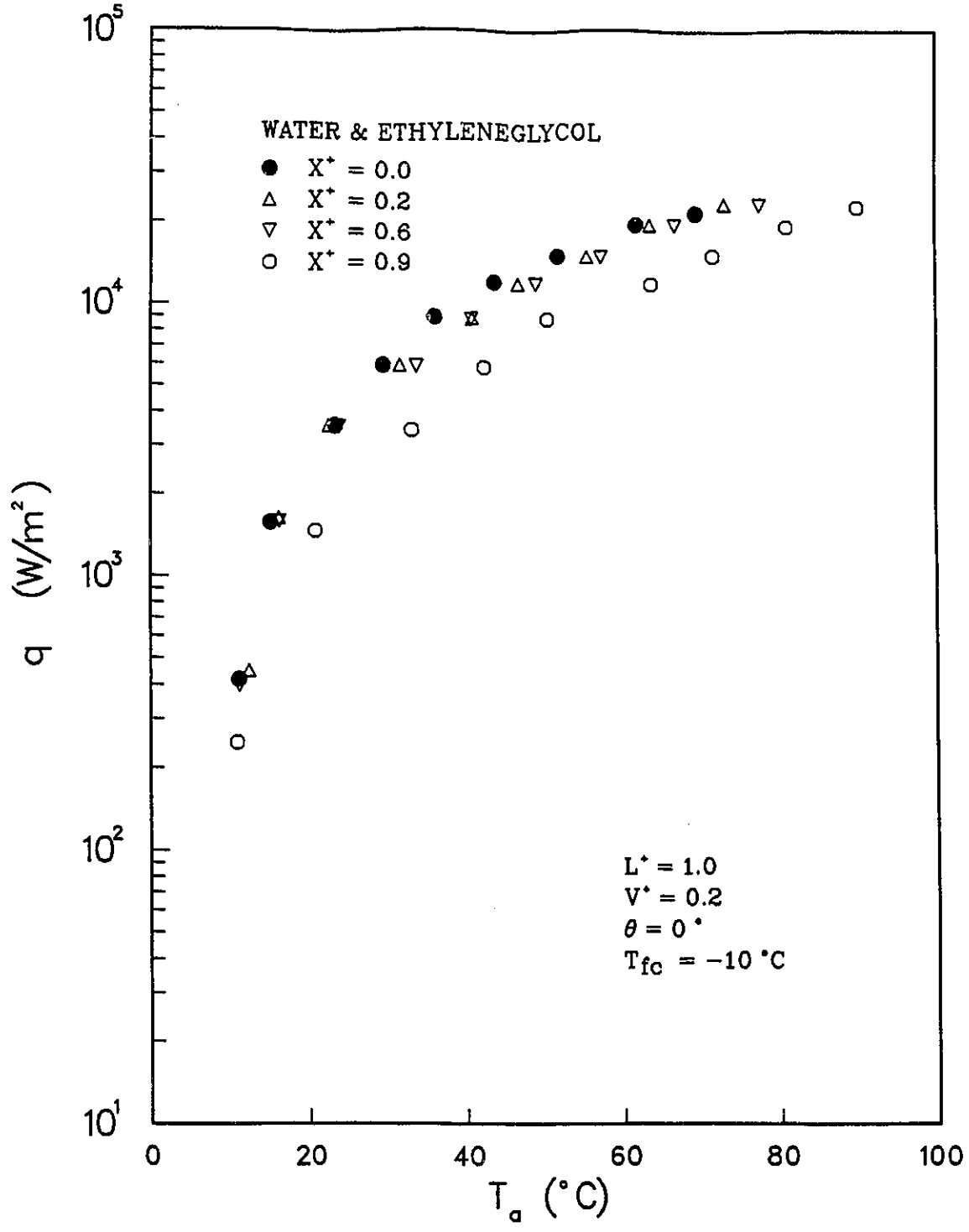

Figure 5.8(a) Effect of T_a on q (water-ethyleneglycol; T_{fc} = -10 °C)

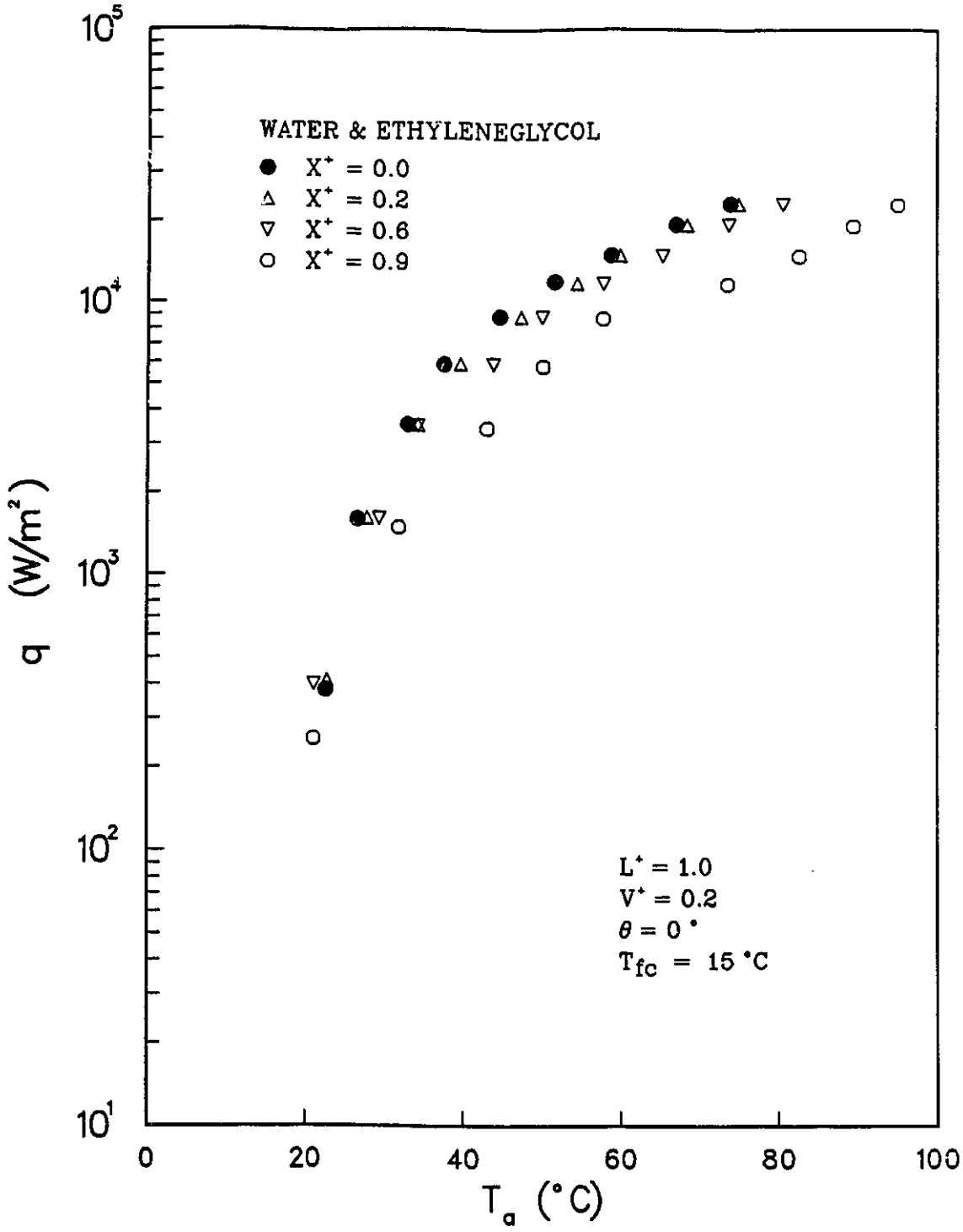

Figure 5.8(b) Effect of T_a on q (water-ethyleneglycol; T_{fc} = 15 °C)

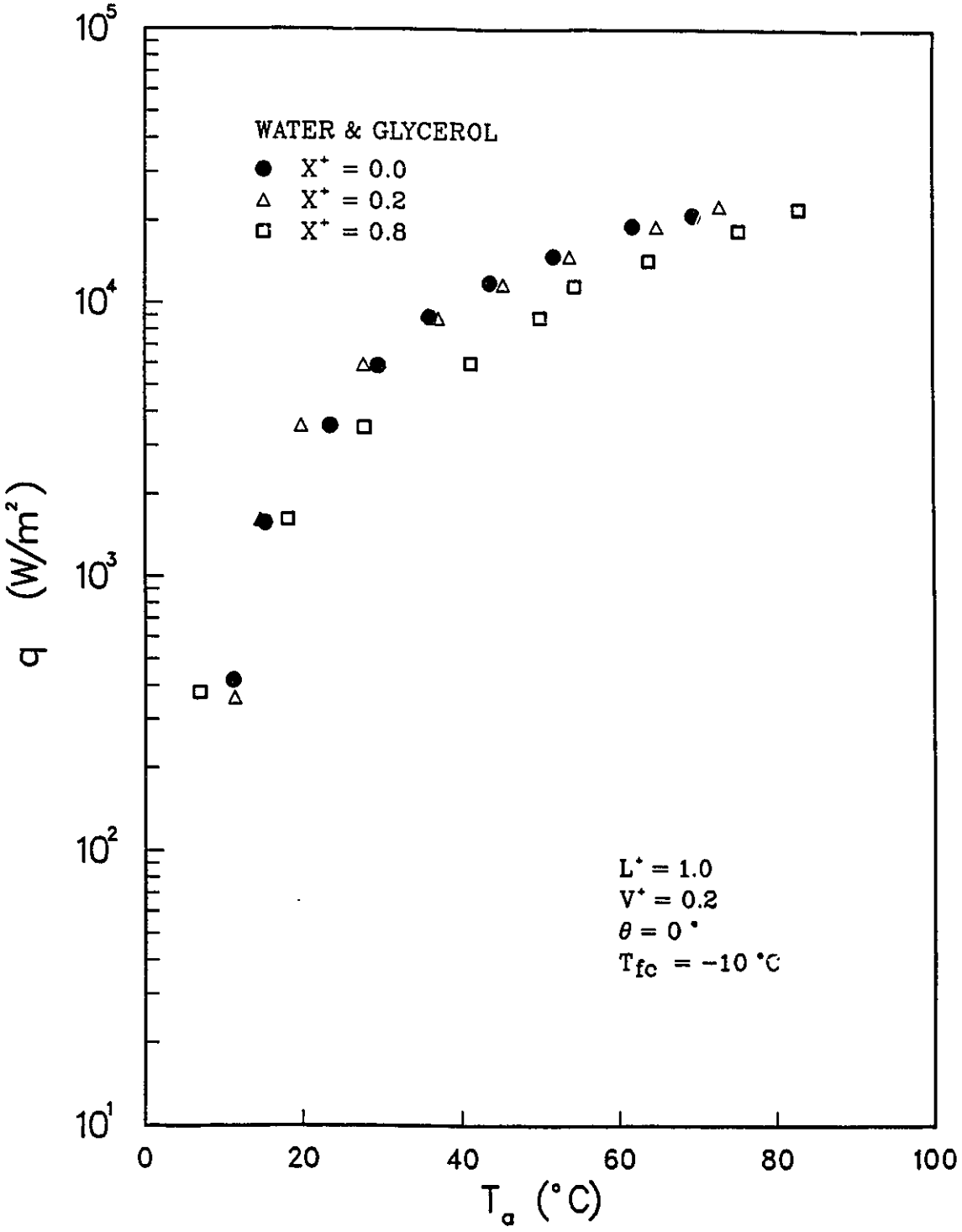

Figure 5.9(a) Effect of T_a on q (water-glycerol; T_{fc} = -10 °C)

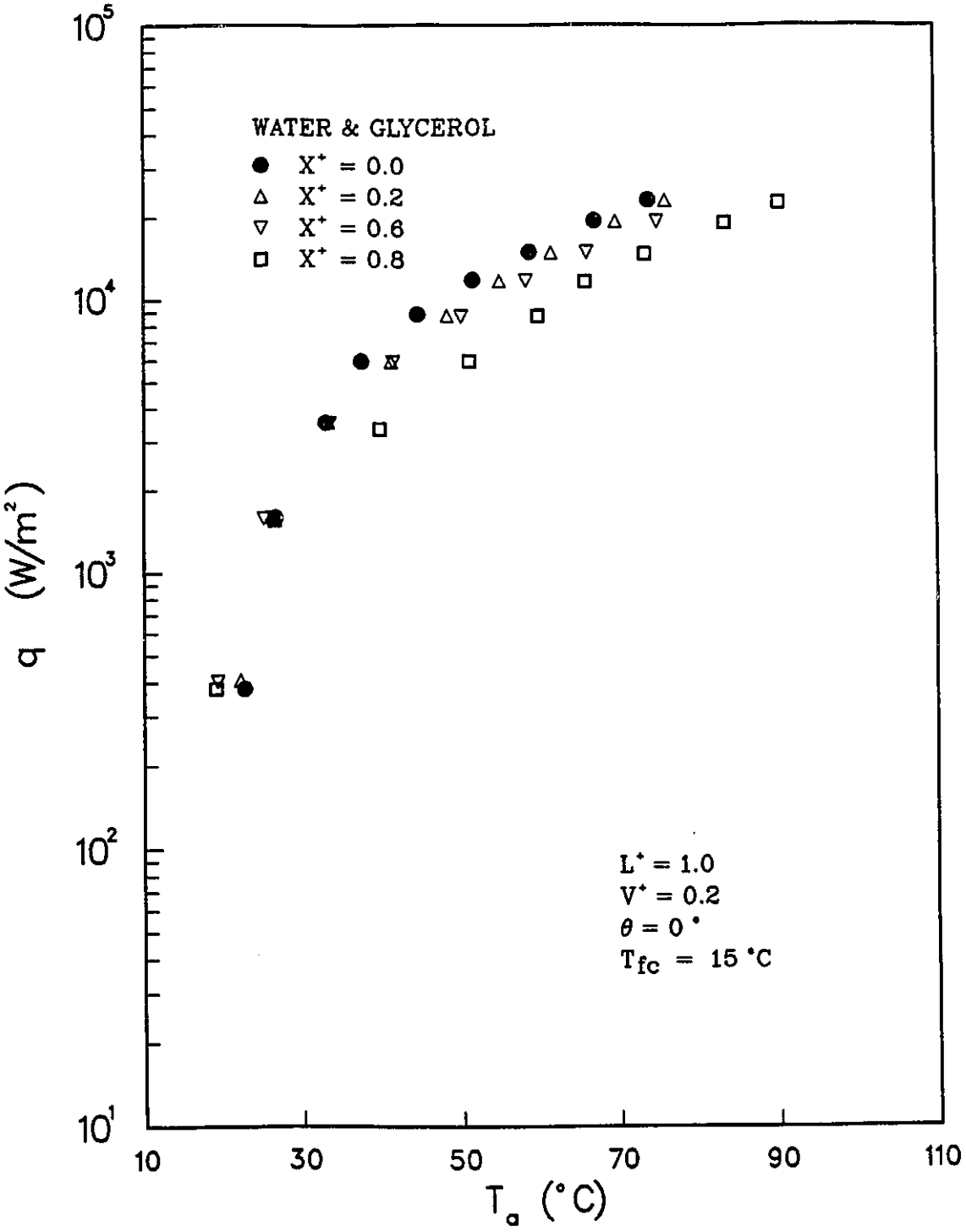

Figure 5.9(b) Effect of T_a on q (water-glycerol; T_{fc} = 15 °C)

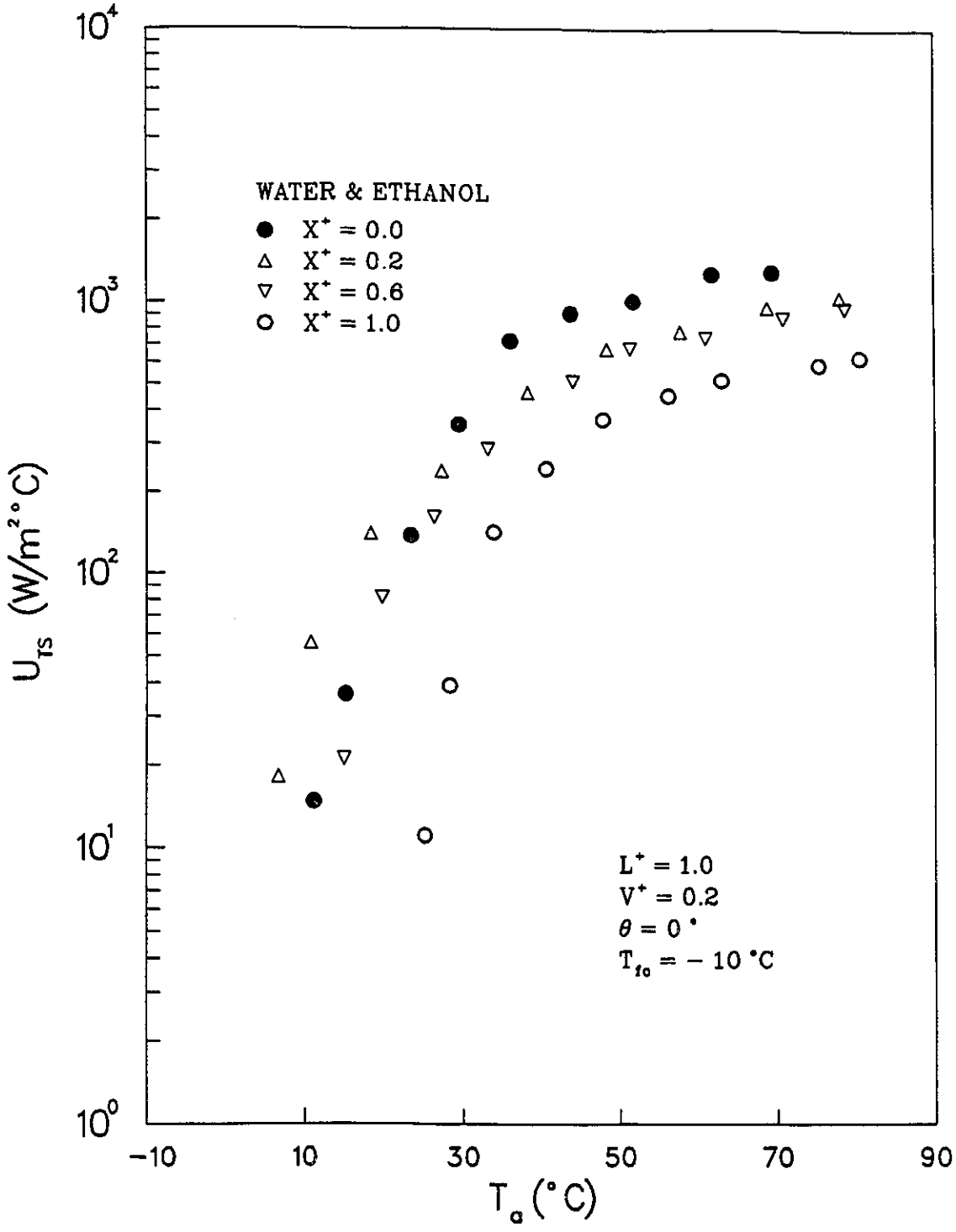

Figure 5.10(a) Effect of T_a on U_{TS} (water-ethanol; T_{fc} = -10 °C)

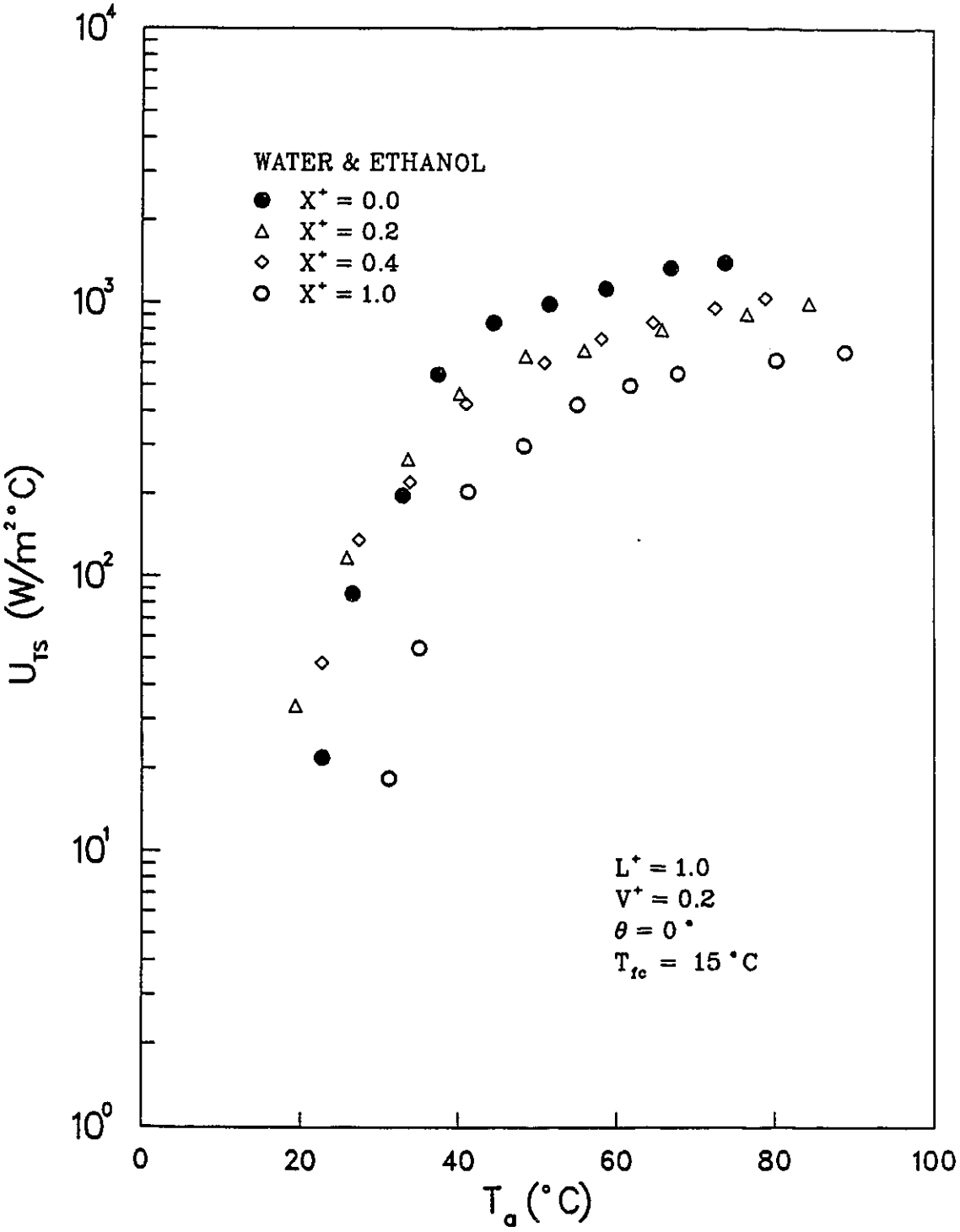

Figure 5.10(b) Effect of T_a on U_{TS} (water-ethanol; T_{fc} = 15 °C)

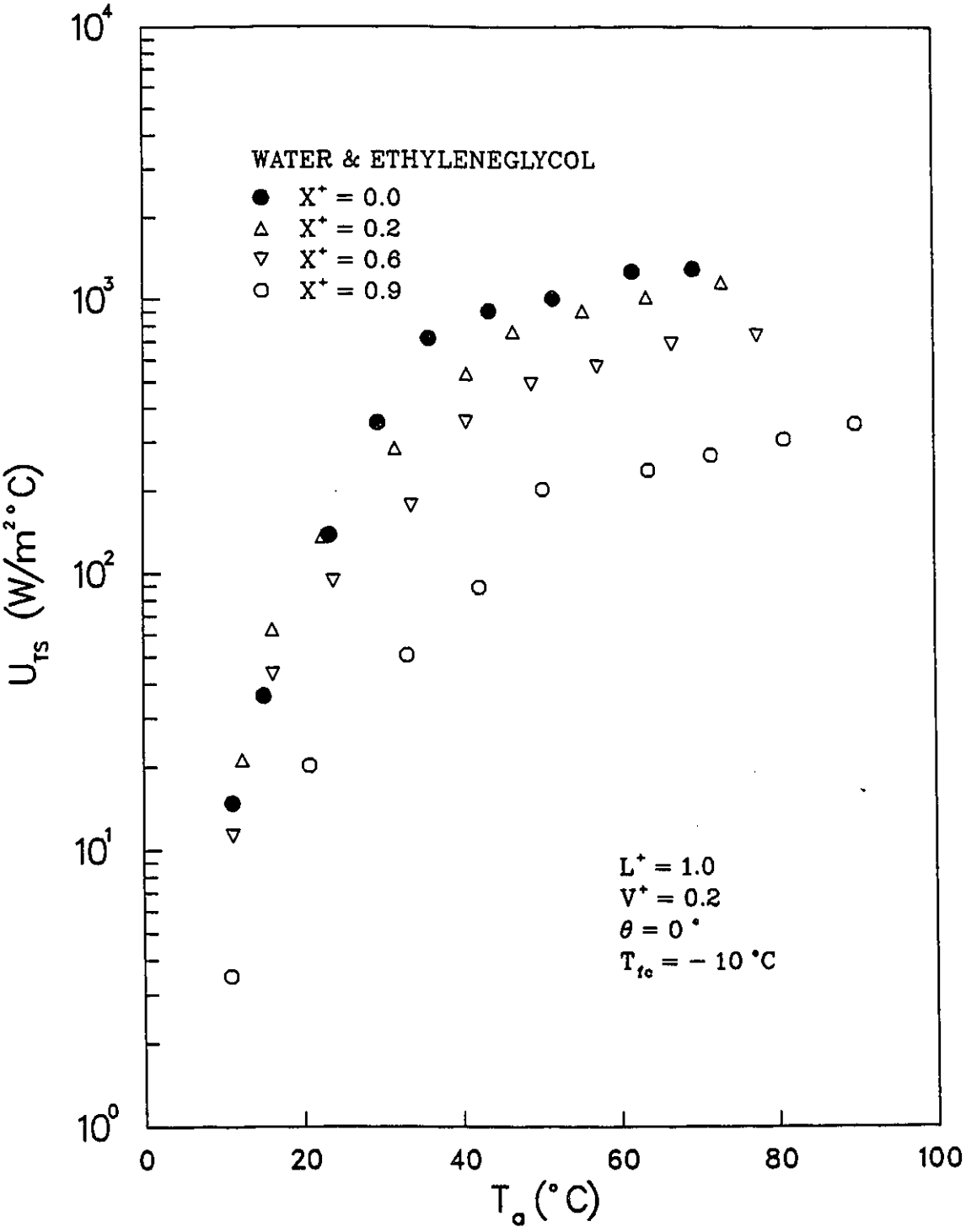

Figure 5.11(a) Effect of T_a on U_{TS} (water-ethyleneglycol; T_{fc} = -10 °C)

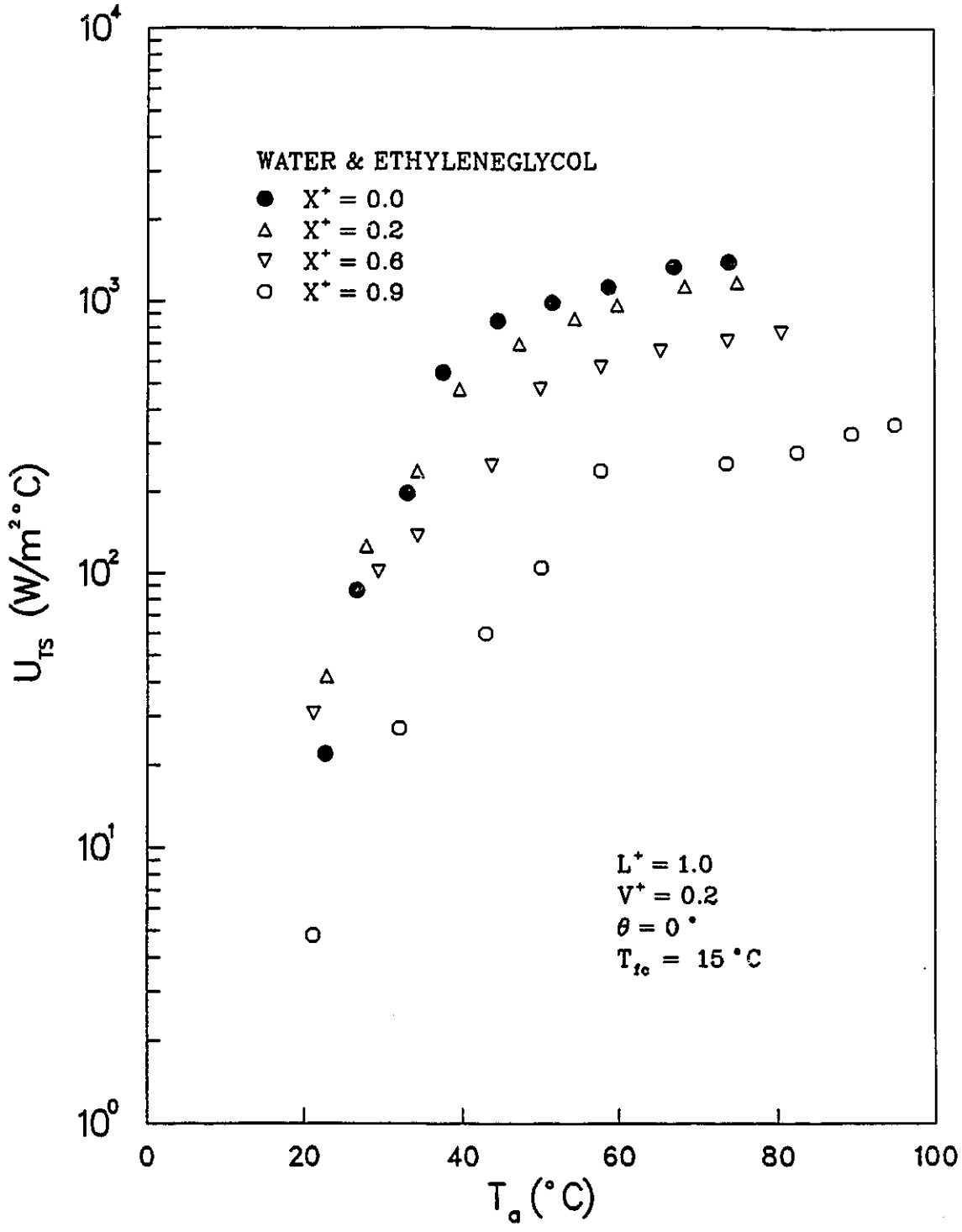

Figure 5.11(b) Effect of T_a on U_{TS} (water-ethyleneglycol; T_{fc} = 15 °C)

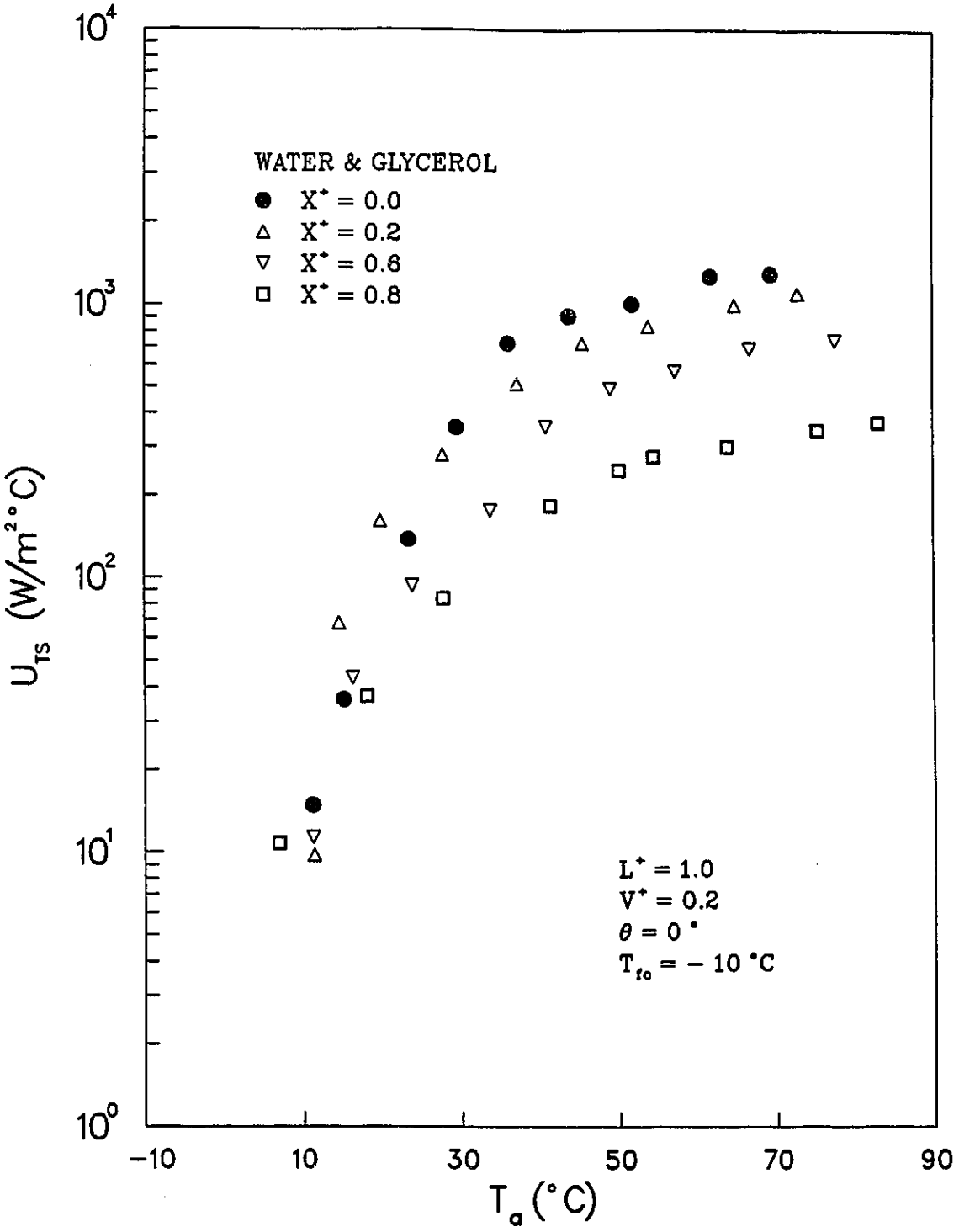

Figure 5.12(a) Effect of T_a on U_{TS} (water-glycerol; T_{fc} = -10 °C)

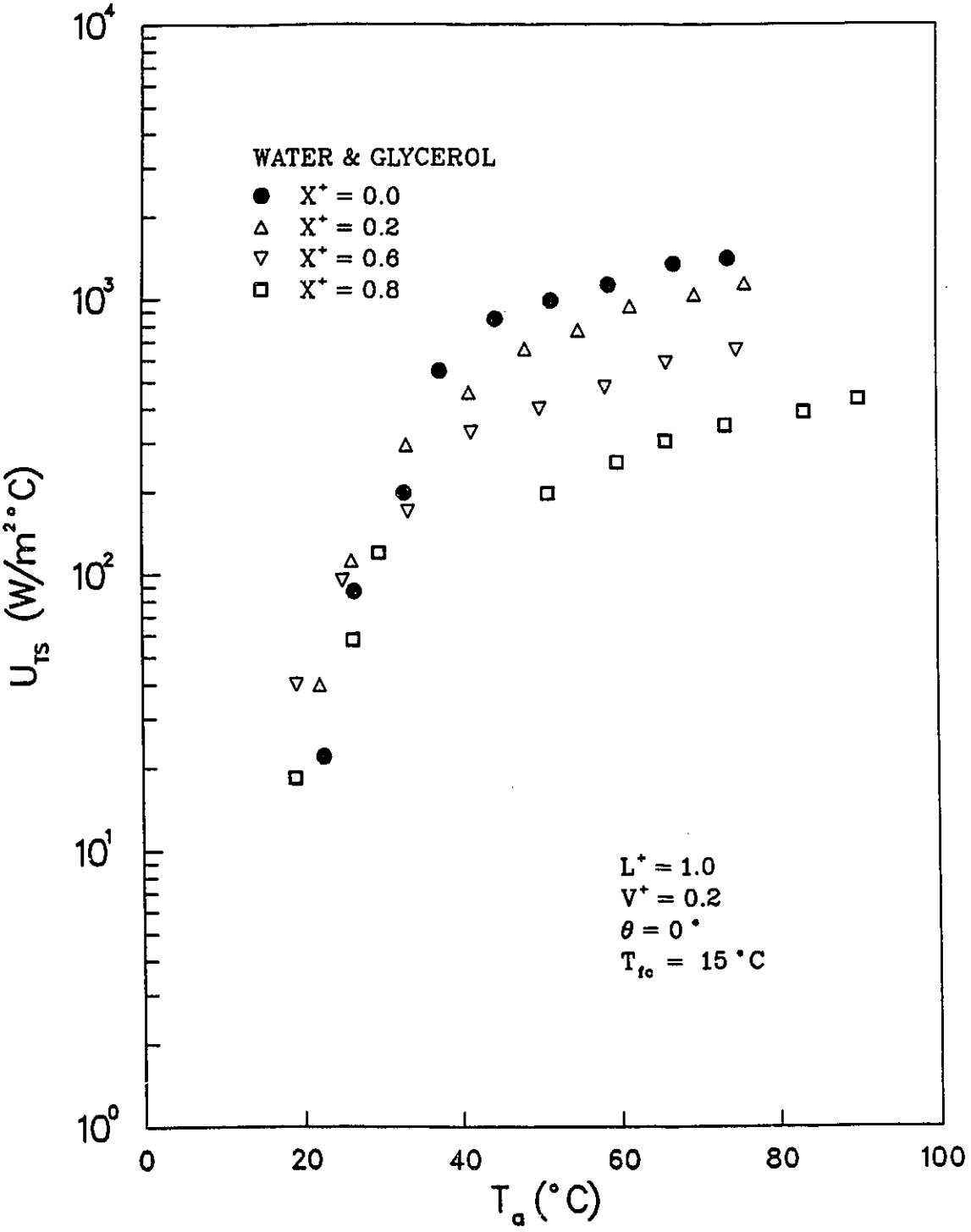

Figure 5.12(b) Effect of T_a on U_{TS} (water-glycerol; T_{fc} = 15 °C)

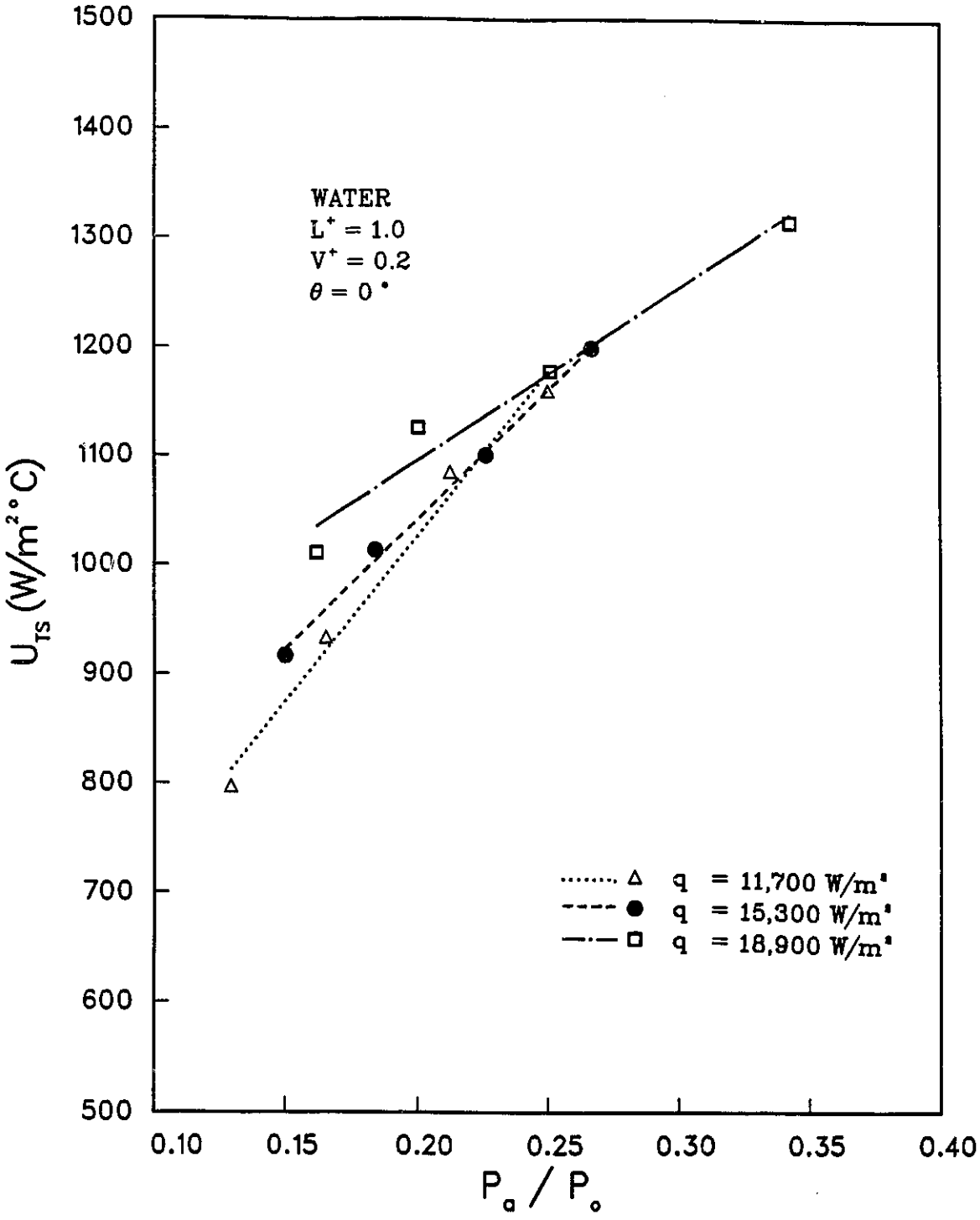

Figure 5.13 Effect of Pressure on U_{TS}

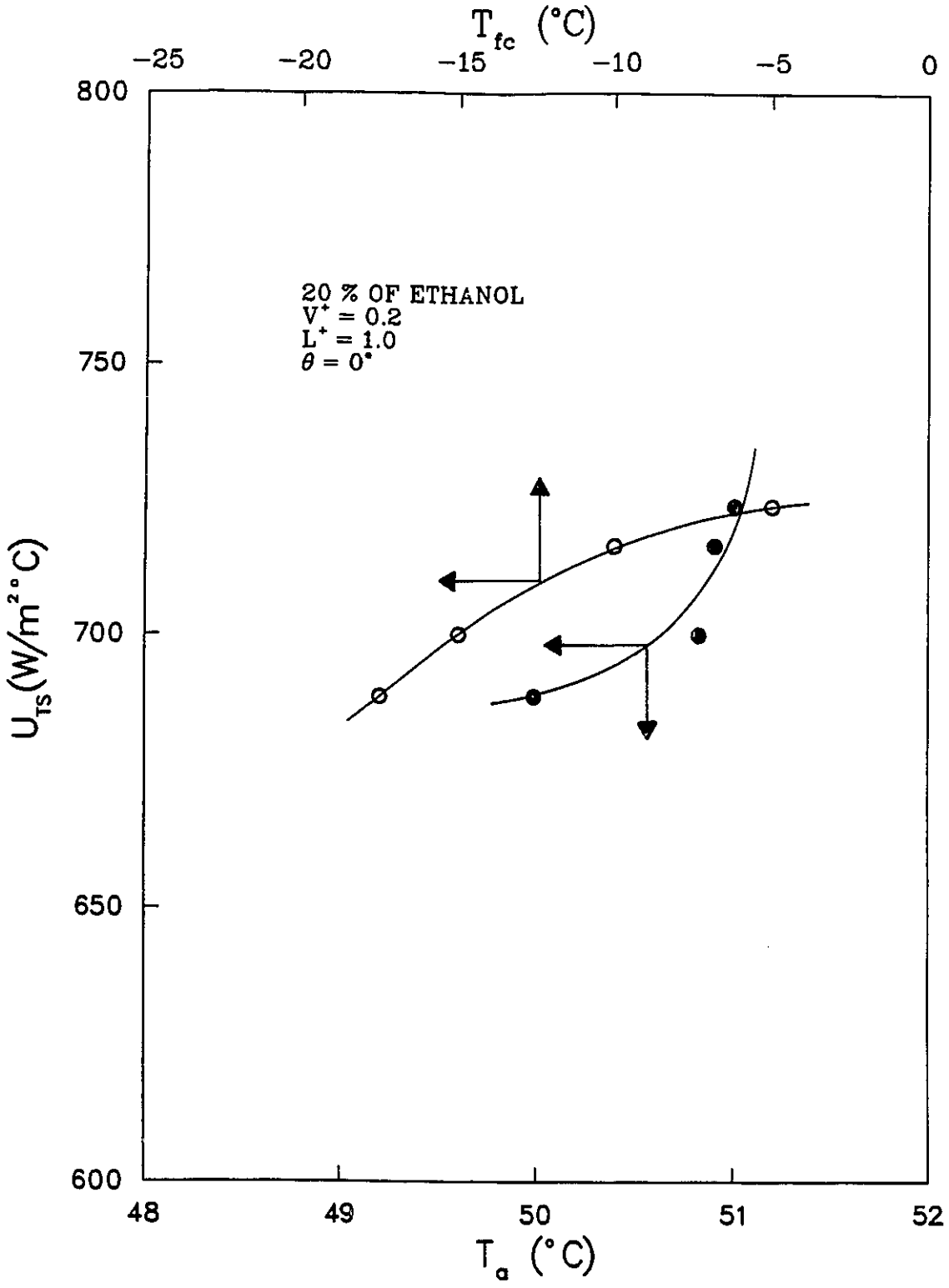

Figure 5.14 Effect of T_{fc} and T_a on U_{TS} at Constant Heat Flux

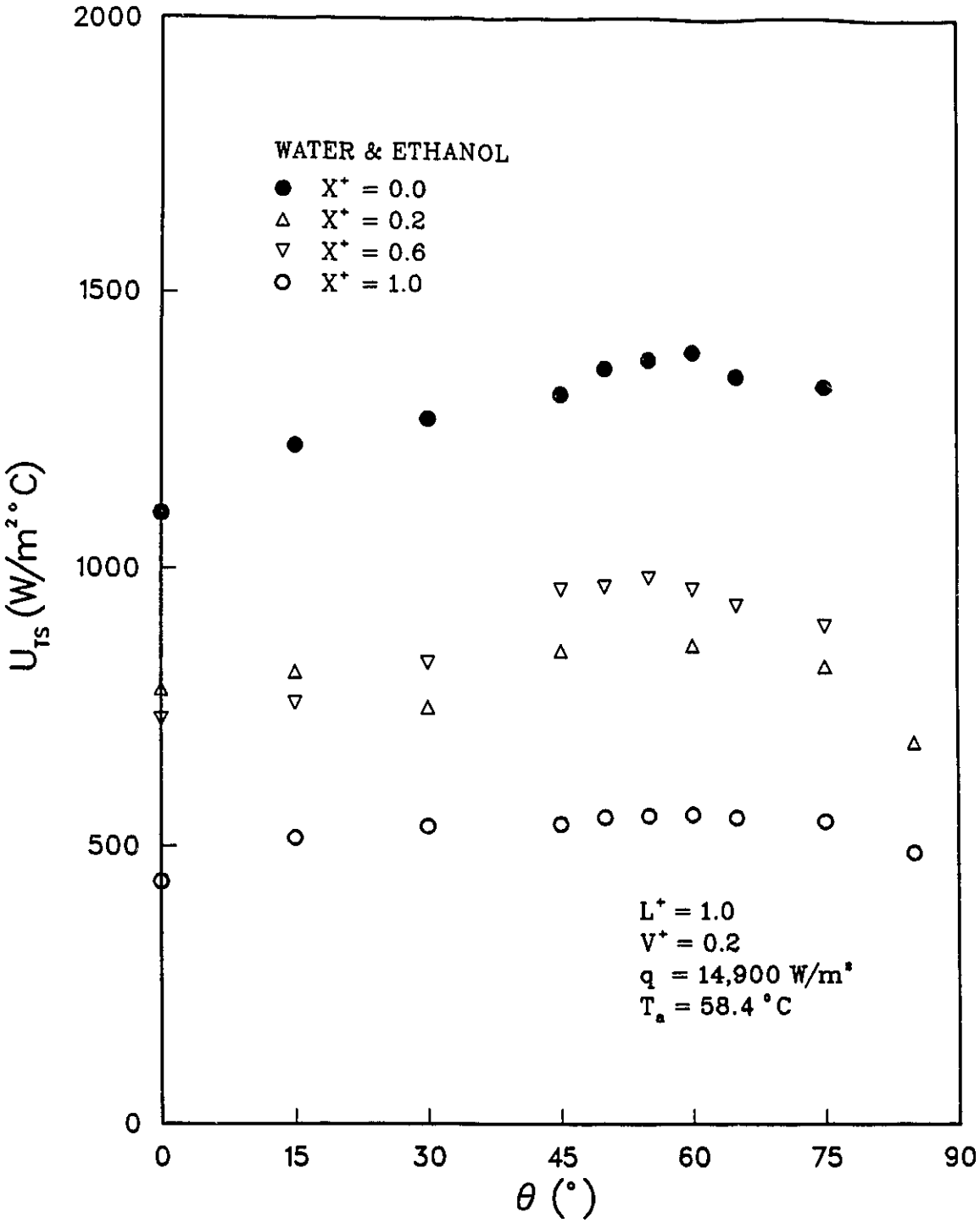

Figure 5.15(a) Effect of Thermosyphon Inclination on U_{TS} (water-ethanol; T_a = 58.4 °C)

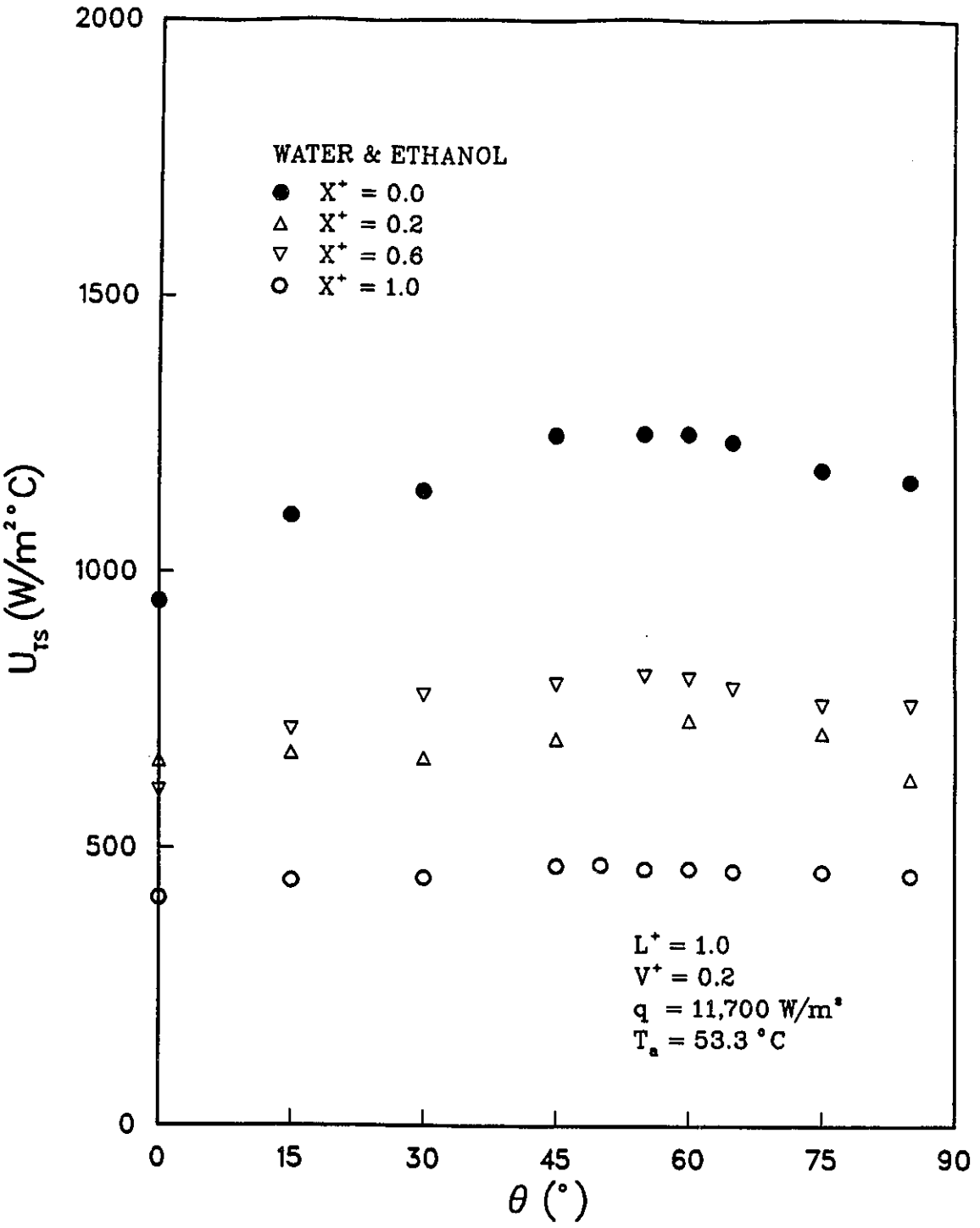

Figure 5.15(b) Effect of Thermosyphon Inclination on U_{TS} (water-ethanol; T_a = 53.3 °C)

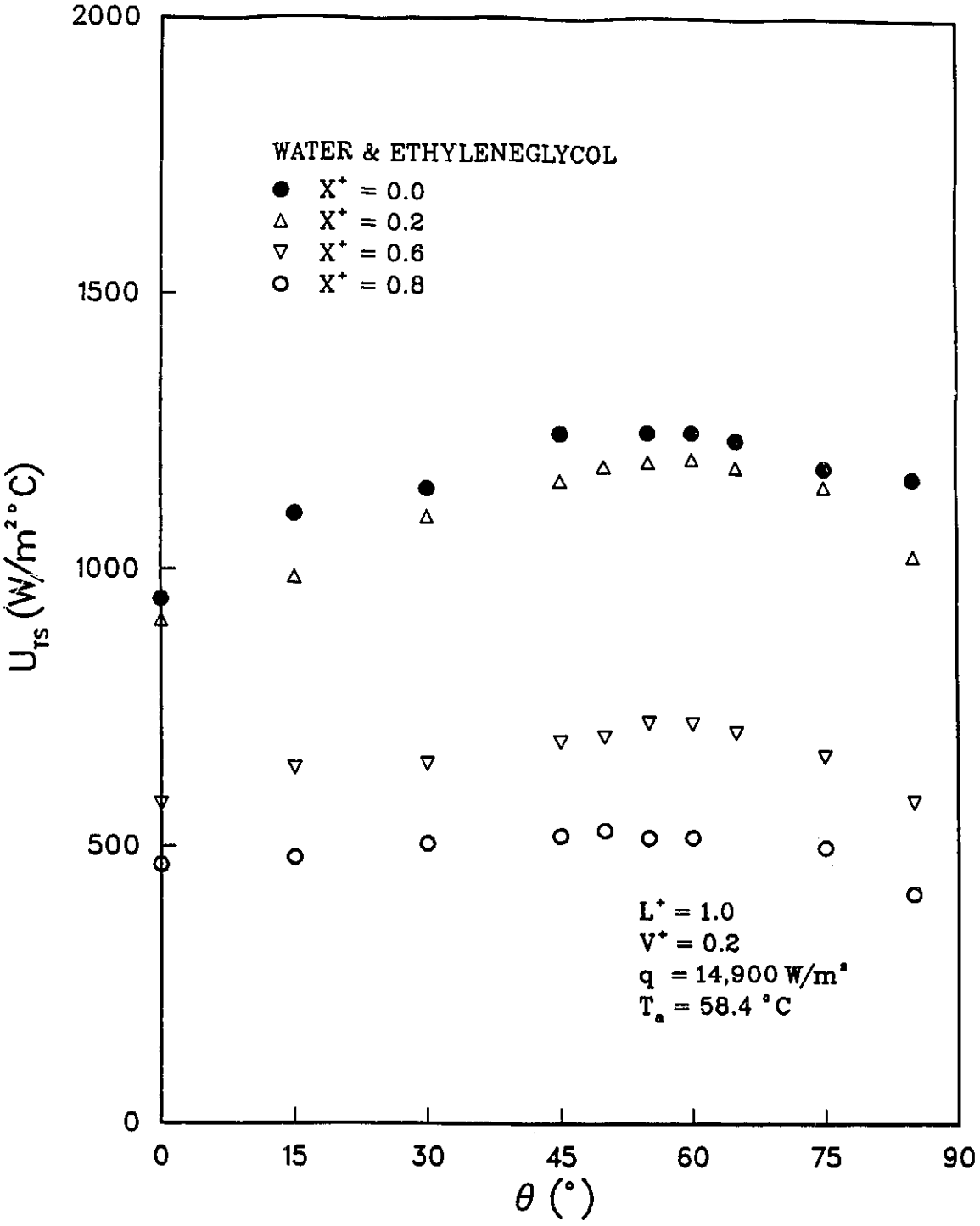

Figure 5.16 Effect of Thermosyphon Inclination on U_{TS} (water-ethyleneglycol; T_a = 58.4 °C)

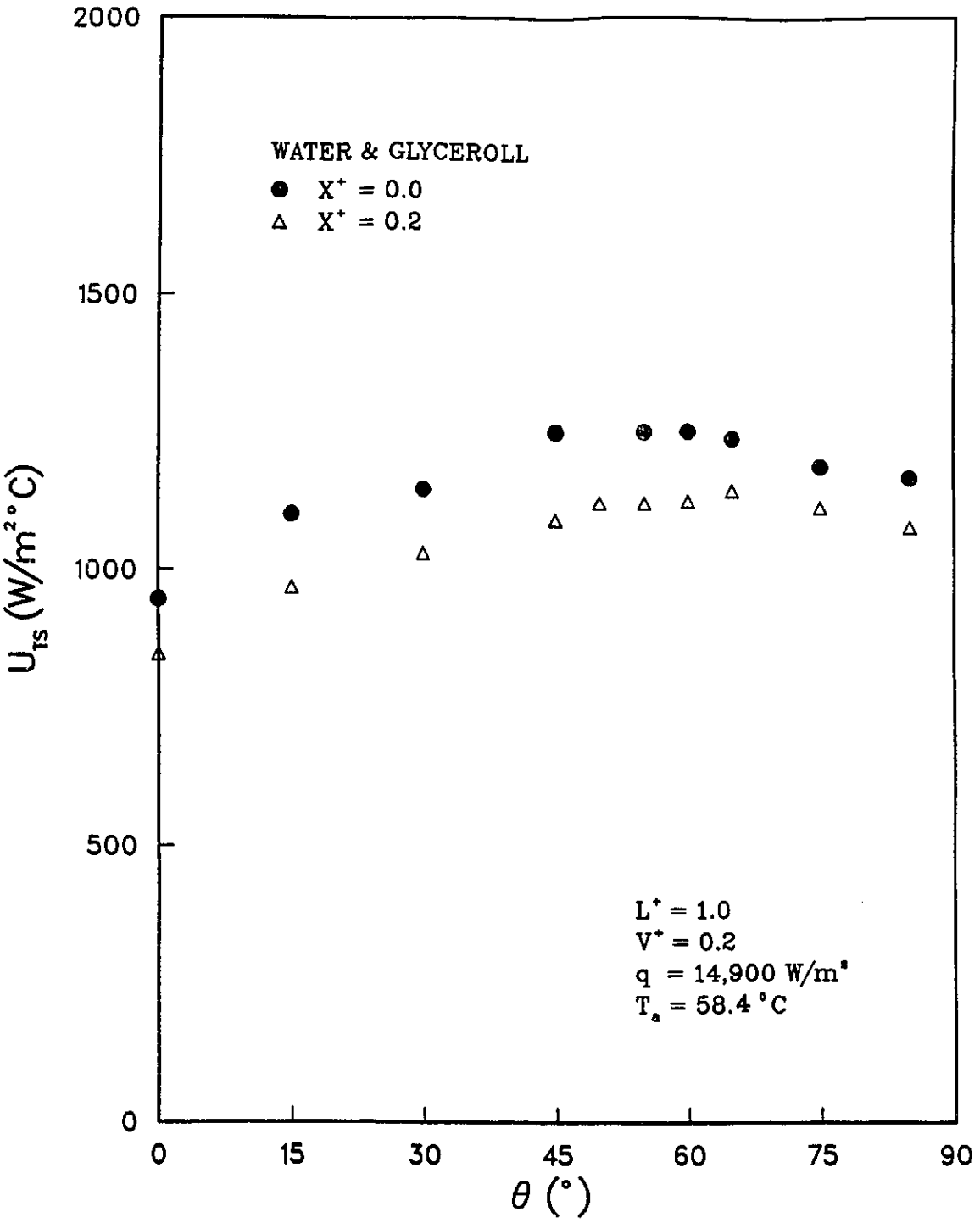

Figure 5.17 Effect of Thermosyphon Inclination on U_{TS} (water-glycerol; T_a = 58.4 °C)

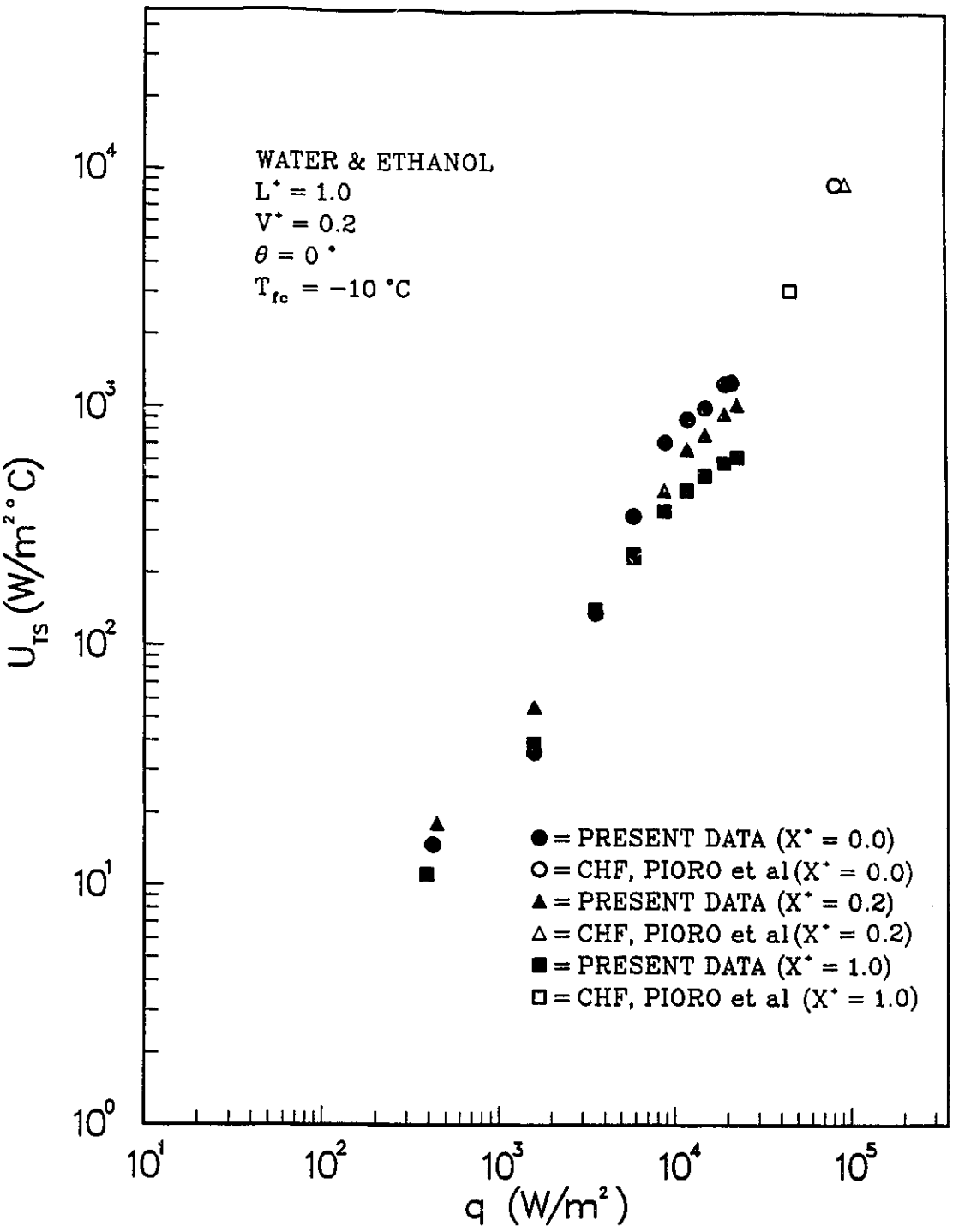

Figure 5.18 Comparison with CHF of Pioro

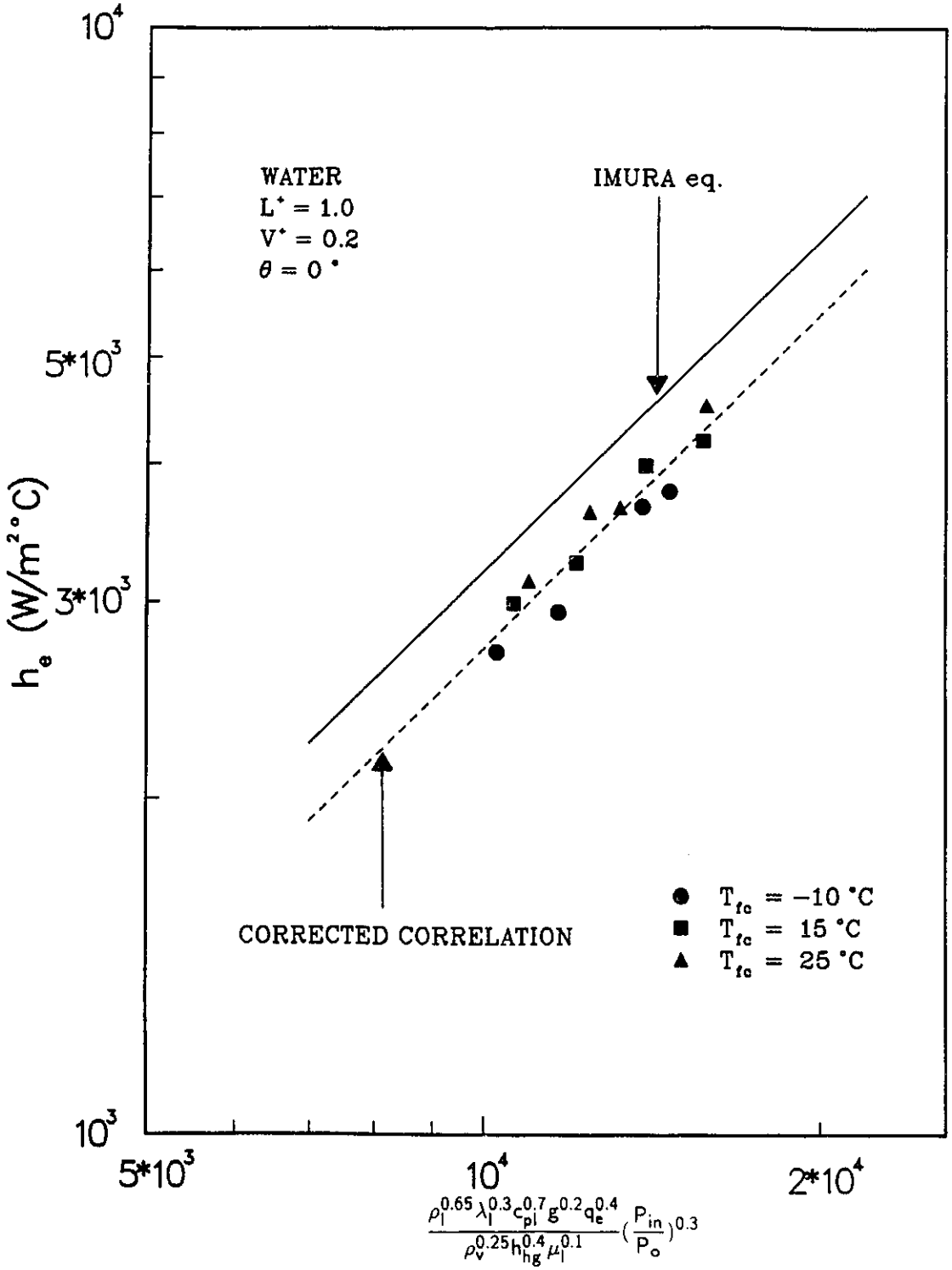

Figure 5.19 Comparison of the Experimental Data with Imura's Correlation (water)

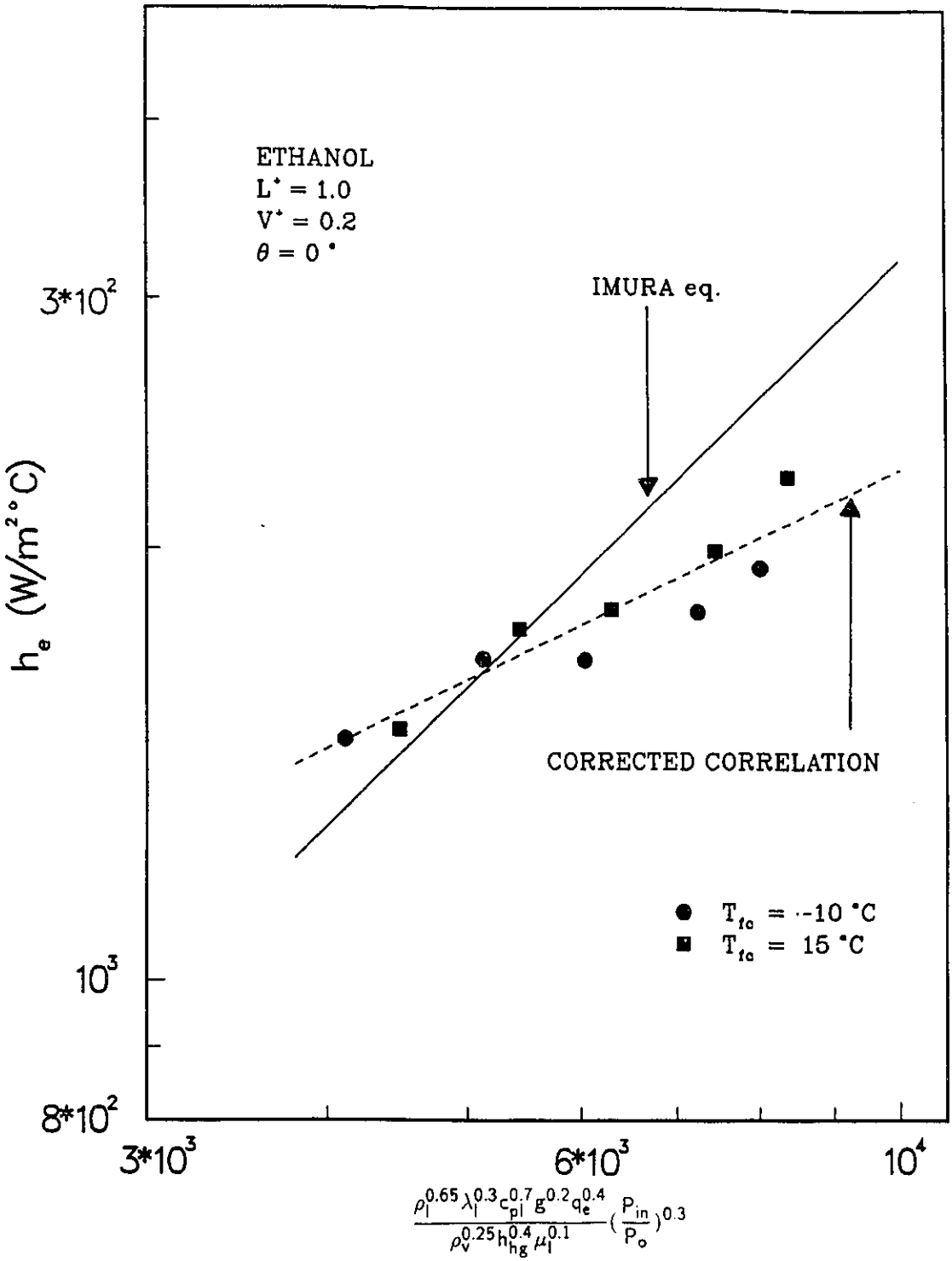

Figure 5.20 Comparison of the Experimental Data with Imura's Correlation (ethanol)

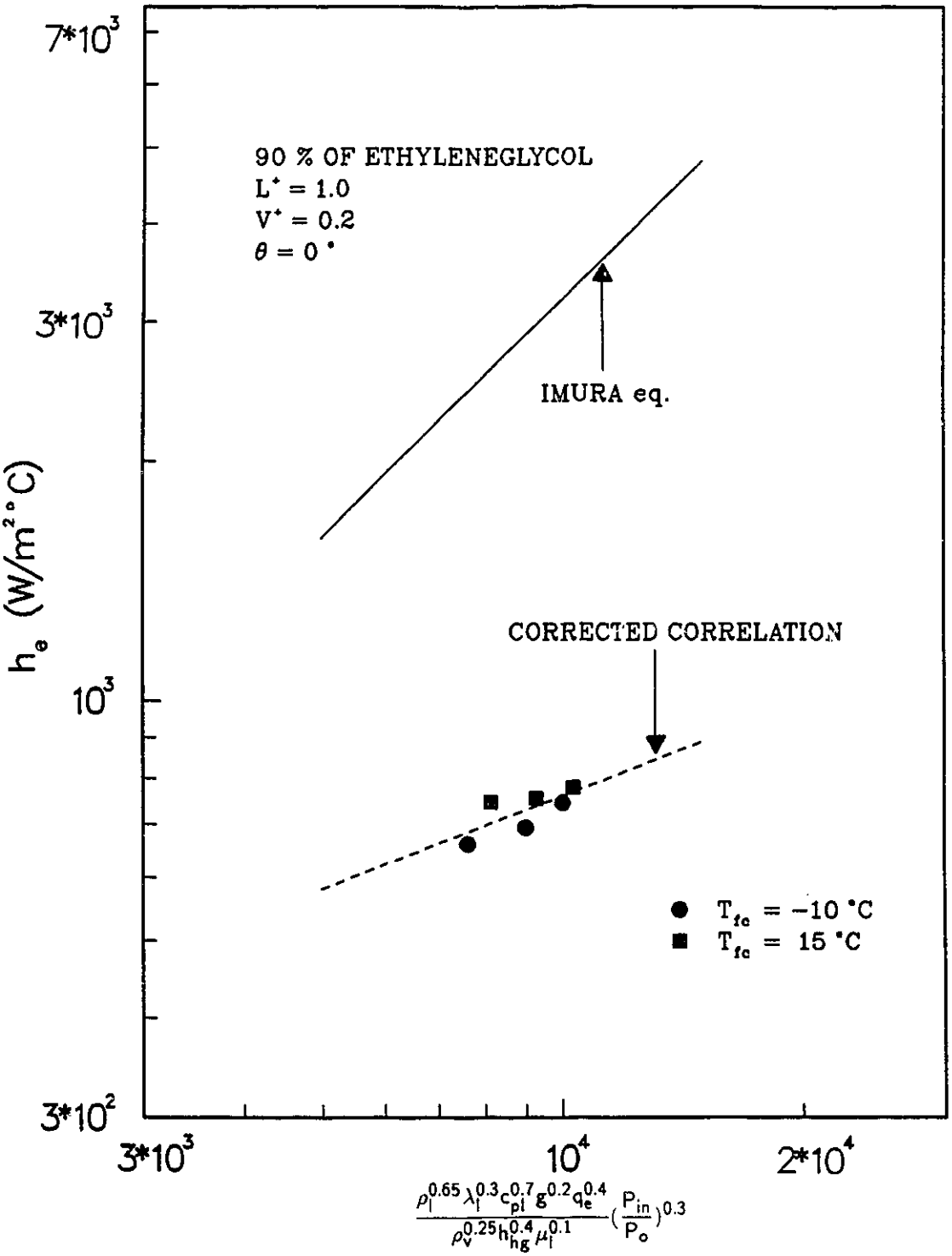

Figure 5.21 Comparison of the Experimental Data with Imura's Correlation (90 % of ethyleneglycol)

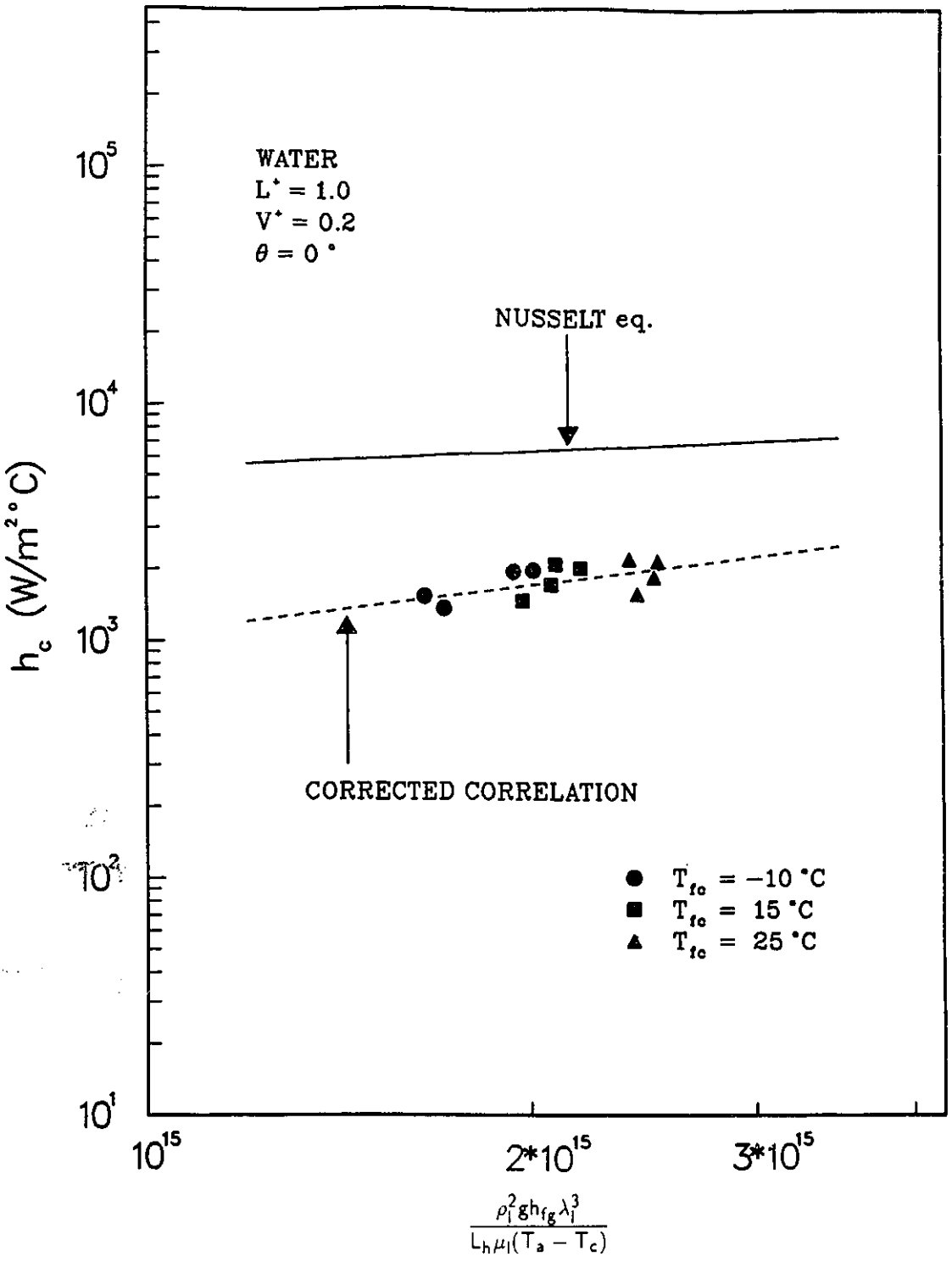

Figure 5.22 Comparison of the Experimental Data with Nusselt's Correlation (water)

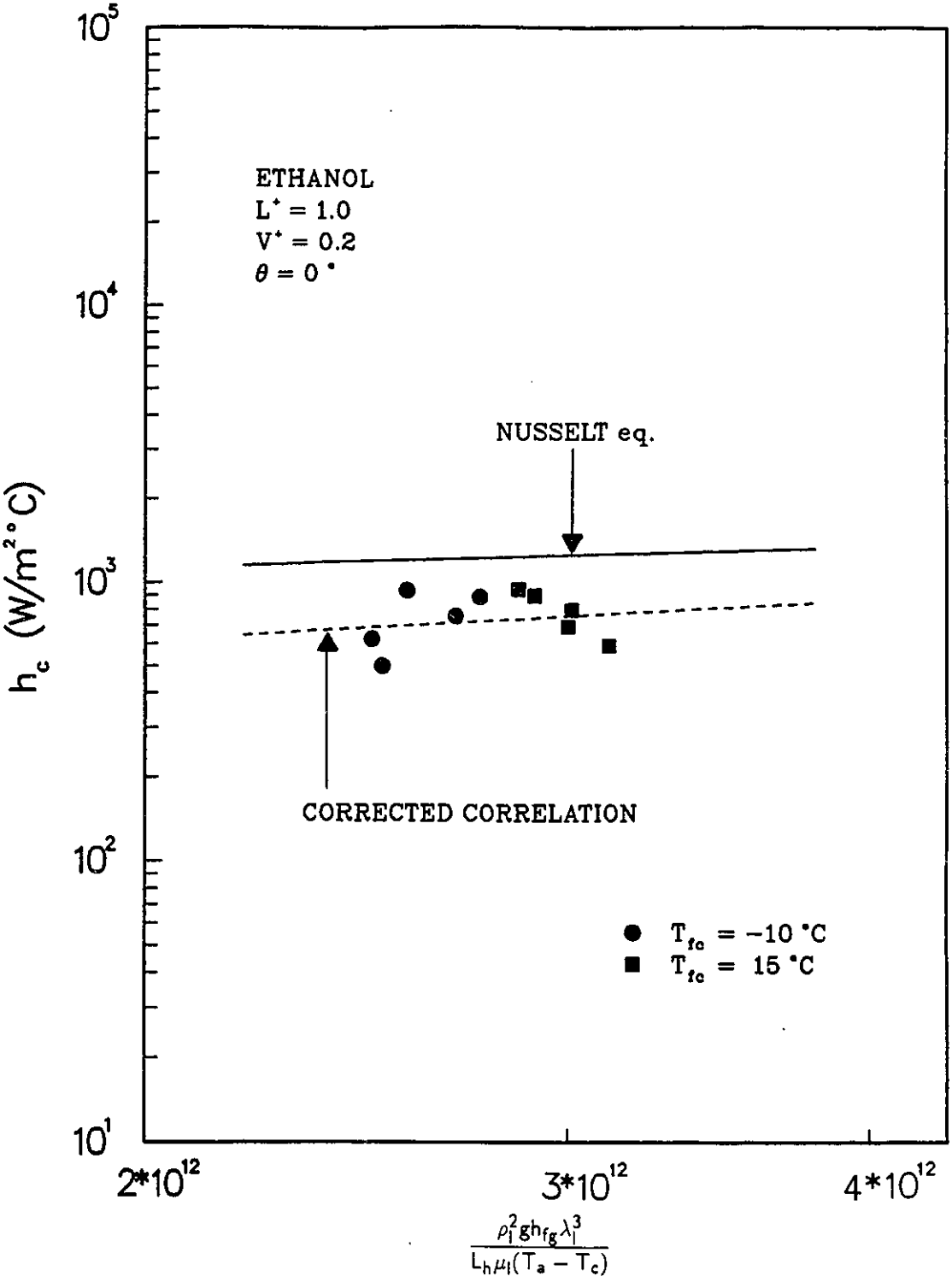

Figure 5.23 Comparison of the Experimental Data with Nusselt's Correlation (ethanol)

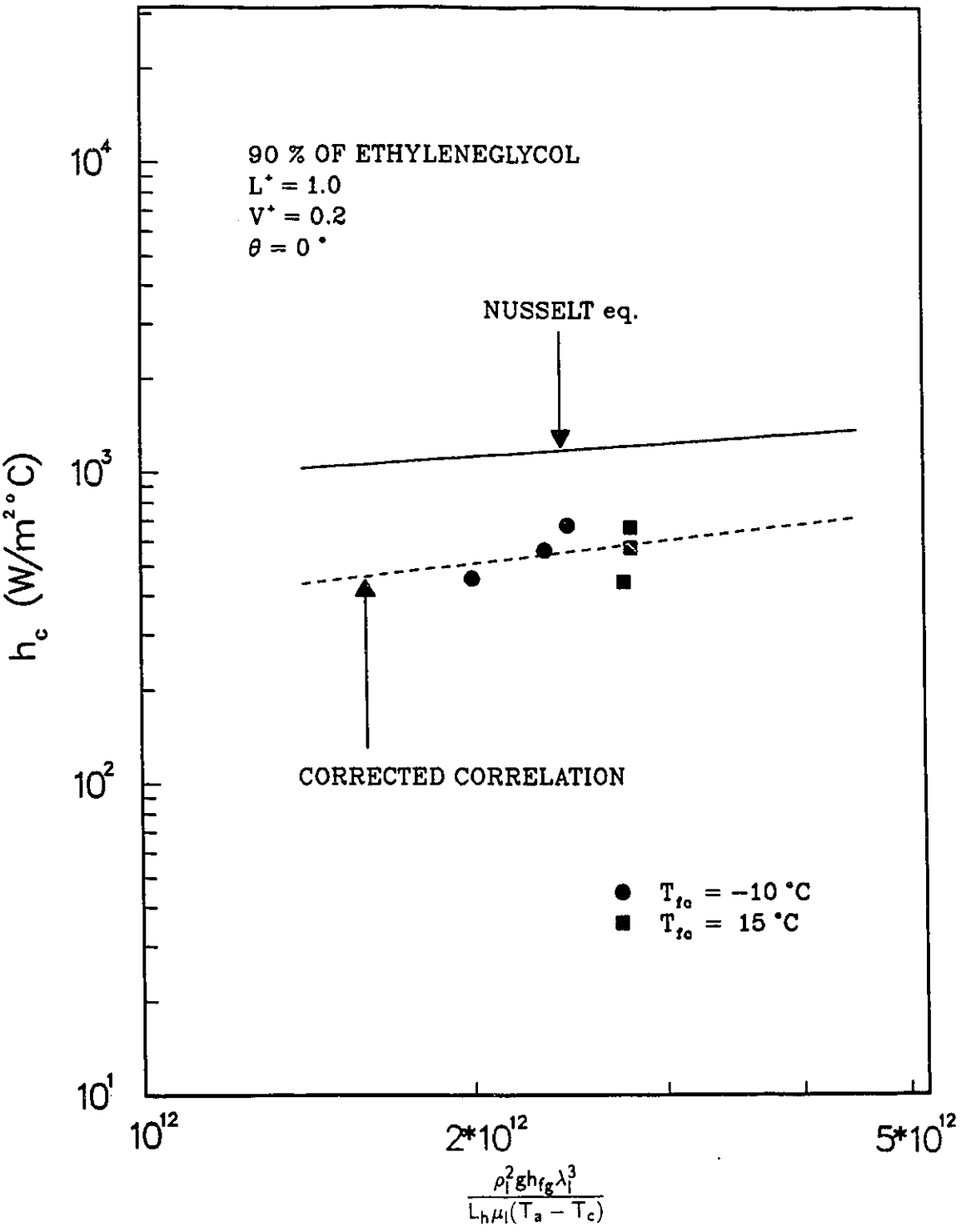

Figure 5.24 Comparison of the Experimental Data with Nusselt's Correlation (90 % of ethyleneglycol)

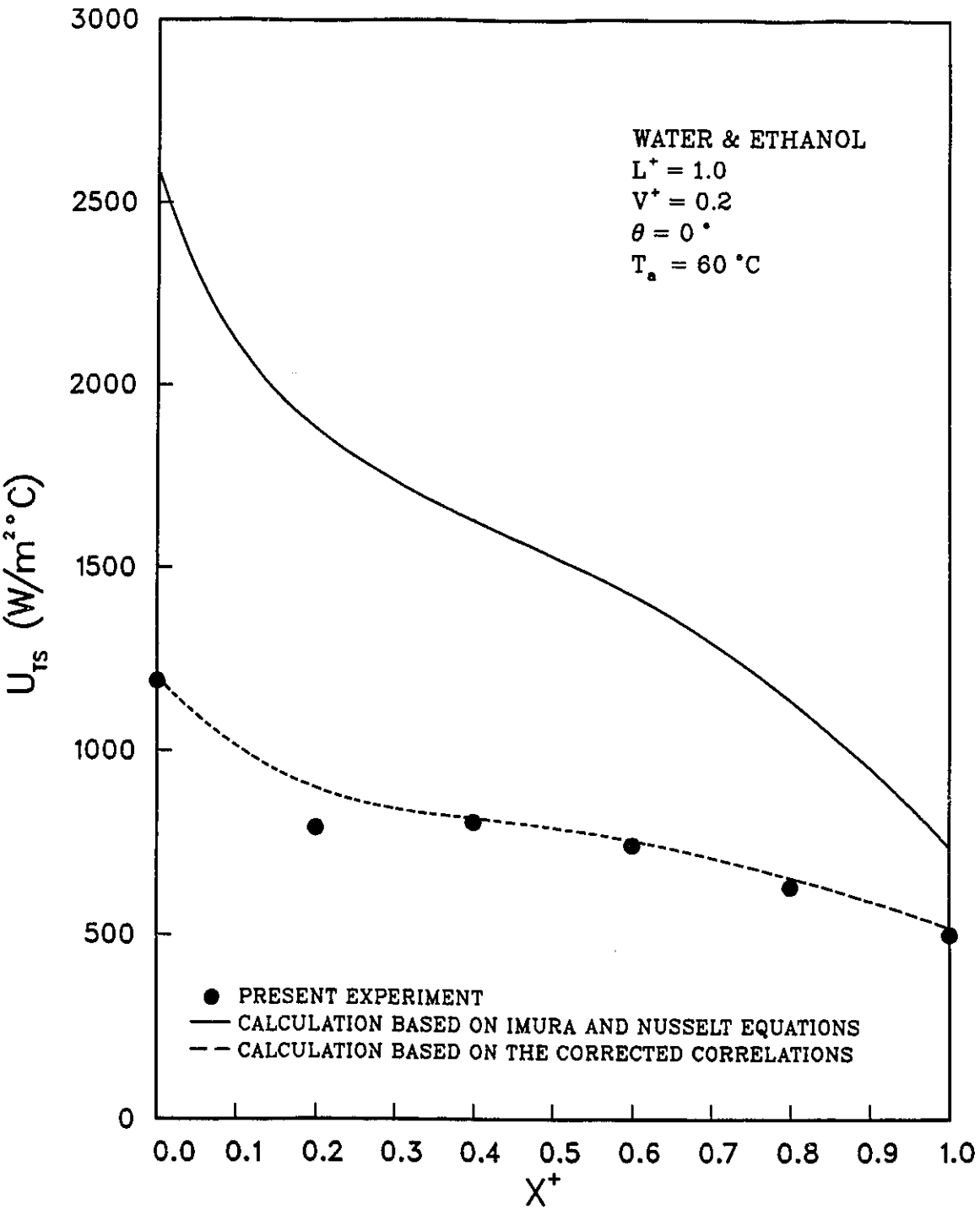

Figure 5.25 Comparison of the Predicted Values of U_{TS} with the experimental results (water-ethanol)

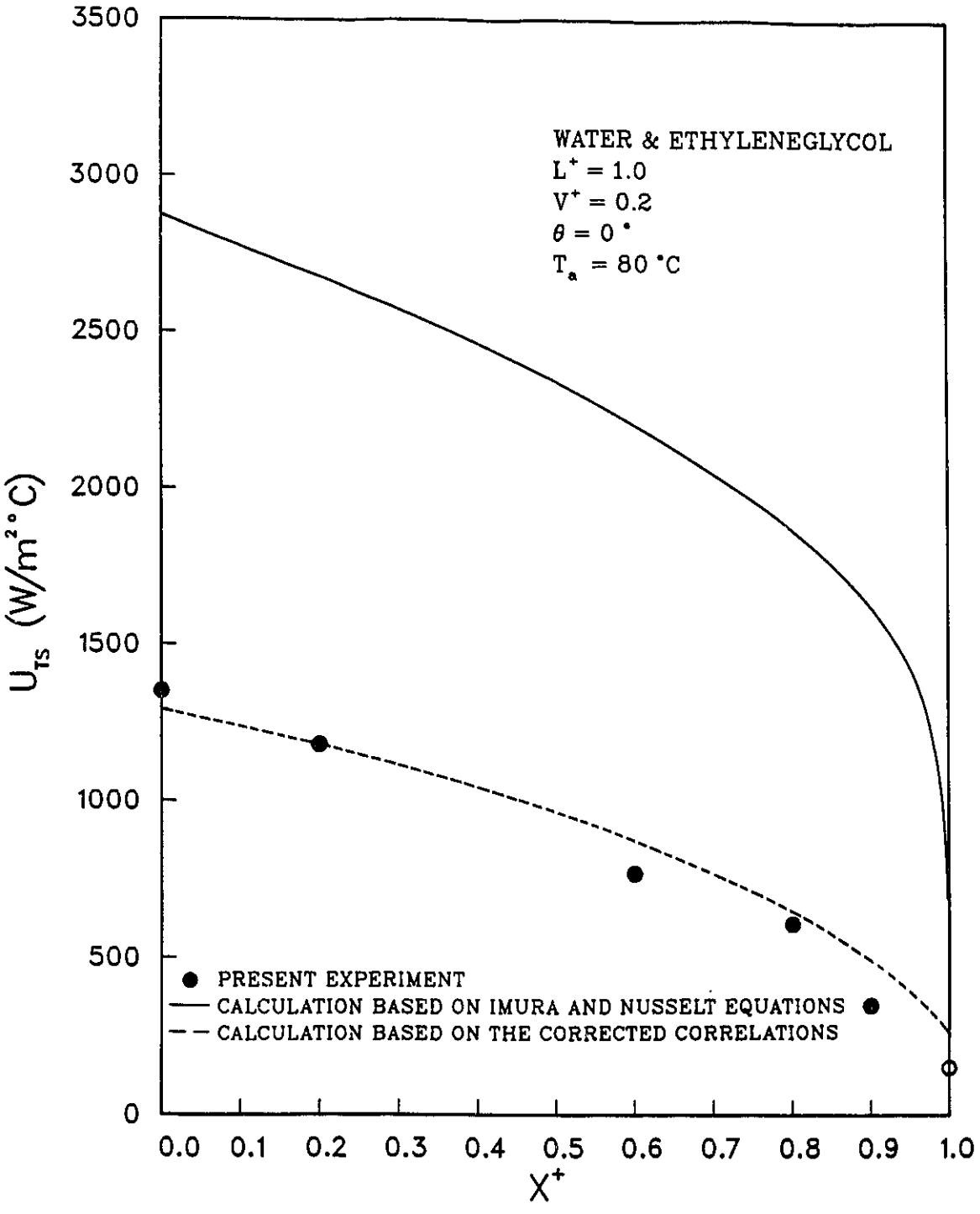

Figure 5.26 Comparison of the Predicted Values of U_{TS} with the experimental results (water-ethylenglycol)

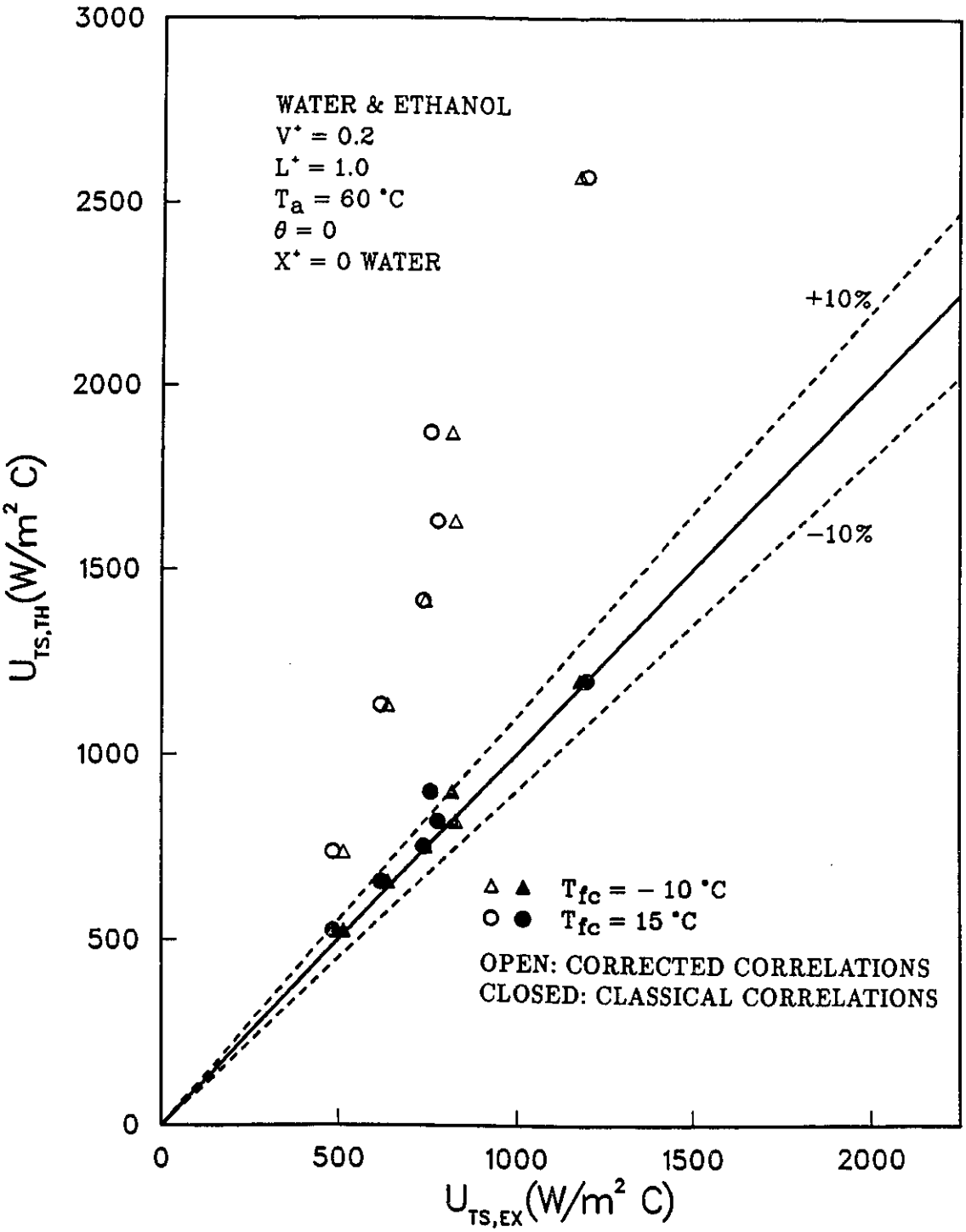

Figure 5.27 Experiment vs. Predictions (water-ethanol)

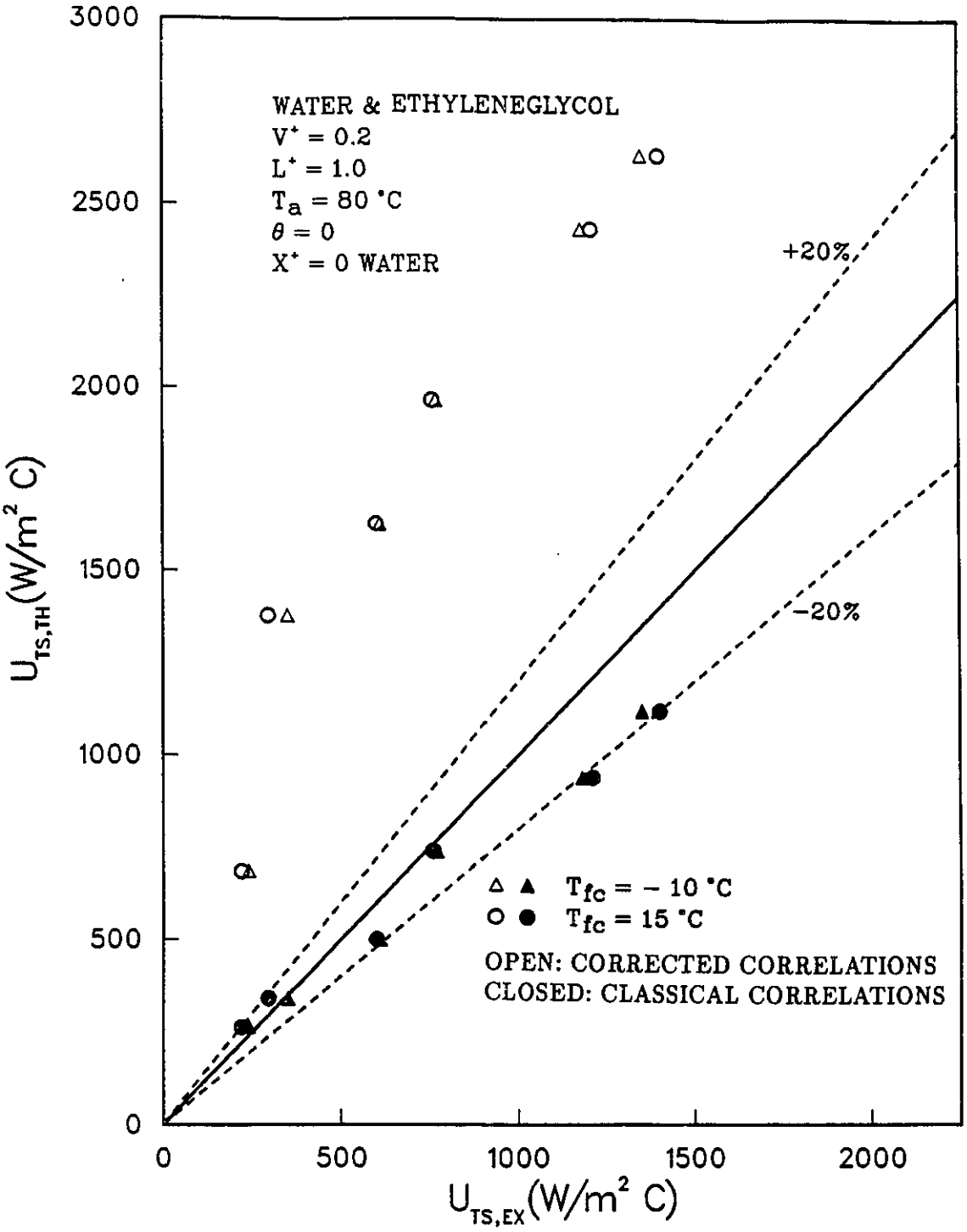

Figure 5.28 Experiment vs. Predictions (water-ethyleneglycol)

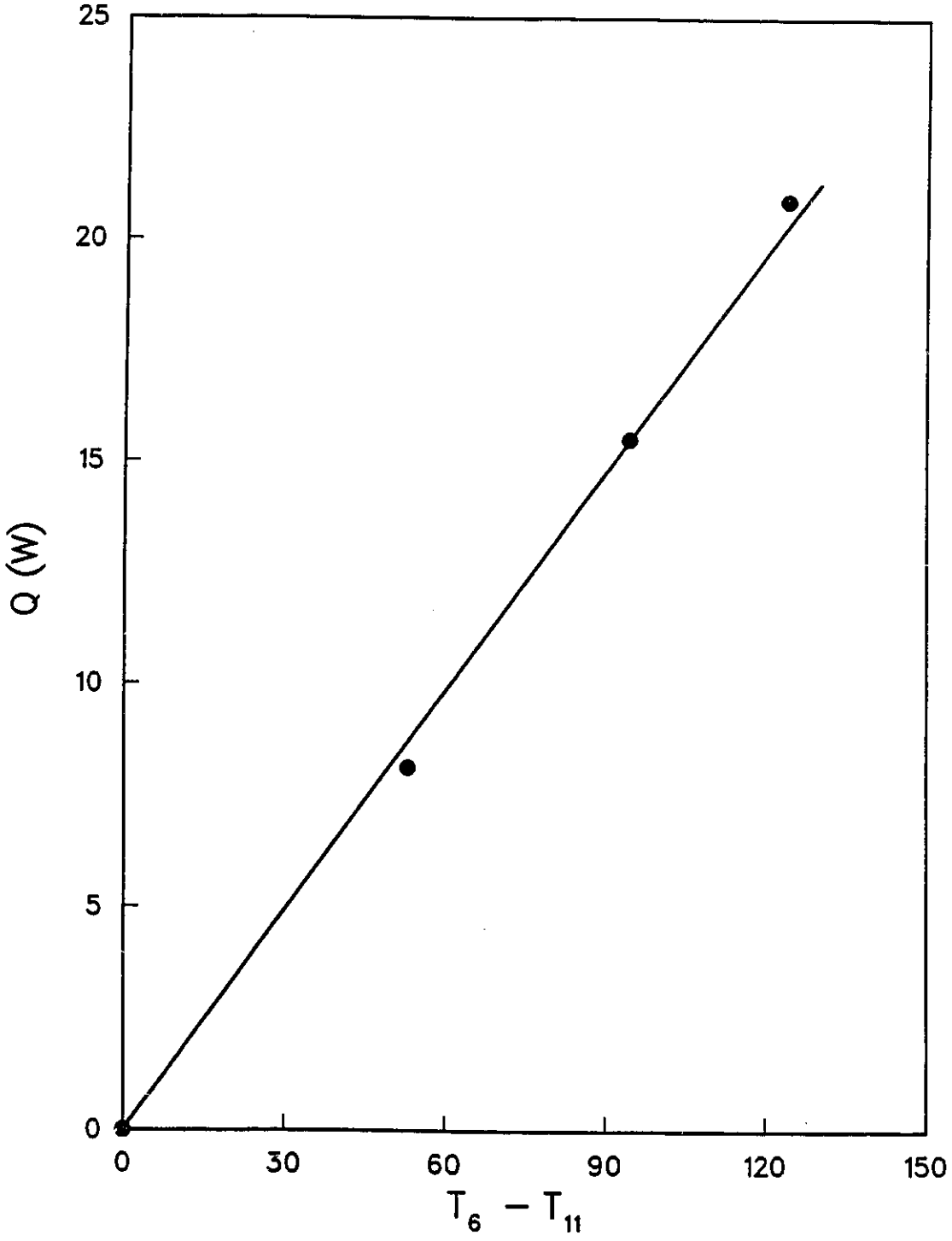

Figure A.1 Heat Loss